Ana Sofia Abrantes Dias

Development and validation of an analytical method for quantification of dopamine metabolism in plasma samples by LC-MS/MS

Dissertação apresentada para provas de Mestrado em Química Forense

Doutor Bruno José Fernandes Oliveira Manadas

Professora Doutora Maria João Moreno

junho 2017

Universidade de Coimbra

Este projeto foi realizado no grupo Life Sciences Mass Spectrometry do Centro de Neurociências e Biologia Celular (Universidade de Coimbra, Portugal), orientado pelo Doutor Bruno Manadas.
O trabalho foi financiado pela Fundação para a Ciência e Tecnologia (FCT), Portugal, com os projetos PTDC/SAU-NEU/103728/2008, PTDC/NEU-NMC/0205/2012, PTDC/NEU-SCC/7051/2014 e UID/NEU/04539/2013, e co-financiado pelo Programa COMPETE 2020 (Programa Operacional Fatores de Competitividade), pelo QREN, a União Europeia (FEDER – Fundo Europeu de Desenvolvimento Regional), e pela Rede Nacional de Espectrometria de Massa (RNEM), sob o contracto REDE/1506/REM/2005.

The present work was performed in the Life Sciences Mass Spectrometry group of Center for Neuroscience and Cell Biology (University of Coimbra, Portugal), and under scientific guidance of Doctor Bruno Manadas.
The work was supported by Fundação para a Ciência e Tecnologia (FCT), Portugal, projects references PTDC/SAU-NEU/103728/2008, PTDC/NEU-NMC/0205/2012, PTDC/NEU-SCC/7051/2014 and UID/NEU/04539/2013, and cofinanced by "COMPETE 2020 Programa Operacional Fatores de Competitividade, QREN, the European Union (FEDER – Fundo Europeu de Desenvolvimento Regional) and by The National Mass Spectrometry Network (RNEM) under contract REDE/1506/REM/2005.

Agradecimentos

A realização desta tese não teria sido possível sem o contributo, estímulo e empenho de várias pessoas e, como tal, gostaria de expressar toda a minha gratidão a todos os que, direta ou indiretamente contribuíram para que esta tarefa fosse possível. A todos deixo aqui os meus sinceros agradecimentos.

Desta forma, quero começar por agradecer ao Dr. Bruno Manadas pela possibilidade de desenvolver este projeto no seu laboratório, no Centro de Neurociências e Biologia Celular. Pela competência e orientação científica, pelos conhecimentos transmitidos e pela disponibilidade revelada ao longo do trabalho, assim como pelas críticas, correções e sugestões relevantes feitas durante a orientação. Agradeço ainda à Prof.ª Maria João pela orientação e ajuda prestadas ao longo do trabalho, assim como pelo interesse e acompanhamento no seu desenvolvimento.

Quero também agradecer à Vera e à Joana pela orientação e transmissão de conhecimentos prestada ao longo do desenvolvimento deste trabalho. Agradeço a disponibilidade e a paciência, assim como toda a partilha de saber que foi um valioso contributo para a elaboração desta tese. Quero agradecer igualmente às restantes colegas de laboratório, Cátia, Margarida e Sandra, pelos momentos de boa disposição, uma vez que foram uma forma de motivação para encarar todos os desafios com mais ânimo.

Aos meus amigos, obrigada pela amizade e cumplicidade, pelos momentos de convívio e descontração que me permitiram relaxar e esquecer todo este stress, mesmo que por breves momentos. Acima de tudo, deixo um enorme obrigada ao Luís. A tua importância na minha vida tornou-se ainda maior. Todo o teu apoio, compreensão e afeição foram fundamentais, peço desculpa por todos os momentos de stress, mas no final sempre me soubeste acalmar e ver as coisas de uma forma positiva. Tenho sorte em ter-te ao meu lado!

Aos meus pais, um obrigada muito especial, por tudo o que fizeram por mim, pelo amor incondicional e pela forma como, ao longo de todos estes anos, me souberam ajudar. Obrigada pela confiança em mim depositada, pelo apoio em todos os momentos bons e menos bons que a vida académica me proporcionou e por toda a compreensão. Por me terem ajudado a crescer, por terem aceite e apoiado todas as minhas escolhas e por me terem tornado na pessoa que sou hoje. Sem vocês eu não teria esta oportunidade de lutar pelos meus sonhos e objetivos e, como tal, quero partilhar convosco a alegria de os conseguir vencer. Sem dúvida são as pessoas mais importantes da minha vida. A vocês devo tudo o que sou!

Agradeço ainda aos restantes familiares, por todo o apoio e palavras de incentivo, assim como todos aqueles que, mesmo não estando aqui diretamente mencionados, tiveram um papel relevante para mim durante este ano.

Table of contents

Abbreviations

AADC	Aromatic L-amino acid decarboxylase or L-DOPA decarboxylase
ACh	Acetylcholine
ACN	Acetonitrile
AD	Alzheimer's disease
AIF	Apoptosis initiator factor
ALDH	Aldehyde dehydrogenase
ALR	Aldehyde reductase
ANOVA	Analysis of variance
APCI	Atmospheric pressure chemical ionization
ATP	Adenosine triphosphate
BBB	Blood-brain barrier
BH4	Tetrahydrobiopterin
CE	Collision energy
CI	Chemical ionization
CID	Collision-induced dissociation
CNS	Central nervous system
COMT	Catechol-O-methyltransferase
CUR	Curtain gas
CV	Coefficient of variation
CXP	Collision exit potential
DA	Dopamine
DAT	DA transporter
DBH	Dopamine beta-hydroxylase
DBS	Deep brain stimulation
DOPAL	3,4-dihydroxyphenylacetaldehyde
DOPET	3,4-dihydroxyphenylethanol
DOPAC	3,4-dihydroxyphenylacetic acid
DNA	Deoxyribonucleic acid
DP	Declustering potential
ECD	Electrochemical detection
EI	Electron ionization

EMA	European Medicines Agency
EP	Entrance potential
ESI	Electrospray ionization
f	Matrix influence factor
F_{crit}	Tabulated F value
FA	Formic acid
FAB	Fast-atom bombardment
FD	Fluorescence detection
FDA	United States Food and Drug Administration
GC	Gas chromatography
GPx	Glutathione peroxide
GS1	Nebulizer gas 1
GSH	Glutathione
H_2O_2	Hydrogen peroxide
HNE	Hydroxynonenal
HPLC	High pressure liquid chromatography
HPLC-MS	High pressure liquid chromatography coupled to mass spectrometry
HVA	Homovanillic acid
ICDs	Impulse control disorders
ISO	International Organization for Standardization
IUPAC	International Union of Pure and Applied Chemistry
L-DOPA	Levodopa or 3,4-dihydroxy-L-phenylalanine
LC	Liquid chromatography
LC-MS	Liquid chromatography coupled to mass spectrometry
LLE	Liquid-liquid extraction
LOD	Limit of detection
LOQ	Limit of quantification
LPLC	Low pressure liquid chromatography
LRRK2	Leucine-rich repeat kinase 2 or PARK8
m/z	Mass-to-charge ratio
MAO	Monoamine oxidase
MAP	Mitogen activated protein
MDA	Malondialdehyde

Mn SOD	Manganese superoxide dismutase
MPP^+	1-methyl-4-phenylpyridinium
MPTP	1-methyl-4-phenyl-1,2,3,6-tetrahydropyridine
MRM	Multiple reaction monitoring
MS	Mass spectrometry
MS/MS	Tandem mass spectrometry
3-MT	3-Methoxytyramine
NADH	Nicotinamide adenine dinucleotide
NO	Nitric oxide
$O_2^{\cdot-}$	Superoxide anion radical
6-OHDA	6-hydroxydopamine
8-OHdG	8-hydroxy-2‘-deoxyguanosine
PARK1	α-synuclein
PARK2	Parkin
PARK7	DJ-1
PD	Parkinson’s disease
PHS	Prostaglandin H synthase
PINK1	PTEN-induced putative kinase 1 or PARK6
PNMT	Phenylethanolamine N-methyltransferase
PPT	Protein precipitation
Prx	Peroxiredoxin
PUFAs	Polyunsaturated fatty acids
Q1	First quadrupole
q2	Second quadrupole (collision cell)
Q3	Third quadrupole
QC	Quality control
R	Coefficient of correlation
R^2	Coefficient of determination
%RE	Percentage relative error
Σ(%RE)	Sum of the percentage relative error
RNS	Reactive nitrogen species
ROS	Reactive oxygen species
R.S.D.	Relative standard deviation

RT	Retention time
ΔRT_{ratio}	Interval of retention time ratio
$S_{y/x}$	Standard error of the residuals
S/N	Signal-to-noise
SIM	Selected ion monitoring
SOD	Superoxide dismutase
SPE	Solid-phase extraction
TCA	Trichloroacetic acid
TH	Tyrosine hydroxylase
TNF-α	Tumor necrosis factor-alpha
TOF	Time-of-flight
TSP	Thermospray
TV	Test value
UCHL1	Ubiquitin carboxyl-terminal hydrolase L1 or PARK5
UPS	Ubiquitin-proteasome system
UV	Ultraviolet
UV-Vis	Ultraviolet-visible
WADA	World Anti-Doping Agency
w_i	Weighting factor
$\sum \lvert \%RE \rvert$	Sum of the relative errors
RT	Retention time
RT	Retention time

Resumo

A doença de Parkinson (DP) é a segunda doença neurodegenerativa mais comum, afetando mais de 6 milhões de pessoas em todo o mundo. Trata-se de um distúrbio neurodegenerativo progressivo caracterizado, neuropatologicamente, por uma perda de neurónios dopaminérgicos numa região específica do cérebro, nomeadamente a *substância negra pars compacta* (SNpc), com uma consequente diminuição da dopamina no corpo estriado, e pela presença de corpos de Lewy nos neurónios sobreviventes. O aparecimento de todos estes sinais neuropatológicos está relacionado com o surgimento dos principais sintomas motores, como tremor em repouso, rigidez, bradicinesia e instabilidade postural, que são utilizados no diagnóstico da patologia. Embora não haja cura para a patologia, há um grupo de medicamentos que podem ser utilizados no controlo dos principais sintomas, sendo a levodopa o mais utilizado.

Devido à relação entre alterações no metabolismo da dopamina e o surgimento da doença de Parkinson, tem havido um interesse crescente na análise dos analitos envolvidos. Uma vez que este metabolismo também ocorre no plasma, existe a possibilidade de utilizar esta matriz para desenvolver um possível teste de diagnóstico que permita detetar a doença numa fase precoce. Desta forma, o principal objetivo do presente trabalho foi desenvolver e validar um novo método analítico para a quantificação do metabolismo da dopamina em amostras de plasma por cromatografia líquida acoplada à espetrometria de massa (LC-MS/MS).

Todas as amostras de plasma foram sujeitas ao mesmo processo de precipitação proteica com metanol, sendo depois analisadas pelo sistema LC-MS/MS, no modo MRM[1].

Após o desenvolvimento do método, foram avaliados alguns parâmetros de validação para assegurar a fiabilidade dos dados, nomeadamente a seletividade, a linearidade, os limites de deteção e quantificação, a precisão, a exatidão, a transferência[2], a eficiência da extração e os efeitos da matriz.

Os resultados mostraram que foi possível desenvolver um método para determinar quantitativamente o metabolismo da dopamina em amostras de plasma, bem como aplicá-lo em amostras reais de plasma, a fim de quantificar estas moléculas. O método mostrou-se seletivo para todos os analitos em estudo, uma vez que não houve interferências da matriz. O método também mostrou ser linear para todas as moléculas, em solvente, na gama de trabalho, nomeadamente nos intervalos: 0,05-5,0 pmol/µL para L-tirosina e DA; 0,03-5,0 pmol/µL para 3-

[1] Do inglês, Multiple Reaction Monitoring
[2] Do inglês, carry-over

MT e HVA; 0,1-6,0 pmol/µL para L-DOPA; e 0,1-5,0 pmol/µL para DOPAC. Nas amostras de plasma, o método foi linear nos intervalos 0,5-10,0 pmol/µL para 3-MT e DOPAC e 0,05-12,0 para HVA.

Em solvente, os limites de deteção foram: 0,381; 0,426; 0,424; 0,377; 0,260 e 0,235 pmol/µL para L-tirosina, L-DOPA, DA, 3-MT, DOPAC e HVA, respetivamente. Os limites de quantificação foram: 1,154; 1,290; 1,284; 1,143; 0,787 e 0,714 pmol/µL para L-tirosina, L-DOPA, DA, 3-MT, DOPAC e HVA, respetivamente. Por sua vez, nas amostras de plasma, os limites de deteção foram de 0,852; 0,963 e 1,015 pmol/µL e os limites de quantificação foram 2,581; 2,617 e 3,077 pmol/µL para 3 MT, DOPAC e HVA, respetivamente.

Na análise da precisão, os resultados da repetibilidade estavam de acordo com os critérios de aceitação, no entanto, a precisão intermediária apresentou altos valores para todas as moléculas. Em termos de análise de precisão, o método mostrou-se preciso para a quantificação dos analitos.

A recuperação do método, nos três níveis de concentração, variou entre 84,9% e 112,1%. Nos efeitos da matriz, obtiveram valores negativos, indicando supressão iónica.

Por fim, o método desenvolvido foi aplicado em amostras de plasma que foram recolhidas de um grupo controlo e dois grupos de estudo. No grupo controlo, nenhum composto foi devidamente detetado. Por sua vez, L-DOPA, DOPAC e HVA foram detetados na maioria das amostras de plasma dos grupos de estudo, no entanto, não foi encontrada nenhuma relação entre a dose diária de medicação e a concentração de L-DOPA no plasma.

Palavras-chave: Metabolismo da dopamina; quantificação; plasma; LC-MS/MS; validação.

Abstract

Parkinson's disease (PD) is the second most common neurodegenerative disease, affecting over than 6 million people across the world. This is a progressive neurodegenerative disorder neuropathologically characterized by a loss of dopaminergic neurons in a specific brain region, namely the *substantia nigra pars compacta* (SNpc), with a consequent depletion of dopamine (DA) within the striatum, and by the presence of Lewy bodies in the surviving neurons. The appearance of all these neuropathological signs is related to the emergence of the main motor symptoms, for instance resting tremor, rigidity, bradykinesia and postural instability, which are used in the diagnosis of the pathology. Even though there is no cure for the pathology, there are a group of medications that can be used in the control of the main symptoms, being levodopa the most used one.

Due to the relationship between changes in DA metabolism and the arise of PD, there has been a growing interest in the analysis of the involving analytes. Since this metabolism also occurs in the plasma, there is the possibility to use this matrix to develop a possible diagnose test that allows to detect the disease in an early stage. Then, the main purpose of the current work was to develop and validate a new analytical method for the quantification of DA metabolism in plasma samples by liquid chromatography coupled to tandem mass spectrometry (LC-MS/MS).

All the plasma samples were subjected to the same protein precipitation procedure with methanol, being then analyzed by the HPLC-MS/MS system, in the MRM mode.

After the development of the method, some validation parameters were evaluated in order to assure the reliability of the current data, namely selectivity, linearity, limits of detection and quantification, precision, accuracy, carry-over, recovery and matrix effects.

The results showed that it was possible to develop a method to quantitatively determinate DA metabolism in plasma samples, as well as to apply it in real plasma samples, in order to quantify these molecules. The method proved to be selective for all the analytes under study, since no matrix interferences occur. The method also showed to be linear for all the molecules in solvent over the working range, namely in the intervals: 0.05-5.0 pmol/µL for L-tyrosine and DA; 0.03-5.0 pmol/µL for 3-MT and HVA; 0.1-6.0 pmol/µL for L-DOPA; and 0.1-5.0 pmol/µL for DOPAC. In plasma samples, the method was linear in the intervals: 0.5-10.0 pmol/µL for 3-MT and DOPAC and 0.05-12.0 for HVA.

In solvent, the limits of detection were: 0.381, 0.426, 0.424, 0.377, 0.260 and 0.235 pmol/µL for L-tyrosine, L-DOPA, DA, 3-MT, DOPAC and HVA, respectively. The limits of quantification were: 1.154, 1.290, 1.284, 1.143, 0.787 and 0.714 pmol/µL for L-tyrosine, L-DOPA, DA, 3-MT, DOPAC and

HVA, respectively. In turn, in plasma samples, the limits of detection were 0.852, 0.963 and 1.015 pmol/µL and the limits of quantification were 2.581, 2.617 and 3.077 pmol/µL for 3-MT, DOPAC and HVA, respectively.

In the precision analysis, the repeatability results were in accordance with the acceptance criteria, however, intermediate precision presented high values for all the molecules. In terms of accuracy analysis, the method proved to be accurate to the quantification of the analytes.

The recovery of the method, at three levels of concentration, ranged from 71.9% to 103.6%. In matrix effects, negative values were obtained, indicating ion suppression.

Finally, the developed method was applied in plasma samples that were collected from a control group and two study groups. In control group, no compound was properly detected. In turn, L-DOPA, DOPAC and HVA were detected in most of plasma samples of the study groups, however, no relation between the daily dose of medication and the concentration of L-DOPA in the plasma was found.

Keywords: Dopamine metabolism; quantification; plasma; LC-MS/MS; validation.

1. Introduction

1.1. Parkinson's disease

The first reports of symptoms that are today associated with Parkinsonism date from 4500 B.C. and are from India. The disease to which the Ayurvedic physicians designated as Kampavata, was treated with *Mucuna pruriens*, one plant of the Fabaceae family and commonly named as "velvet beans." This plant is the only known natural source of levodopa (L-DOPA), the direct precursor of dopamine (DA) [1].

Even though there are possible reports of Parkinson's disease (PD) from very early, the first clear medical description was written in 1817 by James Parkinson, when he published "An Essay on the Shaking Palsy", considered the foundational text of the disease, where he medically described it as a neurological syndrome [2, 3]. In this essay, Dr. Parkinson report the specific group of major symptoms which manifest in afflicted patients as a slowly debilitating disorder of movement that ultimately proves to be fatal [4]. Some years later, in the mid-1800s, Jean-Martin Charcot had an important role in refining and expanding this preliminary description and in disseminating the information about PD in an international level. He was responsible to differentiate PD from other disorders mainly characterized by tremor, and recognized cases that later were then classified as Parkinsonism-plus syndromes [2, 5]. Over the time, Charcot discriminated the difference between bradykinesia and rigidity (both symptoms of PD), recorded the frequency of tremors, recognized the micrograph as a common feature to all patients, and prescribed the first treatments [6]. Despite the stiffness symptoms have been described by Charcot, is the Charcot himself who suggested the name given to the disease, Parkinson [7].

This pathology is a slowly progressive degenerative disorder that affects the motor system and, consequently, the body movements. It is considered the most common neurodegenerative disease of the motor system and the second most common neurodegenerative disease after Alzheimer's disease (AD), affecting six million people around the world [8] and around twenty thousand people in Portugal [9]. It is usually a more prevalent disease in the elderly, giving its clinical onset after 60-65 years of age [8], once some studies show that only in 0.5% of the cases the diagnosis was made before the age of 40, 3.4% before the age 50 of and over 60% were first diagnosed after 65 years of age [10]. However, in some cases of familial forms of the disease it can appear before 40 years of age [11]. Since the incidence of the disease increases with age (major risk factor), it is likely that in future the number of people suffering from this pathology increases [10].

Symptoms appear gradually, usually arise on one side of the body and remains worse on that side, even after symptoms begin to affect both sides. The specific group of symptoms that a patient experience can be different from person to person, but the primary motor signs of PD include trembling of hands, arms, legs, jaw and face; bradykinesia or slowness of the movement; rigidity of the limbs and trunk; and postural instability or impaired balance and coordination [3]. As symptoms get worse, people may have trouble walking or even doing simple tasks. Besides, patients may also experience a wide range of physical and/or psychological symptoms, including depression, anxiety, balance problems, loss of sense of smell, sleeping disorders and memory fails, being that some are side effects of drug therapy [12]. In PD, as in other disorders linked to a dysfunction in the dopaminergic system, it appears to have some gender differences regarding the symptoms and treatment response, and at the level of metabolism in basal ganglia, namely in the frontal monoaminergic activity, in recently diagnosed Parkinson's disease patients [13].

The disease arises when the neurons of a brain region called the substantia nigra (so called because the high concentration of neuromelanin) die, wherein when the first symptoms appear, there is already a loss of 70 to 80% of striatal DA and 50% of nigral DA neurons [14]. Under normal conditions, these cells produce DA, a neurotransmitter responsible for the transmission of messages between the different areas of the brain that control movement and coordination [15]. Being so, DA signals travel from the substantia nigra to the remaining areas of the brain in order to control the movement and balance (Figure 1.1).

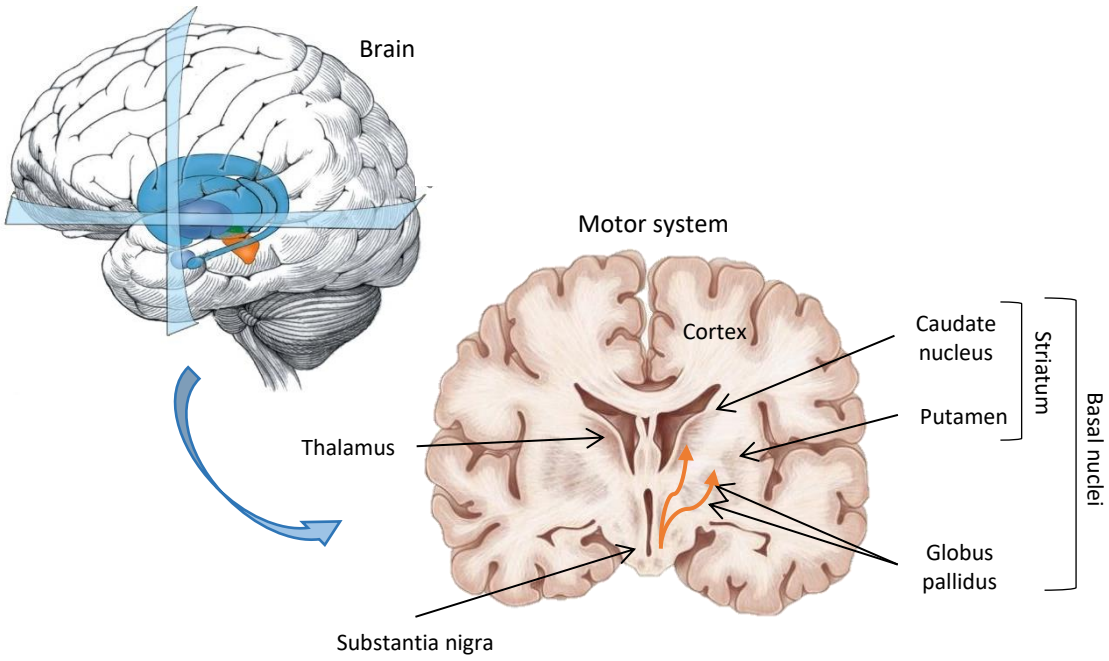

Figure 1.1. Dopamine pathway in the motor system. Under normal conditions, dopamine (DA) signals travel from the substantia nigra to the other brain regions involved in the control of movement and balance, including the corpus striatum, the globus pallidus, and the thalamus. However, in Parkinson's disease (PD), most of these dopamine signals are lost, leading to the appearance of the first symptoms.

The connection between the substantia nigra and the striatum is critical to produce smooth movements. Thus, when the cells of the substantia nigra die DA levels drop and most of the DA signals are lost. The loss of the DA in this circuit leads to the appearance of the first symptoms of the disease [3] because these neurons do not receive the necessary messages about how and when to induce body movement. Unfortunately, the ultimate cause of PD, the reason that these cells become altered and die, is not known in most of the diagnosed cases [16], but researchers suggest that it can result from a combination of both genetic and environmental factors.

The striatum is the main receiving area of neuronal information from the basal ganglia and this can happen by three different pathways: corticostriatal, thalamocortical and nigrostriatal (the most affected by neurodegeneration in PD) [17]. The information is processed in the neural circuits of the basal ganglia, being sent to the thalamus and then to the cerebral cortex and its transmission can be made by direct or indirect means [18]. The direct pathway, by inhibiting the basal ganglia, leads to the inhibition of the thalamus and to cerebral cortex excitation. In turn, the indirect pathway, by stimulating the basal ganglia, promotes the excitement of nerve centers that conduct stimuli to the spinal cord [19]. There are pathologies with a basal ganglia origin and related to dopaminergic neurons, usually known as movement disorders, which are thought to result from imbalanced activities between these two pathways and are characterized by an excessive or restriction of movement [18]. In PD, the degeneration of nigral neurons may lead to excessive inhibition of the thalamus and the base nodes, leading to reduced stimulation of the motor cortex and the onset of akinesia or bradykinesia [19].

There is currently no blood test that helps in diagnosing sporadic PD, and so it can be difficult to diagnose the disease [15]. The diagnosis is usually late, due to the non-specificity of initial symptoms, and usually only with the worsening of the symptoms the patient goes to the doctor. It is best accomplished by a specialist such as a neurologist, being based on the medical history of the patient and in an evaluation of the symptoms, where the patients must present bradykinesia and, at least, another of the major symptoms of the disease. Moreover, it is essential to exclude other causes of Parkinsonism, in order to do a proper diagnosis [7]. Another way to diagnose PD is to prescribe L-DOPA to the patient and monitor its response to the therapy [20]. However, this disease can only be reliably confirmed upon autopsy.

Currently, there is no cure for the disease, but there is a wide variety of medications used to relieve the symptoms and provide a good lifestyle for the patients [15]. Usually, patients are given L-DOPA combined with carbidopa, an inhibitor of the peripheral metabolism of L-DOPA, which delays the conversion of L-DOPA into DA until it reaches the brain. Neuronal cells have the ability to use L-DOPA to synthetize DA, providing the brain cells with the necessary amount of DA [15]. However, a prolonged use of this therapy can be associated with the development of motor

complications, especially when it is used in high doses [21], and nonmotor symptoms. Other medications include DA agonists, that chemically mimic the action of DA, and inhibitors of catechol-O-methyltransferase (COMT) enzyme, inhibiting the degradation of DA and allowing the increase of its concentration within the brain. One of the earliest used drugs was anticholinergics, who have the ability to decrease acetylcholine (ACh) levels in order to achieve a balance with DA levels. Also, it can be used amantadine, that has an anticholinergic activity, increases DA release and acts on the excitatory neurotransmitters of the basal ganglia [15].

There is a minority of patients that can develop compulsive behaviors (or impulse control disorders, ICDs), when receiving DA-replacement medications [22]. These are characterized by an inability to resist an impulse, drive or temptation that lead the patient to perform an act that is harmful to the individual or to the others and, in cases of PD patients, they are usually associated with dopaminergic therapies [23]. Although the reason of the onset of this disorder is not fully understood, due to the fact that it does not affect all the patients, it is thought that they are related to irregularities in the reward system, once it is a DA-mediated system, being sensitive to dopaminergic medications [24]. Thus, people are driven by the sense of pleasure and usually, in PD patients, these behaviors involve hypersexuality, gambling or abuse of anti-parkinsonian medications and can develop tolerance and psychological dependence. In patients whose PD is more advanced these disorders tend to be more pronounced, once they need higher doses of anti-parkinsonian medications to control their motor function. Among the ICDs, modifications of sexual behavior, as well as sexual impulses, have a distinct position in regard to the severity of the clinical cases and, although rare, these modifications may assume larger proportions, like abnormal sexual behaviors, and may eventually have criminal implications [25]. Patients that develop PD at a younger age are more likely to develop ICDs [26]. Hypersexuality in PD patients is associated with male gender, earlier disease onset, dopamine agonist therapy, and depression [27]. In most cases of ICDs, the onset of the impulsive behavior is associated with the addition or increase of the dopaminergic medication (mainly in cases of DA agonists) [28, 29], then, in these cases, the first step is to inform the doctor, to adjust the treatment. In some of these cases, an antipsychotic or antidepressant can be beneficial in the control of ICDs [30]. In legal terms, episodes of hypersexuality involved in cases of rape, for example, can raise important questions, namely if the patients are in full possession of their mental faculties while committing the sexual offence. We can affirm that, on the one hand, patients are capable of understanding the aberrant nature of their actions, however, on the other hand, the urge to commit the action may be so strong that they do not have self-control to resist. Advanced cases of PD are more complex, as there are other psychiatric disorders, such as hallucinations and confusion, and the severity of the character of the action may be more or less lost [25].

There are other cases in which surgery may be necessary, such as in cases where the patient does not respond to the medications. A therapy known as deep brain stimulation (DBS) can also be used, where electrodes are implanted into the brain and connected to a small electrical device [31]. This surgery can reduce the need of L-DOPA and related drugs, which in turn decreases the involuntary movements, resulting from side effects of L-DOPA therapy. Moreover, it also helps in the relief of the main symptoms of the disease.

1.2. Genesis of Parkinson's disease

1.2.1. Histopathology of Parkinson's disease

In terms of characteristic pathophysiological changes in PD, it is common to find in patient's brain a significant neurodegeneration in the substantia nigra pars compacta, due to a loss of pigmented dopaminergic cells, as well as a decrease of DA concentration in all the components of basal ganglia, including the putamen and the caudate nucleus, which constitute the striatum [32]. From the two constituents of striatum, putamen is the most affected, once the DA decrease in the putamen can reach 95%, while in the caudate nucleus the loss is about 80%, being that this difference is present in all patients diagnosed with idiopathic PD. The degree of the decrease of DA in the substantia nigra is positively related with the level of cell loss in this brain area [33]. This loss does not occur only at the striatal area, it also takes place at the extraestriatal nuclei of basal ganglia (internal and external pallidum, substantia nigra pars reticulata, and subthalamic nucleus), which are thought to be involved in the pathophysiologic mechanisms that result in parkinsonian disorders [33, 34], and in other brain areas, such as locus coeruleus, related to non-motor symptoms of the disease [35]. Besides the loss of DA, there is also a decrease of its main metabolite, the homovanillic acid (HVA), of the enzymes involved in its synthesis, and of its transporter sites [32, 33].

Another pathologic characteristic used in PD diagnosis is the presence of Lewy bodies in the surviving neurons from substantia nigra, i.e., deposits or clusters of the brain protein α-synuclein (present in presynaptic terminals), along with other proteins, seen in a microscopic examination of the brain. This deposit is considered a precursor of the neurodegeneration and it can provide a reliable diagnostic marker of cell death [36], once these neuronal inclusions are not found in healthy people, even though there are cases in which they are not present, namely in familial forms of the disease, and are responsible for the appearance of some non-motor symptoms. The composition of these clusters is still unknown but there are evidences of the presence of

neurofilament proteins, ubiquitin [37] and p62 [36]. However, there are some doubts about the reason that lead to their formation as well as their role in the development of the disease and so, several efforts are being conducted to try to understand the (ab)normal function of α-synuclein and its relationship to the genetic mutations involved in PD. In addition to Lewy bodies, there are other cytoplasmic inclusions with a similar composition, called Lewi neurites, detected in other brain structures, such as amygdala and hippocampus [38]. The presence of α-synuclein was identified in most cases of sporadic PD and other neurodegenerative diseases (dementia with Lewy bodies and multiple system atrophy), and in some cases of familial form of AD [39].

There are suggestions of a possible dysfunction of the mitochondrial respiratory chain in the pathogenesis of PD that led to the study of the structure and activity of mitochondrial system (enzymes and proteins). Therefore, postmortem analysis in the substantia nigra of patients with idiopathic PD showed a selective deficiency in the activity of complex I, due to a decrease of the activity of rotenone-sensitive nicotinamide adenine dinucleotide (NADH) CoQ_1 reductase, as well as a decrease in the activity of NADH cytochrome C reductase either in the substantia nigra [40] and frontal cortex [41]. A direct consequence of complex I inhibition is an increased lactic acid production and, consequently, a higher lactate concentration [42].

Also, there are evidences of changes in the antioxidant mechanisms, since there is a depletion of reduced glutathione (GSH) levels and GSH peroxidase activity, which is involved in the detoxification of peroxides in brain and, consequently, in the removal of hydrogen peroxide (H_2O_2). This reduction occurs especially in substantia nigra, putamen, globus pallidus and frontal cortex, compromising the detoxification process [43]. This failure in the defense system against reactive oxygen species (ROS) is associated with a potentiation of lipid peroxidation, once they act on polyunsaturated fatty acids (PUFAs) present in cell membranes. Then, studies about oxidative stress as a factor in the pathogenesis of this disease showed an increase in lipid peroxidation, with decreased levels of PUFA (indicator of the amount of substrate available for the process) and increased levels of malondialdehyde (MDA, an intermediate of the process that indicates the rate of lipid peroxidation at the time of death) in substantia nigra, when compared with other brain regions, probably due to an exposure to free radicals [44, 45]. Measurements of protein oxidation were made to compare oxidative stress in several brain regions, and it was showed an increase in the substantia nigra, when compared with basal ganglia or prefrontal cortex, meaning that it is a more vulnerable region to the oxidative damage [46]. This increase may be due to high levels of 8-hydroxy-2‘-deoxyguanosine (8-OHdG), a product of free radical attack on deoxyribonucleic acid (DNA), in the substantia nigra [47].

Loss of protective mechanisms against oxygen toxicity also has more consequences, rather than those presented before. In idiopathic Parkinson’s patients brains there is an increase in the

activity of the enzyme superoxide dismutase (SOD), with a particular relevance in the substantia nigra and basal nucleus [48] and a reduction of catalase and peroxidase activity in the substantia nigra and putamen [49], both enzymes involved in the defense system. These changes suggest an enhanced free radical production, and may be related to the inhibition of complex I activity from the mitochondrial respiratory chain [45].

All these biochemical changes appear to result from the nigral cell death, as well as the presence of Lewy bodies in the brain, characteristic features in Parkinson's patients.

1.2.2. Etiology and pathogenesis of Parkinson's disease

As previously mentioned, besides all the research made over the years, the etiology of PD, as well as its pathogenesis, is not yet well understood, but it is known that 95% of the cases are idiopathic, have a multifactorial cause, resulting from environmental and genetic contributions [50], and the other 5% result from genetic mutations. However, both forms share pathological, biochemical and clinical features [51]. It is believed that there is an interaction between these factors, genetic predisposition and environmental factor, being associated with mitochondrial dysfunction and oxidative stress in idiopathic cases [7]. Also, in idiopathic cases, there are other hypothesis such as the inhibition of proteasome activity and a possible genetic susceptibility, being that they all appear to be related.

The discovery of onset of Parkinson's symptoms in young accidentally intoxicated with 1-methyl-4-phenyl-1,2,3,6-tetrahydropyridine (MPTP) supported the idea of interactions between genetic and environmental factor in the development of PD. The administration of MPTP causes toxicity in mice and human and it leads to symptoms that mimic neurological symptoms of PD, once it causes dopaminergic neurodegeneration. This happens because the toxic metabolite, 1-methyl-4-phenylpyridinium (MPP^+), is a potent complex I inhibitor in DA neurons [50].

There are other substances with a similar structure to MPTP, as 6-hydroxydopamine (6-OHDA), rotenone and paraquat, which are used in the agricultural industry for the manufacture of pesticides, herbicides and insecticides [52]. Depending on dose and time of exposure, these substances can induce neurotoxicity, by inhibiting mitochondrial function, and lead to a disorder in the complex I of the mitochondrial respiratory chain, which may induce cell death [50]. Thus, the progressive neurodegeneration may be caused by a chronic exposure to dopaminergic neurotoxins, or only by a brief exposure that, in some way, can lead to the initiation of a cascade of damaging events [3].

Therefore, increased oxidative stress, mitochondrial dysfunction, accumulation of oxidized aggregated proteins, inflammation process, genetic mutations, and defects in protein clearance constitute some of the complex stakeholders in the neurodegeneration of neurons.

1.2.2.1. Oxidative stress

There is a basal level of oxidative damage in all cells, namely in DNA, lipids and proteins, once some of the reactive species play important biological roles, being essential the existence of antioxidant mechanisms to repair or replace oxidized molecules, then the cells must have a balance between the production of the reactive species and the defense systems. Thus, when there is a failure in these defense systems, something that occurs with age, it can contribute to cell death and, consequently, to neurodegeneration, due to the increase of reactive species, such as oxygen free radicals [53]. These reactive species responsible for the oxidative damage in cells are related with an increase of the endothelial permeability. Blood-brain barrier (BBB) is essential to maintain central nervous system (CNS) homeostasis and is important to limit the transport of neurotoxic substances from blood into the brain. The increase of its permeability allows the entry of potentially harmful substances in the brain [54], being thought that this has a potential relevance in the pathogenesis of PD. This change of permeability is related with alterations in the regulation of occludin, a protein located in tight junctions that regulates the diffusion of substances between these structures [54].

Human brain is an extremely sensitive area to oxidative stress, due to the high oxygen consumption (20% of the oxygen from the body) required by the adenosine triphosphate (ATP) needs, but its metabolism is a natural producer of ROS during oxidative phosphorylation [55], specially of H_2O_2, a product of SOD and monoamine oxidase (MAO) A and B activity [53]. Once H_2O_2 is produced during brain metabolism, there is the need to remove it, so it does not have harmful consequences in the brain. This process is usually mediated by peroxiredoxin (Prx), catalase or glutathione peroxide (GPx) [56].

The relationship between oxidative stress and the pathogenesis of PD has its basis on the following evidences: increase of manganese superoxide dismutase (Mn SOD, involved in the protection of mitochondria from the oxidative damage of free radicals) activity, increase in lipid peroxidation (showed by an increase in the levels of hydroxynonenal (HNE)-modified proteins in nigral neurons, a product of lipid damage), increase in iron content and decrease in reduced form of glutathione [57].

Metals, such as iron, are suspected of having a role in cytotoxicity and cell degeneration. There are clear evidences of an increase in the content of total iron, iron (III) and ferritin (protein-

bound iron) in substantia nigra, being that the action of this metal in hydrogen peroxide leads to the production of highly reactive radicals, involved in oxidative damages [58]. There seems to be a relationship between the development of PD and the iron concentration in the substantia nigra with consequent formation of iron and DA complexes, which promotes oxidative stress as oxygen radicals are formed as products of oxygen reduction by these complexes [59].

Dopaminergic neurons are highly exposed to oxidative stress, since some ROS are naturally produced during DA metabolism, leading to H_2O_2 formation. This can occur spontaneously, in the presence of iron, or enzymatically, through MAO-B enzyme [60].

Therefore, oxidative stress plays a key role in neurodegeneration, especially in substantia nigra, and is currently accepted as a fundamental factor in the pathogenesis of PD.

1.2.2.2. Mitochondrial dysfunction

Mitochondria are organelles that are involved in several cellular processes including energy production, calcium homeostasis, apoptosis and fatty acids metabolism. They have a key role in electron transport and oxidative phosphorylation, being therefore the main cellular source of free radicals, once they are products of oxidative phosphorylation. However, in pathologies where there is a deficit of mitochondrial respiratory chain, the amount of ROS produced by the electron transport chain increases, surpassing the antioxidant protection mechanisms [51]. So, when mitochondrial dysfunction starts to appear it affects some cellular mechanisms that can cause cell death, including oxidative stress, induction of excitotoxicity and apoptosis. These facts support the idea that abnormal mitochondrial function and increased oxidative stress may have an important role in the pathogenesis of PD [61].

The implication of the mitochondrial dysfunction in the development of PD derivate from epidemiological studies that associate the exposure to environmental factors (like pesticides) to the disease development [51]. The clearest evidence of abnormal mitochondrial function, which is thought to be the main responsible for the mitochondrial dysfunction, is the decreased activity of complex I (major component of electron transport chain) in the substantia nigra of patients with PD. Also, it was demonstrated an increased oxidative stress and reduced electron transfer rate through complex I subunits [51, 61]. This process leads to an increase of the vulnerability of cells to apoptosis inducers (such as Bax) that act in the mitochondria, which allows the permeabilization of the outer mitochondrial membrane and the release of cytochrome c and apoptosis initiator factor (AIF) to the cytosol, promoting caspase activation [61, 62].

Impaired catalytic activity of complex I leads to a decrease of ATP production and decreased rate of electron transfer along the respiratory chain, being verified a protein loss in one of the

subunits of the complex. In line with this, studies have proved that these functional alterations at the level of complex I are in the basis of the pathogenesis of sporadic cases of PD, once these changes are not present in other forms of Parkinsonism [63].

Another evidence of the involvement of mitochondrial dysfunction in sporadic PD is the fact that findings showed that complex I inhibition can decrease proteossomal activity, which in turn make dopaminergic neurons more susceptible to damage by some neurotoxins. The relationship between complex I inhibition and ubiquitin-proteasome system (UPS) impairment is the fact that the degradation process requires ATP. Moreover, as mitochondrial dysfunction, increased oxidative stress is also thought to be related to an overload of UPS, leading to the accumulation of misfolded or damaged proteins [61]. This suggests that a decline in the proteossomal activity could be the mechanism behind UPS impairment, leading to the development of pathological protein aggregates.

1.2.2.3. Ubiquitin-proteasome system impairment

There are evidences that a dysfunction at the level of protein degradation by UPS might be an important factor in the neurodegenerative process, typically observed in various forms of PD. Some studies show high levels of damaged proteins and protein aggregates as well as impaired proteolysis in the substantia nigra of patients with sporadic PD, being that this is consistent with the idea that a failure at protein clearance is involved in the pathogenesis of cell death in PD [64].

All intracellular proteins and many extracellular proteins are continually hydrolyzed into their constituent amino acids, being replaced by new proteins. Then, protein degradation is an essential step to prevent the development of proteins with structural anomalies, incapable of performing their function correctly, reusing amino acids and peptides. These abnormal (short-lived, misfolded, mutant, damaged) proteins are degraded in the cytosol of eukaryotic cells through ATP-dependent mechanisms, namely the UPS. The UPS exists naturally in cells and play an essential role in the clearance and degradation of abnormal proteins. This process involves the identification of the abnormal proteins that are, then, linked with ubiquitin protein residues, as signal for degradation, by proteasome. Proteasome, the most complex component of the ubiquitin-proteolytic pathway, comprises three conjugated enzymes. In the first step, ubiquitin-activating enzyme (E1) activates the ubiquitin molecule, then, ubiquitin is transferred to the ubiquitin-conjugating enzyme (E2) and, finally, ubiquitin protein ligase (E3) recognizes and bonds to the targeted protein, to ensure selective protein targeting, forming a non-covalent complex. Lastly, ubiquitin-protein aggregates are recognized and degraded by 26S proteasome complex,

resulting in short peptide fragments and amino acids that can be recycled to produce new proteins [64].

The 26S proteasome complex, located in the cytosol of cells, is responsible for proteolysis of ubiquitin-conjugated protein, an ATP-dependent process, and it consists in a 20S proteasome complex (the "core catalytic" unit) and two 19S regulatory complexes. It also contains, at least, one ubiquitin C-terminal hydrolase involved in the recycling of ubiquitin [65]. Analysis to brain areas of patients with sporadic PD and healthy people with the same age showed a loss of α-subunit of 26/20S proteasomes and a dysregulation of 20S proteossomal enzymatic activity in the substantia nigra of PD patients when compared with the control group. Moreover, levels of proteasome activators, PA700 and PA28, are reduced in the substantia nigra when compared with healthy people, however PA700 expression is increased in other brain regions [66].

In addition to neurodegeneration of substantia nigra neurons, another characteristic of PD is the accumulation of non-degraded dysfunctional proteins, forming aggregates in cytoplasmic inclusions (Lewy bodies) in the remaining dopamine cells in substantia nigra, in cases of sporadic PD. This finding supports the idea that impaired protein degradation might be an important factor in neuronal death that occur in various forms of PD, being thought that defects in the 26/20S proteasome could exceed the degradation capacity of the UPS. A failure in the UPS lead poorly degraded proteins to aggregate and allow α-synuclein accumulation, that promotes the formation of insoluble inclusions in dopaminergic neurons [67]. The presence of α-synuclein and ubiquitin in Lewy bodies appears to be related to an incomplete degradation of α-synuclein fibrils (cytotoxic molecules) after labeling with ubiquitin via UPS, due to a downregulation of this complex, which leads to protein accumulation. Dysfunction of autophagy is also correlated, once α-synuclein can also be degraded by the autophagy-lysosomal pathway [68]. Fibrillar α-synuclein can also form inclusions in neuronal processes, termed Lewy neurites [69].

All these findings suggest that a failure in the UPS may raise the vulnerability of substantia nigra neurons, leading to a selective neurodegeneration in both sporadic and familial PD.

1.2.2.4. Neuroinflammation

The CNS is capable of triggering an immune response against exogenous agents and also in response to an immune process inherent to CNS itself. This inflammatory response is known as neuroinflammation and is mediated by glial cells, namely microglial cells, responsible to respond to neuronal damage through phagocytosis of damaged cells, then, activation of microglia is a hallmark of brain pathology. However, it remains unclear if glial cells have a neuroprotective or deleterious function in neuropathological diseases, as, on one hand, they are responsible for

scavenging oxygen free radicals and, on the other hand, they can cause neuronal damage through the release of potentially cytotoxic molecules, such as proinflammatory cytokines [70].

When it comes to PD, it is known that neuroinflammation is present in this pathology, as there is an activated microglia response and an increased microglial cytokine (like interleukins and tumor necrosis factor-alpha (TNF-α)) expression in the substantia nigra of brain patients [50], even though it is involved in the progression of the disease and not in its pathogenesis. The alterations in cytokines levels is thought to be due to the activated microglia, which promotes apoptotic cell death. However, the cause for the activation of microglial cells in PD, as well as in individuals exposed to MPTP, is still unknown [71]. It is important to highlight that inflammatory response in PD, or neuroinflammation, is different from the normal inflammation process, which refers to the defense reaction of the living tissues to an injury.

Activation of microglia cells can even be associated with oxidative stress, which also has a role in the pathogenesis of PD. This relationship relays on the fact that microglia activation can produce a variety of toxic compounds, such as ROS, reactive nitrogen species (RNS), cytokines, among others. Moreover, nitric oxide(NO)-mediated stress appears to be essential in the pathogenesis of PD, once when NO enters the neurons it can be combined with the superoxide anion radical ($O_2^{\cdot -}$), resulting in peroxynitrite, a very reactive specie [72, 73].

1.2.2.5. Neuromelanin

As said, substantia nigra owes its name to the presence of high levels of brown pigmented granules of neuromelanin in its neurons, being that these pigments can also be found in locus coeruleus. Neuromelanin has a similar structure to cutaneous melanin, begins to form at 2 to 3 years of age and increases with age, accumulating in central catecholaminergic neurons [74].

In terms of its synthesis it can occur enzymatically, by tyrosine, tyrosine hydroxylase (TH), peroxidase or prostaglandin H synthase (PHS) or non-enzymatically, due to the autoxidation of DA into polymeric material, a process that can be accelerated by interaction with transition metal ions [75]. It is believed that neuromelanin is related with the vulnerability of dopaminergic neurons in the substantia nigra, as in PD there is a selective loss of pigmented neurons in the substantia nigra and, consequently, a decrease in the neuromelanin content as the disease progresses, even though non-pigmented neurons survive [76]. There are evidences about the neuroprotective role of neuromelanin, by sequestering reactive metal species and organic toxic compounds, also providing a protective mechanism against DA toxicity. However, there are also some suggestions about the fact that neuromelanin plays a neurotoxic role, acting as a source of free radicals that will react with H_2O_2 [74, 77].

The neuromelanin released by the degenerating neurons is thought to be associated with neuroinflammation, once it can lead to an activation of microglial cells, allowing the release of cytotoxic molecules that damage the other neurons and lead to the progression of the disease [73]. Moreover, the accumulation of toxic chemical compounds that have high melanin affinity, such as MPTP [78] and paraquat (which has a similar structure to MPTP metabolite, MPP^+) [79] is related to a possible increase of the potency of these compounds in pigmented nerve cells. This is due to the fact that there is a gradual release of these substances into the neurons of the substantia nigra that may ultimately cause lesions in these neurons, leading to the progression of PD [78, 79].

Neuromelanin also has the ability to bond to metals, for instance iron, reinforcing the protective role of this polymer. The presence of iron in neurons is required to neuromelanin synthesis, being that neuromelanin has a central role in preventing cytotoxic processes resulting from all the metals. Ferritin, a protein that stores and releases iron, is only present in astrocytes and oligodendrocytes but not in the substantia nigra of dopaminergic neurons, then, the only way of these neurons can get iron is through neuromelanin, that also acts as the defense system against iron and other metals toxicity in these neurons, once it prevents their potential role in inducing oxidative stress [80].

1.2.2.6. Genetic changes

The characterization of monogenic forms of PD allowed to identify sixteen *loci* with a potential relevance in the development of PD (PARK1 to PARK16) and six genes were associated with mutations that were showed to cause familial forms of PD, in which the transmission can have a dominant nature like α-synuclein and leucine-rich repeat kinase 2 (LRRK2) or a recessive nature such as Parkin, PTEN-induced putative kinase 1 (PINK1) and DJ-1 [52, 81]. Among the most known, the SNCA gene encodes α-synuclein, located mainly in Lewy bodies in cases of idiopathic PD. Mutations of these genes and DA interaction can increase protofibrils inclusions, considered the most toxic form of α-synuclein [52]. Thus, it is essential to understand the linkage between gene products and monogenic forms of PD, highlighting the normal function of each one and how its dysfunction may contribute to PD pathogenesis.

The first gene for familial PD is SNCA gene and there were discovered 3 different mutations at 3 different families with familial forms of PD [81]: A53T [82], A30P [83] and E46K mutation [84]. It was also discovered a genomic triplication in a region spanning the α-synuclein gene [85] and a mutation adjacent to E46K (E46KΔG) which increased the aggregation propensity [86]. A53T and A30P mutations promote amyloid fibrils and nonfibrillar oligomers formation, when compared to

the wild-type α-synuclein [87]. There are evidences that overexpression of different types of α-synuclein can disturb catecholamine homeostasis and increase the cytosolic concentration of these neurotransmitters, which can then trigger cellular oxyradical damage and, consequently, damage dopaminergic neurons [88].

It was identified a genetic mutation in the gene encoding Parkin protein, linked to a rare form of autosomal recessive juvenile Parkinsonism, which encodes a ubiquitin ligase of type E3, one of the UPS components. Defects on parkin gene may interfere with the ubiquitin-mediated proteolytic pathway and lead to the death of neurons of substantia nigra, even though there is no Lewy bodies formation [89]. The majority of familial cases result from Parkin gene mutations and, in these cases, most of the patients have an onset before the age of 40, the clinical response to L-DOPA therapy is good and they present a severe loss of nigral dopaminergic neurons but not Lewy bodies formation [90]. On one hand, it is though that the inactivation of Parkin gene could be involved in the pathogenesis of the disease, due to the decreased ligase activity and, consequently, to the UPS impairment, however, on the other hand, the overexpression of Parkin protein may also have a protective role, once it confers resistance to stimuli that promote mitochondria-dependent apoptosis [81]. Moreover, there are evidences of Parkin role in the maintenance of mitochondria function and that Parkin mutants exhibit dramatic mitochondrial defects in its morphology [91].

A missense mutation in the gene that encodes ubiquitin carboxyl-terminal hydrolase L1 (UCHL1) causes a partial loss of the catalytic activity of this protease, leading to irregularities in the proteolytic pathway and in aggregation of proteins, causing neuronal degeneration [92]. As in the case of Parkin, this gene also encodes an important enzyme of the UPS, whose function is the cytoplasmic protein degradation, recycling free ubiquitin [93]. Once this mutation was only identified in one specific family it is controversial whether or not this variant is significant for the development of the disease [81, 94].

Research for PINK1 mutations in autosomal recessive early-onset familial cases revealed several different new mutations, however, these are less common than mutations in the Parkin gene in early-onset PD cases [81]. Also, it is thought that PINK1 has a neuroprotective role, once the overexpression of this gene leads to a reduction of cytochrome c release, which limits the activation of the members of the apoptotic cascade [95]. Being so, a loss of PINK1 function leads to an increased sensitivity to apoptotic stress, as well as to mitochondrial dysfunction (due to a decrease of complex I activity) and impaired DA release [96].

A deletion in the DJ-1 gene is related with the development of autosomal recessive early-onset Parkinsonism, once the loss of DJ-1 function causes neurodegeneration [97]. Although there are some doubts about the role of DJ-1, there are evidences that it acts as a cytoplasmic redox-

sensitive molecular chaperone and when there is a deficiency of this gene it sensitizes cells to oxidative stress, leading to an increase of the apoptosis [81, 98]. Moreover, this protein can also reduce α-synuclein aggregation [98].

More recently, it was discovered a mutation in the LRRK2 gene, which encodes a mitogen activated protein (MAP) kinase, the most common genetic cause of autosomal dominant, late-onset Parkinsonism [81, 99]. LRRK2 is involved in several neurodegenerative diseases and it may be responsible for the phosphorylation of α-synuclein and tau (protein present in nerve cells and that stabilize microtubules) and for its aggregation within degenerating neurons [99].

In order to summarize all these factors and their interactions, Figure 1.2 presents a scheme with the potential physiological factors involved in the pathogenesis of PD and their relationship.

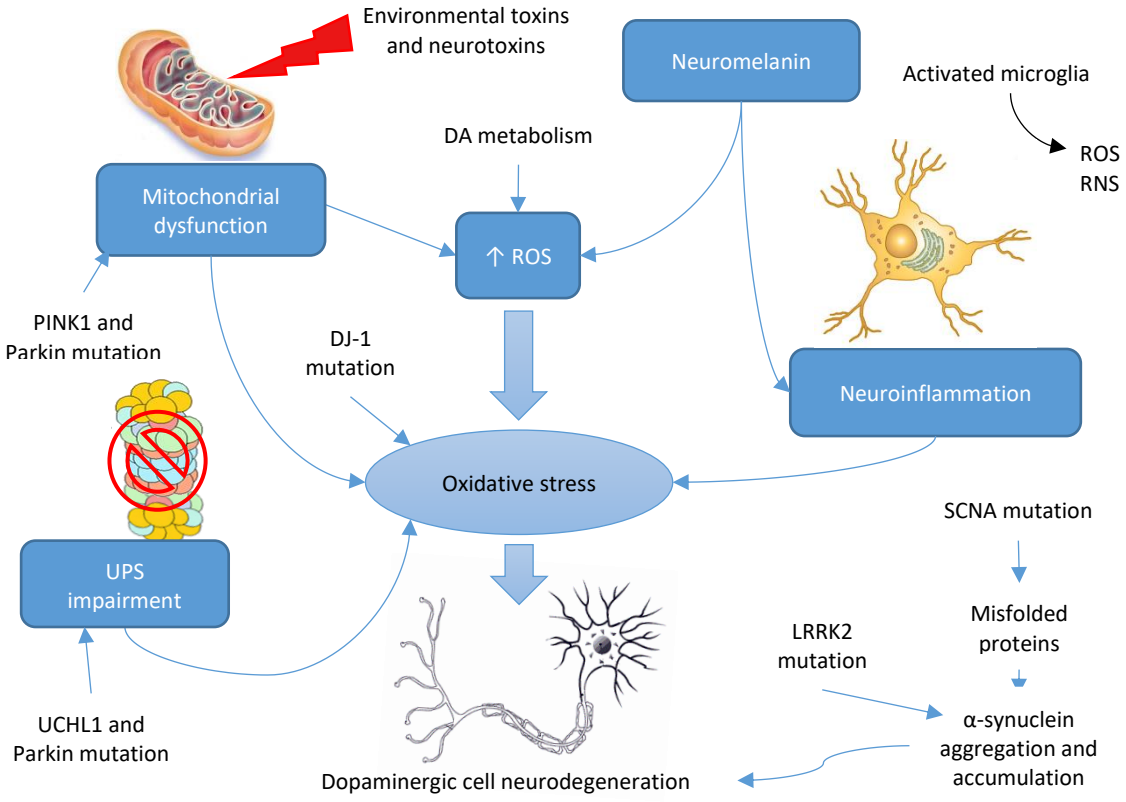

Figure 1.2. Potential physiological factors related to the pathogenesis of Parkinson's disease (PD). There are different pathways in which dysfunction results in genetic modifications in PD-related genes, leading to increased oxidative stress. Mutation of these proteins results in oxidative stress, mitochondrial dysfunction, ubiquitin-proteasome system (UPS) impairment and protein misfolding, affecting cell's integrity. Increased levels of reactive oxygen species (ROS) may also result from dopamine metabolism. Environmental toxins impair mitochondrial function, increase the generation of ROS, and lead to aggregation of proteins, such as α-synuclein and tau. Mitochondrial dysfunction increases oxidative stress and decreases ATP production, leading to cell death. Neuromelanin is involved in the activation of microglial cells and in the production of ROS. At least, neuroinflammatory mechanisms might contribute to the cascade of consequences that lead to cell death.

1.3. Dopamine role in Parkinson's disease

The onset of cerebral function disorders such as neurodegenerative diseases (like PD) and neurological disorders (schizophrenia) are associated with DA metabolism, in particular with a possible disruption in this metabolism. This relation exists because DA metabolism represents an additional source for oxidative stress, once its degradation generates ROS, and investigators considerer that oxidative stress has an important role in the loss of dopaminergic neurons [100]. This idea first came from Arvid Carlsson in 1958, when he discovered that DA is a transmitter present in the brain and that it had a great importance in the capability to control movements. He also developed the first method which allows to determine the concentration of DA in the brain and discovered that this neurotransmitter is found in high concentrations in a specific brain region, closely related to the movement, the basal ganglia. He found out that a depletion of DA induces Parkinson's syndrome and that a treatment with L-DOPA alleviate the symptoms by restoring the dopamine level [101]. Moreover, Paul Greengard and Eric Kandel had important roles for their discoveries about signal transduction in the nervous system [102].

1.3.1. Dopamine biosynthesis

Dopamine (Figure 1.3) is a neurotransmitter from the catecholamine family, formed by a biogenic amine in the aliphatic part and a catechol group at the aromatic, with a special relevance in the CNS [103].

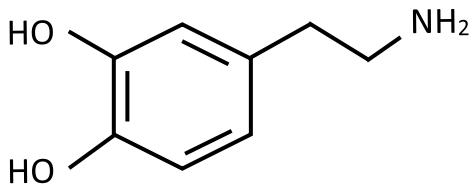

Figure 1.3. Chemical structure of dopamine.

The biosynthesis of DA is a two-step procedure that takes place in the cytosol of neurons and starts with the hydroxylation of the L-tyrosine at the phenol ring, at the *meta* position, by TH, resulting in 3,4-dihydroxy-L-phenylalanine (also known as L-DOPA), being that this is the rate-limited step of the process. This oxidation is strongly regulated and depends on tetrahydrobiopterin (BH4), that acts as cofactor. In the second step of the synthesis, L-DOPA is decarboxylated to DA by aromatic L-amino acid decarboxylase (AADC, also known as DOPA decarboxylase) [103]. This enzyme has a very wide distribution in the body, being found in

catecholaminergic and serotonergic neurons and some non-neuronal tissues (like the kidneys and blood vessels).

Even though the action of DOPA decarboxylase is the last step in the DA biosynthesis, this neurotransmitter also acts as a precursor for the synthesis of other neurotransmitters, such as norepinephrine, which, in turn, is the precursor of epinephrine. Therefore, in the epinephrine-producing neurons, DA is converted to norepinephrine by the enzyme DA beta-hydroxylase (DBH), and then to epinephrine, through the transference of a methyl group by the enzyme phenylethanolamine N-methyltransferase (PNMT) [103].

1.3.1.1. L-tyrosine

L-tyrosine (Figure 1.4) is a non-essential amino acid once under normal conditions the body synthesizes sufficient quantities from phenylalanine. This amino acid can be found in many food products, it is present in fish, soy products, poultry, eggs, almonds, peanuts, sesame seeds, bananas, among others. It is incorporated into proteins of all life forms and it is a precursor for synthesis of thyroxin, melanin, and the neurotransmitters DA and norepinephrine [104]. It can enter the neurons by active transport.

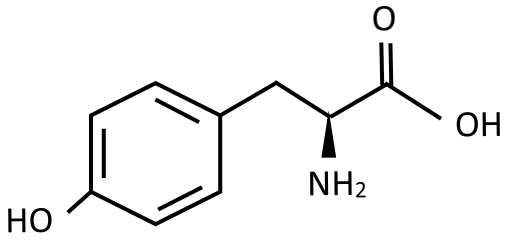

Figure 1.4. Chemical structure of L-tyrosine.

From the numerous mechanisms of action of this amino acid, the most clinically significant is its role as a precursor in DA biosynthesis. However, there are some clinical conditions in which tyrosine supplementation provides a therapeutic benefit, like depression, hypertension, stress, cognitive function and memory, PD, phenylketonuria and narcolepsy. By improving the rate of neurotransmitter synthesis [105], tyrosine stimulates the CNS and acts as an antidepressant [106].

Although the use of L-tyrosine as a clinical therapy in PD is not well understood, there are some studies made on animal models and in live Parkinson's patients that indicate L-tyrosine may be of therapeutic interest [107]. Being so, this amino acid may actually prove to be a better therapy than L-DOPA, once it is usually present in the diet and side effects tend to be minimal [108].

1.3.1.2. Levodopa

The hydroxylation of L-tyrosine in DA biosynthesis leads to the formation of L-DOPA (Figure 1.5), an amino acid and a hormone that is naturally synthesized by some plants and animals.

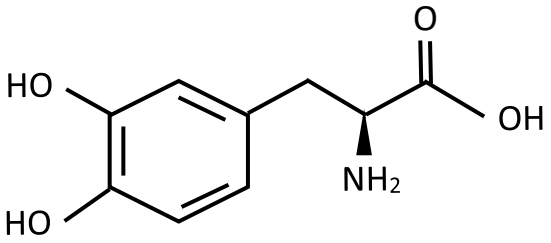

Figure 1.5. Chemical structure of levodopa (L-DOPA).

Besides its involvement in DA biosynthesis, L-DOPA is also a precursor for norepinephrine and epinephrine. In its pure form, it is considered a psychoactive chemical, being used in the treatment of PD and other conditions related to decreased levels of the mentioned neurotransmitters [109].

1.3.2. Dopamine metabolism

When dopaminergic neurons are excited, synaptic vesicles containing DA open and there is exocytosis of the neurotransmitter into the synaptic cleft, being that the molecules will interact with the postsynaptic receptors. However, after the signaling, the extracellular DA present in the synaptic cleft needs to be removed to avoid an over-stimulation of the receptors. This DA can be recycled if it is reuptaken by the dopaminergic neurons or degraded if it is reuptaken by glial cells [103].

Some of the DA that is reuptaken by dopaminergic neurons can be degraded by MAO, a mitochondrial bound isoenzyme, which catalyzes the oxidative deamination of dietary amines, monoamine neurotransmitters and hormones [103]. This degradation is based in the degradation of the monoamine to its correspondent aldehyde, which is then oxidized to acid by aldehyde dehydrogenase (ALDH) or converted into alcohol by aldehyde reductase (ALR) [110]. There are two isoenzymes of MAO, MAO-A and MAO-B, having different affinities for substrates and inhibitors [111]. Although both isoforms exhibit similar affinity for DA, it is though that MAO-A is the main responsible for DA degradation. Oxidative deamination of DA by MAO-B leads to 3,4-dihydroxyphenylacetaldehyde (DOPAL) and H_2O_2 formation. This H_2O_2 is thought to be involved in the progression of some neurological disorders, such as PD, and in the oxidative damage of the mitochondrial membrane [112]. The metabolite formed can suffer reduction to its corresponding

alcohol, 3,4-dihydroxyphenylethanol (DOPET), by ALR, or oxidation to carboxylic acid, 3,4-dihydroxyphenylacetic acid (DOPAC), by ALDH. In this step, the oxidation is the major pathway. Being so, DOPAC can then be metabolized by COMT enzyme, forming HVA, the final degradation product of DA metabolism, released in urine [103].

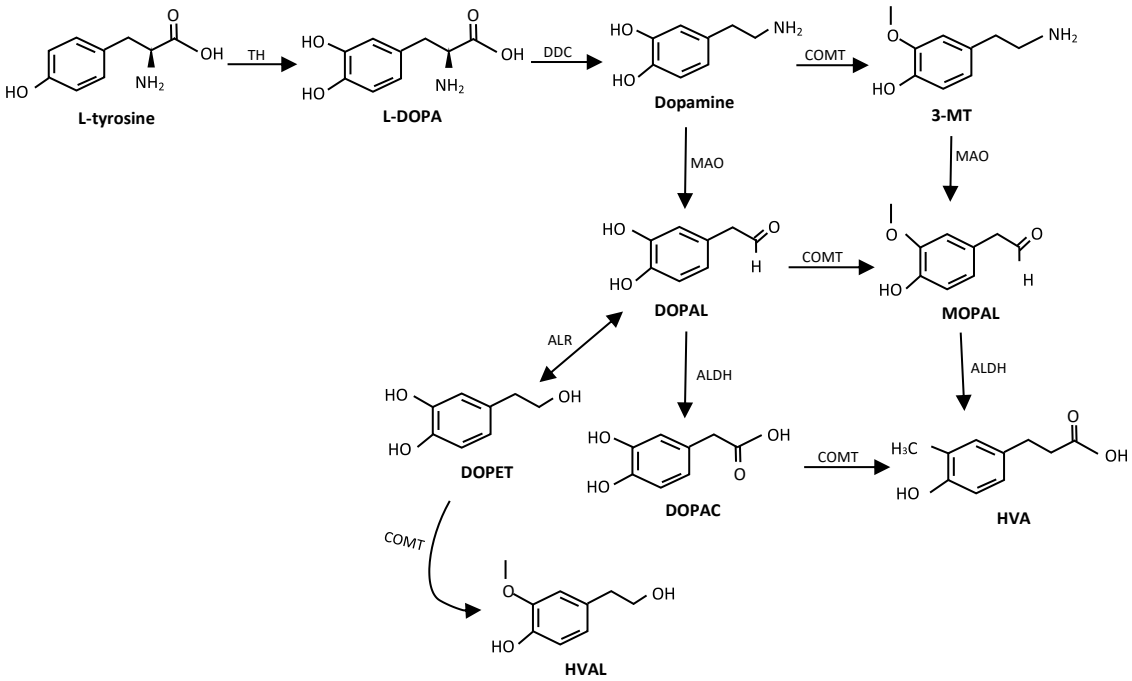

Figure 1.6. Dopamine metabolism. Dopamine is synthetized in the neurons from levodopa (L-DOPA), its direct precursor, which results from L-tyrosine hydroxylation. Then, dopamine is degraded either by monoamine oxidase (MAO) or catechol-*O*-methyl transferase (COMT), resulting in 3-methoxytyramine (3-MT) or 3,4-dihydroxyphenylacetic acid (DOPAC), the main metabolites of dopamine metabolism. The final product is homovanillic acid (HVA), which is then excreted in urine. ALDH - aldehyde dehydrogenase; ALR - aldehyde reductase; DDC - dopa decarboxylase; DOPAL - 3,4-dihydroxyphenylacetaldehyde; DOPET – 3,4-dihydroxyphenylethanol; HVA – homovanillic acid; HVAL – homovanillyl alcohol; MOPAL – 3-methoxy-4-hydroxyphenylacetaldehyde; TH – tyrosine hydroxylase.

DA that is reuptaken by the surrounding glial cells can be degraded by MAO or by COMT. Also, the remaining DA present in the synaptic cleft diffuses into the circulation and is destroyed in the liver, either by MAO and COMT (Figure 1.7).

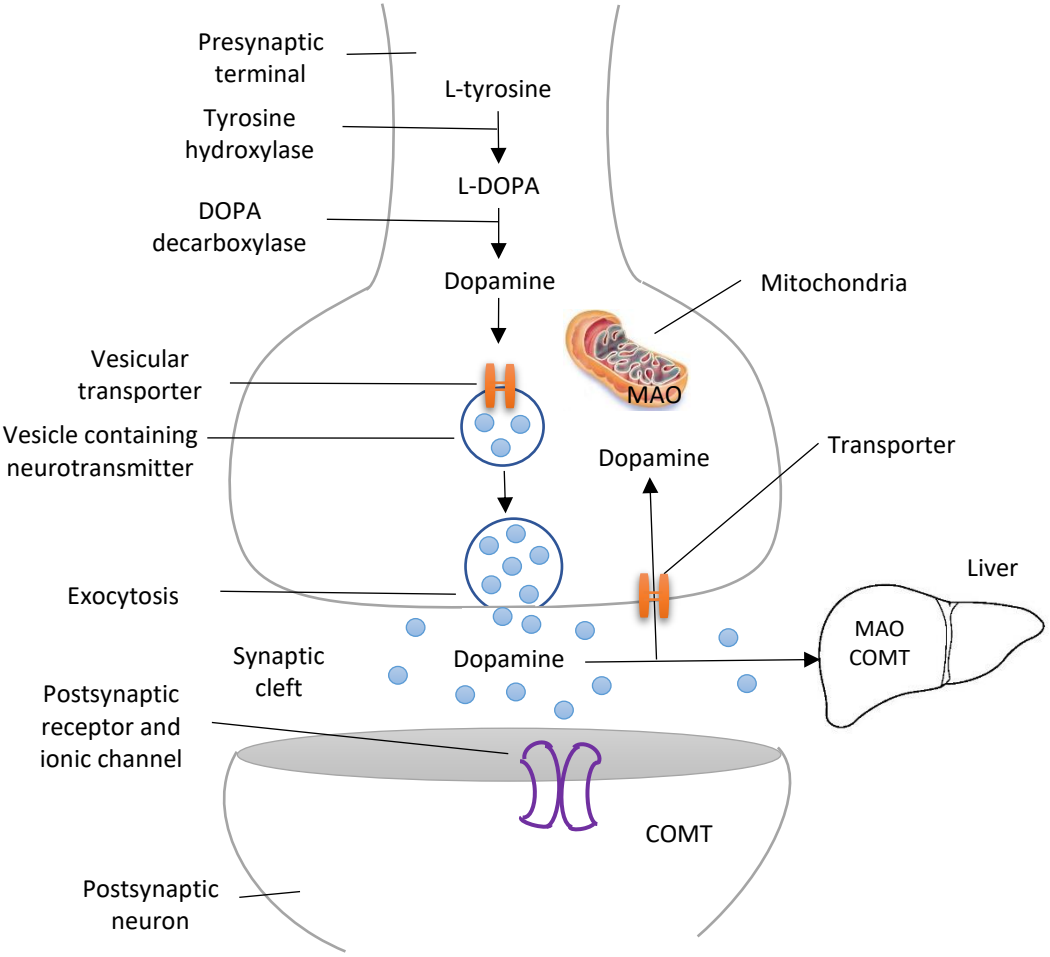

Figure 1.7. Steps involved in the synthesis and release of dopamine. Once synthetized, it is stored in vesicles. When the neuron is excited, it is released into the synaptic cleft. After signaling, it has to be removed, being that it can be recycled or degraded, by glial cells or in the liver by monoamine oxidase (MAO) or catechol-*O* methyl transferase (COMT).

It is important to notice that the oxidative deamination of DA by MAO produces potentially cytotoxic species, such as superoxide and hydroxyl radicals, while the reaction with the enzyme COMT forms no reactive species, and is thought to be a vital antioxidant defense mechanism [113]. Moreover, expression of MAO enzyme is age dependent and its concentration increases in the brain. This increase may contribute to neurodegeneration due to the natural production of ROS [58, 114], which are released into the extracellular environment and, because of its high membrane permeability, can enter the neighboring neuronal cells [115].

Under normal physiological conditions, DA metabolism is responsible for the production of ROS. After being synthetized in dopaminergic neurons or transported into the cell, DA is rapidly stored in the synaptic vesicles, as a protection mechanism against possible deleterious effects of DA auto-oxidation or its presence in high concentrations in the cytoplasm [116].

1.3.2.1. 3-methoxytyramine, 3,4-dihydroxyphenylacetic acid and homovanillic acid

It is known that the concentration of DOPAC and HVA, the major metabolites of DA, in brain samples depends on the rate of neuronal impulse flow in dopaminergic pathways. Treatments which increase impulse flow in such pathways also increase the concentration of DA metabolites in brain regions [117-119] and, likewise, conditions which inhibit impulse flow in dopaminergic pathways decrease the concentration of these metabolites in brain regions. On the other hand, the concentration of brain DA is more resistant to change, even under conditions that rapidly changes its release. Also, there are evidences that suggest that these metabolites present in the plasma derive, in part, from DA-rich areas of the brain, and that any changes in the brain concentration of these metabolites results in parallel changes in the plasma [120]. Therefore, measurements of DA metabolites in the plasma may reflect their concentration in the brain and provide a more reliable guide of dopaminergic cell activity, when compared with those obtained with measurements of DA levels. HVA is produced in the human body and it has been found in the plasma [121], cerebrospinal fluid [122] and urine [103].

1.3.3. Peripheral synthesis of dopamine

Despite the fact that DA plays a vital role as a neurotransmitter in the brain, a significant part of the total DA present in the body is produced outside the brain in mesenteric organs [103]. Also, besides being a neurotransmitter of the autonomic nervous system, it has an important role in physiological regulation outside the CNS, with effects in the kidney and gastrointestinal tract (Figure 1.8) [123].

In pharmacological doses, DA is a potent natriuretic and vasodilator agent. The mechanisms of this natriuretic action appear to be multiple: DA increases renal plasma flow and glomerular filtration rate, induces redistribution of internal blood flow [124] and increases sodium excretion [125]. It was also showed that a suppressor of DA had a greater vasodilator action on renal medullary blood flow than in cortical blood flow, supposing that the action in the renal medulla may contribute to the diuretic and natriuretic action of DA [124]. The kidney is a source of DOPA decarboxylase, an enzyme located in the proximal and distal tubules. Therefore, the main source of renal and urinary DA is L-DOPA, that reaches the kidney through the renal circulation.

DA in the gastrointestinal tract is an important enteric neuromodulator, stimulates exocrine secretions, inhibits gut motility, modulates sodium absorption and mucosal blood flow and is protective against gastroduodenal ulcer disease [126, 127]. Here, the main source of L-DOPA for

posterior DA synthesis is not the blood flow but the ingested food, since, as already mentioned, there are numerous foods rich in L-tyrosine, which is converted to L-DOPA and, subsequently, to DA.

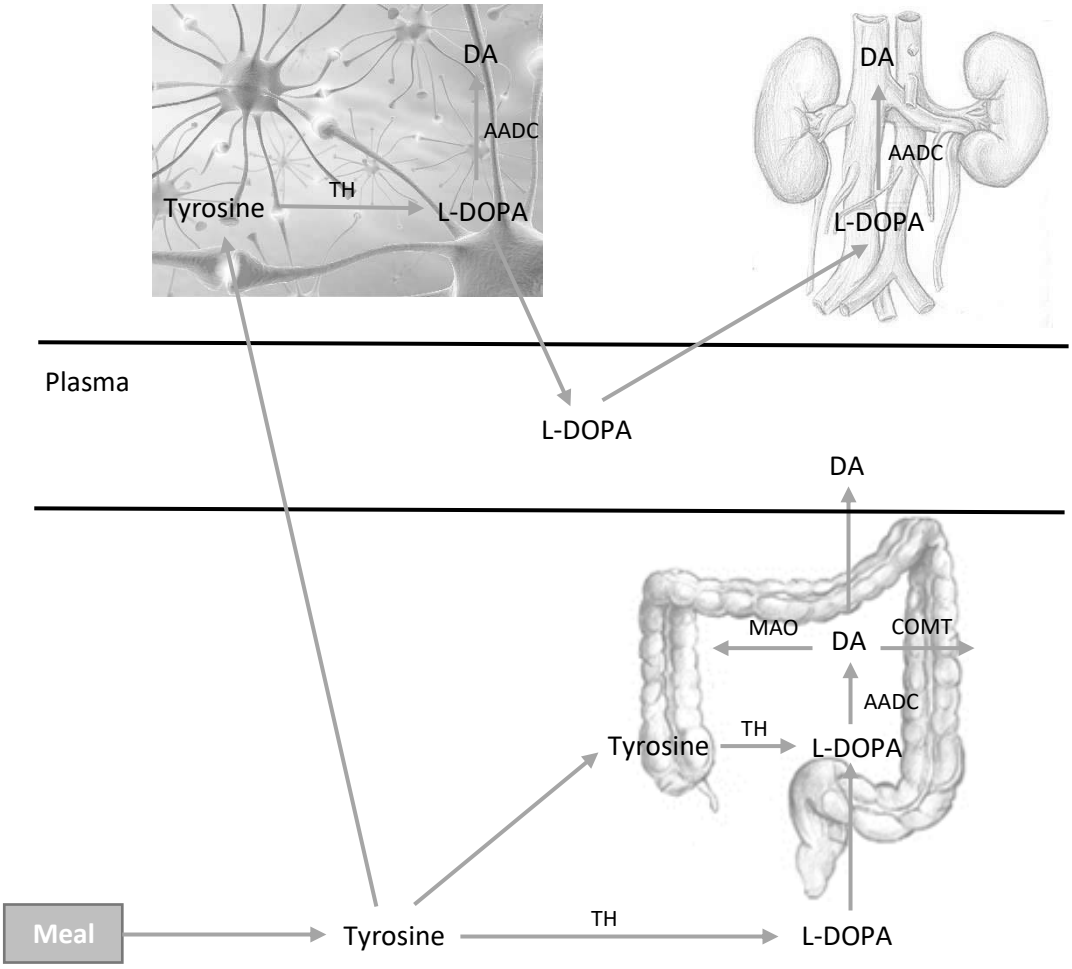

Figure 1.8. Peripheral synthesis of dopamine. The ingested food is the main source of tyrosine, being converted into levodopa (L-DOPA) in the gut wall by tyrosine hydroxylase (TH), and then converted into dopamine (DA) by aromatic L-amino acid decarboxylase (AADC). Tyrosine can also be converted into DA in the dopaminergic neurons. The kidneys use L-DOPA present in the plasma, that reaches the kidneys through the renal circulation, and convert it to DA by AADC. Adapted from: [128].

2. Analytical methodologies

2.1. Analytical methodologies for sample preparation

An appropriate sample preparation is essential to obtain reliable results in many fields, such as biomedical analysis. Therefore, it is essential to make a biological sample suitable for the selected method for the quantification of the analytes of interest, without the interference of other components, to obtain reliable results [129]. Moreover, the operator must know the chemistry of the analyte, the biological matrix being study, and the detection method used, in order to choose the best method of separation, as well as the optimal conditions of separation.

This process is a major step with an important relevance in the development of a method, once most of the samples used in the study of metabolites, biomarkers, or even some drugs are present in biological matrices that contain a large amount of proteins and other organic and inorganic compounds. Therefore, sample preparation is specific to the sample matrix. For example, plasma is frequently used as an experimental material to start with because it is easy to collect. Therefore, before performing bioanalysis that include chromatographic separation, the sample preparation is essential to remove or reduce the number of lipids and proteins, to ensure compatibility for the subsequent separation and detection, and to remove endogenous compounds [129]. This process is important due to the fact that lipids and proteins affect the ability to quantify the analyte, interfere with most detectors, with the retention time, or can affect the sensibility of the method. In analysis with mass spectrometry detection, lipids can contribute to ion suppression, generating background “noise” and to some matrix effects [130]. Besides, this process also aims to concentrate the analyte to achieve adequate signal intensities, decreasing lower limits of quantification, and to avoid saturation effects of detection and non-linearity [131].

In terms of the existing sample preparation technologies, these include pre-extraction and post-extraction sample processing, such as protein precipitation (PPT), liquid-liquid extraction (LLE), and solid-phase extraction (SPE).

2.1.1. Sample preparation of plasma

2.1.1.1. Protein precipitation

Protein precipitation is commonly used as a method of sample preparation, allowing the removal of proteins in samples for downstream analysis. For example, in the analysis of blood samples, proteins must be eliminated, otherwise they may absorb in the column and interfere with the analysis. One advantage of protein precipitation is the fact that it is considered the simplest sample preparation approach in the study of biological fluids [132]. In chromatographic analysis, this step improves the reproducibility and sensitivity of the analysis and protects the chromatographic column. Among the different methods for protein precipitation there is salting out, isoelectric point precipitation and precipitation with organic solvents [133].

The basic theory of protein precipitation relies on the interaction between the reagent and the proteins present in the matrix. As reagent, it can either be used an organic solvent (usually acetonitrile, methanol, isopropanol, or acetone) or an acid, such as the trichloroacetic acid (TCA) or perchloric acid [129].

Protein precipitation with a miscible organic solvent is the most convenient technique of sample preparation of complex matrices, such as the plasma, because of its low cost and has minimal method development requirements, even when compared with SPE and LLE procedures [134]. The procedure begins with the addition of a volume of the precipitant (organic solvent) three or four times the volume to the biological sample, which should then be agitated to homogenize the mixture. After that, the sample is centrifuged for several minutes, leading to the separation of the organic solvent layer (supernatant), which contains the analyte, from the protein aggregate (pellet). Before the centrifugation, the mixture may be refrigerated to improve the efficiency of protein removal [129].

In some approaches, an isotope-labeled internal standard can be used to account for sample lost and help overcome matrix effects during sample preparation and analysis [129, 132]. In these cases, there is the possibility to add the solution of internal standard and the organic solvent that will be used as precipitant as a single solution [129].

However, this method has the disadvantage of not allowing to concentrate the analyte, instead, it allows a dilution of the solution [131].

2.2. Techniques

Plasma concentrations of catecholamines (and metabolites), in general, are often useful for the diagnosis of psychiatric and neurological disorders, as well as in the development of new possible treatments [121, 135]. For example, a dysregulation in DA metabolism is related with PD, making DA detection and quantification in biological fluids a subject of growing interest from a clinical perspective. Thus, there has been a continuous interest in the development of new and improved analytical methodologies for quantitative determinations of these compounds in a variety of biological fluids, including plasma, blood, urine and cerebrospinal fluid [136]. Although several reports have been made in the last years, a quantitative analysis of DA, as well as its metabolites, has inherent challenges, like its physiological levels (pg/ml), complex matrix interferences, the chemical instability of these compounds and the potential tendency of catechol group oxidation [121, 137].

In this field, high-performance liquid chromatography (HPLC) and capillary electrophoresis coupled with various detection methods, such as ultraviolet (UV) detection [135, 138], fluorescence detection (FD) [139, 140], electrochemical detection (ECD) [141-151], and mass spectrometry (MS) [121, 136, 137, 152, 153] have been widely explored. However, besides all the developed methods, all of them present some limitations, for instance insufficient sensitivity and difficult sample preparation.

Nowadays, high-performance liquid chromatography coupled to mass spectrometry (HPLC-MS) has become the method of choice in these analyses due to the need of using a highly sensitive analytical technique, capable to detect the low levels present in samples. This is a powerful technique that offers excellent specificity and sensitivity. However, when analyzing biological samples by MS, some interfering peaks may occur in the low mass-to-charge (m/z) region [154]. More recently, some liquid chromatography coupled to mass spectrometry (LC-MS) methods have adopted tandem mass spectrometry because of its high selectivity [155].

Some of the most relevant reports regarding the quantitative detection of DA metabolism in plasma samples during the past few years are summarized in Table 2.1. During the collection of information about the existing methods for identification and quantification of these compounds, the opportunity to write a review article arose.

Table 2.1. Methods for the determination of catecholamines in plasma samples.

Substance	Sample volume (mL); matrix	Separation and detection	Derivatization step	Run time (min)	Linearity (ng/mL)*	LOD (ng/mL); LOQ (ng/mL)*	Reference
L-DOPA, NE, E, DA, NM, M, 3-MT, DOPAC, HVA, DOPEG, MOPEG, MOPET, DOMA, VMA	0.7; HP	HPLC-FD	Yes	100	2.0-1000 pmol (L-DOPA) 0.2-200 pmol (NE, E, DA, NM, M, 3-MT, DOPAC, HVA, DOPEG, MOPEG, MOPET) 10-3000 pmol (DOMA, VMA)	1.97; - (L-DOPA) 0.10; - (NE) 0.085; - (DOPEG) 0.18; - (E, NM, MOPEG) 0.56; - (DA) 0.59; - (M) 0.50; - (3-MT, DOPAC, MOPET) 0.55; - (HVA) 18.42; - (DOMA) 19.82; - (VMA)	[156]
DA	0.2; HP	UPLC-MS/MS	Yes	≥7	0.01-1.0	-; 0.01	[121]
Free and total DA	0.1; HP	LC-MS/MS	Yes	≥5	0.05-20	-; 0.05 (free DA)	[153]
L-DOPA, DA	0.1; RP	LC-MS/MS	No	≥4	2.5-1000	-; 2.5	[136]
DA, DOPAC, HVA, NE, VMA, MHPG, 5-HT, 5-HIAA, Glu, GABA	0.3; HP	LC-MS/MS	Yes	27	0.17-49.94 (DA) 0.17-49.94 (DOPAC) 0.16-49.91 (HVA) 0.02-50.01 (NE) 0.16-49.94 (VMA) 0.21-62.93 (MHPG) 0.16-50.05 (5-HT) 0.17-50.10 (5-HIAA) 1.34 $x10^3$-3.97$x10^3$ (Glu) 20.63-6.0 $x10^3$ (GABA)	-; 0.087 (DA) -; 0.062 (DOPAC) -; 0.064 (HVA) -; 0.068 (NE) -; 0.069 (VMA) -; 0.21 (MHPG) -; 0.046 (5-HT) -; 0.082 (5-HIAA) -; 0.10 (Glu) -; 0.17 (GABA)	[152]
NE, E and DA	0.25; HP	UPLC-MS/MS	No	2	0.0022-0.27 (E) 0.0083-1.06 (NE) 0.031-0.39 (DA	0.02; 0.04 (NE) 0.005.5; 0.0092 (E) 0.0077; 0.02 (DA)	[137]
NE, E, DA, L-DOPA, 5-HT	1; P	MEKC-UV	No	-	-	125.19; - (NE) 124.58; - (E) 125.61; - (DA) 177.47; - (L-DOPA) 125.12; - (5-HT)	[135]

Table 2.1. Methods for the determination of catecholamines in plasma samples (cont.).

Substance	Sample volume (mL); matrix	Separation and detection	Derivatization step	Run time (min)	Linearity (ng/mL)*	LOD (ng/mL); LOQ (ng/mL)*	Reference
NE, E and DA	1; RP	HPLC-UV	No	≥15	$6.25 \times 10^5 – 5.0 \times 10^6$	-; 1.56×10^5	[138]
NE, E and DA	-; HP and SP	HPLC-ECD	No	≥10	HP: 0.03-0.2 SP: 0.03-0.18	0.025; - (NE) 0.01; - (E) 0.005; - (DA)	[141]
NE, E and DA	0.25; HP	HPLC-AD	No	11	0-10 (NE) 0-5.0 (E) 0-72 (DA)	0.0035; - (NE) 8.7×10^{-4}; - (E) 0.0083; - (DA)	[147]
NE, E and DA	1; HP	HPLC-AD	No	25	0.025-1.0	0.0057-0.0069; - (NE) 0.0074-0.011; - (E) 0.011-0.017; - (DA)	[151]
NE, E, DA and	0.1-0.5; HP, RP	HPLC-ECD	No	10	20-400	< 10 pg; -	[144]
L-DOPA and carbidopa	0.9; DP	HPLC-AD	No	≥10	10-2000 (L-DOPA) 5.0-250 (Carbidopa)	0.3; - (L-DOPA) 1.5; - (Carbidopa)	[146]
L-DOPA and carbidopa	1; HP	HPLC-AD	No	12	5.0-500	-; 5.0	[150]
L-DOPA, carbidopa, 3-OMD and DA	1; HP	HPLC-AD	No	12	25-2000	15; - (DA)	[149]
L-DOPA, 3-OMD, DOPAC, DA, carbidopa	0.5; HP	HPLC-ECD	No	20	-	-; 4.0 (L-DOPA) -; 5.0 (3-OMD) -; 5.0 (DOPAC) -; 5.0 (DA) -; 40 (Carbidopa)	[142]
DOPA, NE, E, DA, DOPAC and DHPG	-; HP	LC-ECD	No	≥30	50-2000 pg (DHPG)	15 pg; - (L-DOPA) 6.0 pg; - (NE) 10 pg; - (E) 14 pg; - (DA) 18 pg; - (DOPAC) 6.0 pg; - (DHPG)	[143]

Table 2.1. Methods for the determination of catecholamines in plasma samples (cont.).

Substance	Sample volume (mL); matrix	Separation and detection	Derivatization step	Run time (min)	Linearity (ng/mL)*	LOD (ng/mL); LOQ (ng/mL)*	Reference
LDME, L-DOPA, DA, 3-OMD	0.5; RP and HP	HPLC-CD	No	35	30-1000 (LDME, L-DOPA, DA) 60-2000 (3-OMD)	-; 9.7 (LDME) -; 19.6 (L-DOPA) -; 2.9 (DA) -; 47.2 (3-OMD)	[145]
5-HT, 5-HIAA, HVA, DOPAC	0.1; HP	MHPLC-AD	No	10	5-20 pg	0.1-0.5 pg; -	[148]
NE, E and DA	1; HP	HPLC-FD	Yes	15	0.01-10	6×10^{-4}; - (NE) 9×10^{-4}; - (E) 0.002; - (DA)	[139]
NE, E and DA	0.5; HP	HPLC-FD	Yes	≥8	0.02-10 pmol	1.18×10^{-3}; NR (NE) 1.28×10^{-3}; NR (E) 1.53×10^{-3}; NR (DA)	[140]
NE, E and DA	0.5; HP	HPLC-CD	No	≥9	0.04-1.6 (5 nA full scale); 0.2-30 (50 nA full scale)	0.012-0.04	[157]
NE, E and DA	0.5; P	LC-AD	No	≥20	0.06-3.00	0.03-0.06	[158]
NE, E and DA	0.01; RP	LC-CLD	Yes	35	5.0-500 fmol	0.91 fmol; 3.0 fmol (NE) 0.36 fmol; 1.2 fmol (E) 1.1 fmol; 3.7 fmol (DA)	[159]

Abbreviations AD – amperometric detection; CD – coulometric detection; CLD – chemiluminescence detection; DA – dopamine; DHBA – 3,4-dihydroxybenzylamine; DHPG – dihydroxyphenyiglycol; DOMA - 3,4-dihydroxymandelic acid; DOPA – dihydroxyphenylalanine; DOPAC – 3,4-dihydroxyphenylacetic acid; DOPEG – 3,4-dihydroxyphenylethyleneglycol; DP – dog plasma; E – epinephrine; ECD – electrochemical detection; FD – fluorescence detection; GABA – Ɣ-aminobutyric acid; Glu – glutamate; 5-HIAA – 5-hydroxyindole-3-acetic acid; HP – human plasma; HPLC – high-performance liquid chromatography; 5-HT – 5-hydroxytryptamine; HVA – homovanillic acid; LC – liquid chromatography; LDME – levodopa methyl ester; L-DOPA – levodopa; M – metanephrine; MEKC – micellar electrokinetic chromatography; MHPG – 3-methoxy-4-hydroxyphenylglycol; MOPEG – 4-hydroxy-3-methoxyphenylethyleneglycol; MOPET – 4-hydroxy-3-methoxyphenylethanol; MS/MS – tandem mass spectrometry; 3-MT – 3-methoxytyramine; NE – norepinephrine; NM – normetanephrine; 3-OMD – 3-*O*-methyldopa; P – plasma; rP – rabbit plasma; RP – rat plasma; SP – swine plasma; ST – serotonin creatinine; UPLC – ultraperformance liquid chromatography; UV – ultraviolet; VMA – vanillymandelic acid.

2.2.1. Chromatography

Chromatography is a method of separation and identification used to separate a mixture of chemical substances into its individual components, so that these can be thoroughly analyzed, wherein the separation depends on the distribution of different molecules between two phases: a stationary phase and a mobile phase [160]. Because of the simplicity in effecting the separation and identification of the chemical species, chromatography occupies a prominent place among the methods used for chemical analysis and it may be used alone or in conjunction with other instrumental analysis techniques. This method can be useful in the identification of compounds, in the purification of the compounds, separating undesired substances, and in the separation of all the different components present in a mixture, so they can be quantified.

There are numerous possibilities of stationary and mobile phase combinations that can be used in the chromatographic separation of a complex mixture, and so we can distinguish the different types of chromatography based on the physical states of these phases.

2.2.1.1. High-performance liquid chromatography

Liquid chromatography (LC) is an analytical chromatographic method in which the mobile phase is liquid, not limited to only volatile and thermally stable samples, like in the case of GC analysis [161]. The basis of LC analysis is that the separation occurs according to the mechanism of interaction between the molecules and the stationary phase, after being inserted into the column. The different components of the sample will present different degrees of interaction with the stationary phase, eluting at different speeds as the solvent flows. This process leads to the separation of the components, which elute at different times (Figure 2.1) [162]. The components that have a stronger adhesion to the stationary phase will elute at a slower speed than those with a weaker adhesion. In the end of the process a chromatogram is obtained, which is then analyzed in order to quantify the analytes present in the eluate. Each one of the distinct peaks represents one of the components separated by the chromatographic column [162], and the area under each curve corresponds to the amount of that component in the analyzed sample.

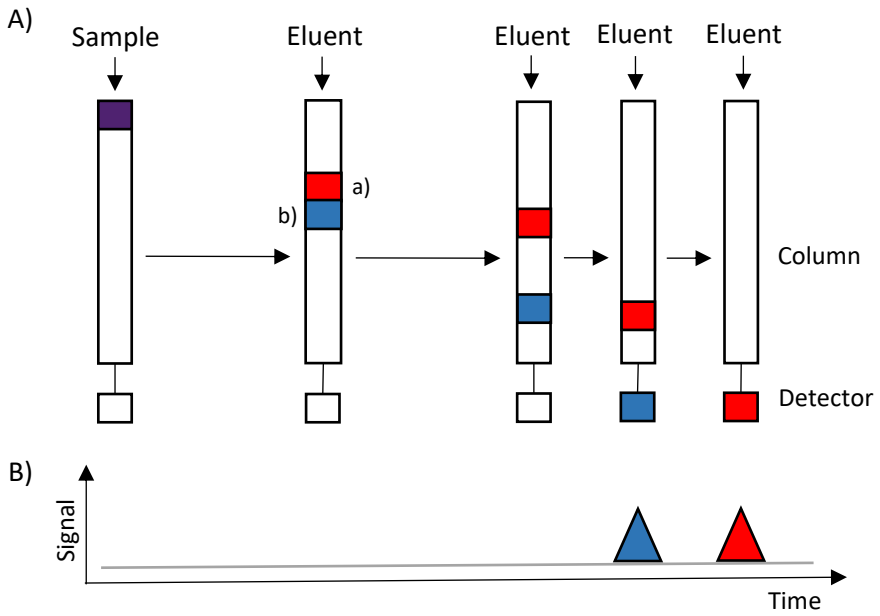

Figure 2.1. Schematic illustration of a chromatographic separation of two components (a and b). The analyte is loaded into the column and the solvent (mobile phase) is added. The components start to separate out as distinct bands according to them interaction with the stationary phase (matrix), being detected at different times. Adapted from [163].

Chromatography systems are defined by their pressure characteristics and in LC low pressure liquid chromatography (LPLC) can be distinguished from HPLC. While LPLC is used to separate molecules that do not require high resolution, HPLC allows a high efficiency in the separation process.

The use of HPLC, considered an expansion of the classic technique, is characterized by the use of narrowed stainless steel columns and smaller particle size for the column packing material [163, 164], resulting in a greater surface area for interactions between the stationary phase and the molecules, allowing a better separation of the components. In HPLC analysis, the mobile phase circulates at a high pressure through the chromatographic column, forcing the solvent to pass through, providing faster analysis [165]. In these analysis, the presence of the bands can be detected through different instrumental analysis techniques, such as ultraviolet-visible (UV-VIS) spectroscopy or MS.

This technique is considered one of the most efficient chromatographic methods, face to the development of automatized instrumentation, that allows the injection of sample volumes increasingly smaller and the detection of lower quantities of the analyte. It has the capability to separate and identify compounds that are present in the sample matrix in trace concentrations.

When comparing it with gas chromatography (GC), this technique is complementary when it comes to the type of samples that are separated, once GC only separates volatile and thermally stable compounds. It also presents an advantage in analytes with lower retention time, provides

a higher number of chromatographic analysis by unit of time and involves the use of lower quantity of mobile phase, allowing the use of toxic solvents [163]. However, as other techniques, it presents some disadvantages, for instance, the fact that the equipment and its maintenance are expensive and complex, its low sensibility to some components, and is dependent on the operator experience.

Due to the numerous advantages the method presents it can be applied in both qualitative and quantitative analysis. In qualitative analysis, the most common parameter used to identify the analyte is its retention time (time that it takes to elute from the column after the injection), as well as its chemical structure or molecular weight, depending on the detector used. The identification of the peaks is followed by the quantification of each compound (quantitative analysis), which is accomplished by the use of peak areas or heights.

An HPLC system basically consists in four main components: a high pressure pump, a sample injection device, a chromatographic column and a detector (Figure 2.2) [165]. The pump is essential to force solvents through packed stationary phase beds, by providing a constant and continuous flow of the mobile phase through the HPLC system [166]. When it comes to the injector, in HPLC analysis the loop injector is used to introduce the sample into a flowing liquid stream [162]. In what concerns the detector, there is a wide variety that can be coupled with HPLC, such as the UV, MS, FD or ECD, whose choice depends on the type of analysis (qualitative or quantitative) [165]. Besides the main components, there is also a solvent reservoir, which stores HPLC solvents for a continuous operation of the system. It is important to notice that it is used a computer-based system to control the parameters of the HPLC instrument (temperature, eluent composition, injection sequence) and to acquire the data from the detector [166].

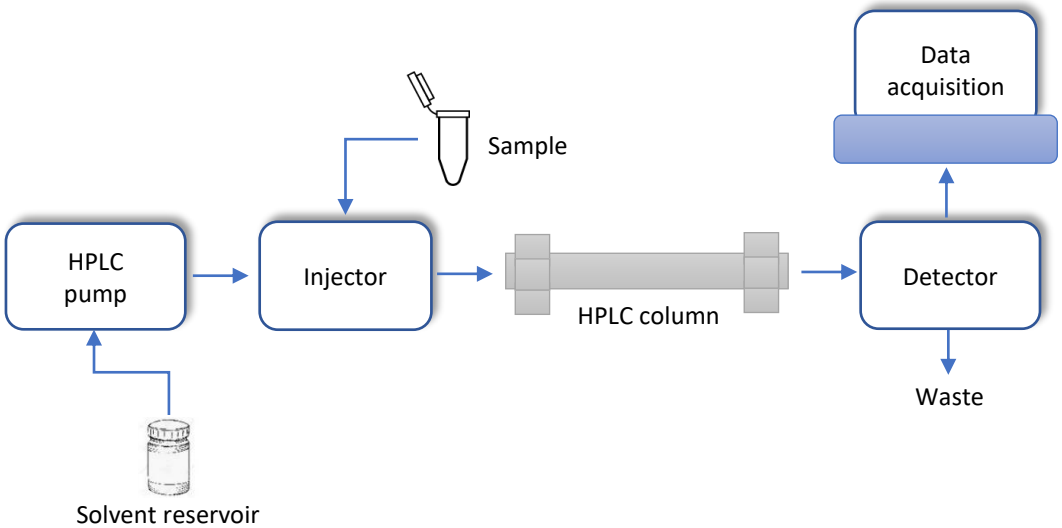

Figure 2.2. Components of an HPLC system. The basic components of an HPLC system include solvent reservoir (HPLC solvents), high-pressure pump, sample injector valve, analytical column, detector, data acquisition system, and waste reservoir.

The correct selection of the column packing and the mobile phase are the most important factors in successful HPLC. Therefore, HPLC can be divided into two mains groups: normal phase liquid chromatography and reversed phase liquid chromatography.

A normal phase chromatography is characterized by a high polarity of the stationary phase (usually silica) and the lower polarity of the mobile phase. In normal phase chromatography, there is a very non-polar environment, where hydrophilic molecules tend to associate with each other. In this case, the stationary phase is polar and the more polar solutes strongly adhere to the stationary phase, leading to less polar components being eluted faster than the more polar [163]. The silica functional group is the hydroxyl group (-OH), which interacts with the polar groups of the analyte through electronic attraction between the atoms. It is a very powerful technique that often requires non-polar solvents [162].

In reversed phase chromatography, the polarities of the mobile and stationary phases are opposite to those in normal phase chromatography, resulting in the adsorption of hydrophobic molecules in a hydrophobic column [166]. This technique is more versatile, being the most used in HPLC analysis. Here, the stationary phase is more hydrophobic than the mobile phase, resulting in a strong retention of the hydrophobic analytes, allowing the more polar compounds to be eluted first [165], and the following components are eluted in decreasing order of polarity. The more hydrophobic molecules will have a stronger interaction with the column, and so, they will need higher concentration of organic solvent to be eluted. When it comes to the functional groups, they usually present a low polarity, being C18 and C8 the most popular [162]. The chromatographic column packing will influence the resolution and efficiency. Usually, most HPLC analysis are made by reversed phase chromatography, due to its high application field.

2.2.2. Mass spectrometry

The MS is a sensitive analytical technique used to identify and quantify molecules in simple and complex mixtures based on their ions m/z ratio [167]. An advantage of this method is that it can be used with small quantities or low concentrations in chemically complex mixtures, due to its high sensitivity. Besides, it also provides quantitative information with high accuracy [165]. This method has become a fundamental tool in a wide range of fields, being the most widely used detector in LC analysis.

A mass spectrometer has three basic components: a source of ionization (convert sample molecules into gas phase ions), one or several mass analyzer(s) (sorts the ions by their m/z ratio) and a detector (quantify the ions) (Figure 2.3) [168]. Upon detection, the signal is processed and presented as a mass spectrum.

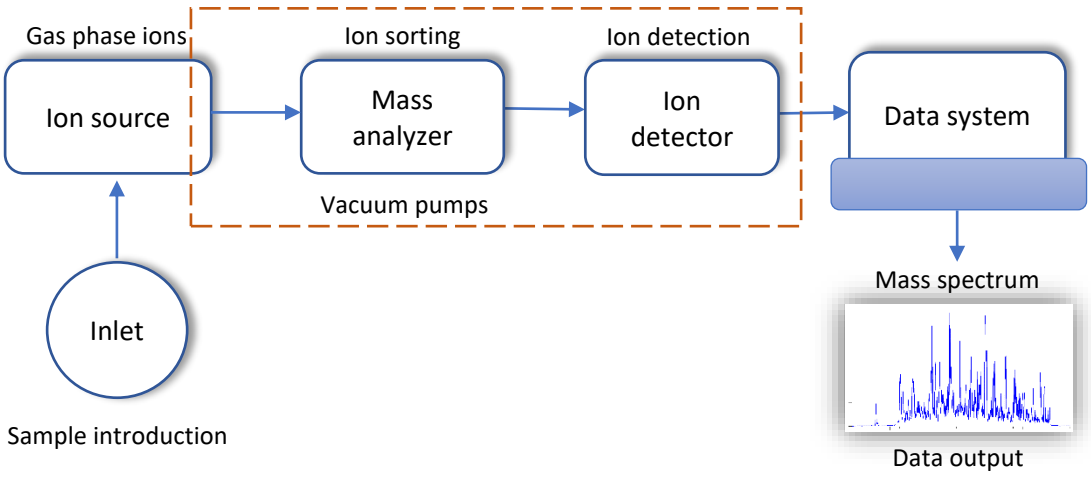

Figure 2.3. Scheme of a mass spectrometer, showing its main components. A mass spectrometry analysis starts with the production of ions from the sample in the ionization source, which are separated according to their mass-to-charge (m/z) ratio in the mass analyzer. The ions are then detected electronically and the resulting information is stored and analyzed in a computer. Adapted from [169].

The first step in a mass spectrometry analysis is the ionization process, leading to formation of gas phase ions from the sample. Once inside the mass spectrometer, the presence of a pressure gradient and voltage allows to accelerate and direct the ions along its route, reaching the detector that detect them qualitatively and quantitatively by their respective m/z ratios and abundance [164].

To associate MS with chromatographic techniques it is necessary to use an interface, in order to remove the mobile phase and ionize the analyte. Among the ionization methods there are electron ionization (EI), chemical ionization (CI), thermospray (TSP), fast-atom bombardment (FAB), electrospray (ESI) and atmospheric pressure chemical ionization (APCI) [165].

Electrospray, the method presented in Figure 2.4, is a soft technique, used in the analysis of thermally labile compounds, that leads to a low quantity of ions which helps to identify the analytes in study and it can be used in the positive or negative mode [170]. It has become one of the most used ionization techniques, due to its versatility, ease of use and efficacy in biomolecules studies. This involves the application of a high electrical potential, under atmospheric pressure, in a liquid sample flowing through a capillary [168]. In the positive mode, the electric field at the tip of the capillary acts on the ions in solution and positive ions migrate toward the tip of the capillary, forming a drop enriched of positive ions. As the charge density increases in the droplet, the electric field formed between the capillary and counter electrode increases causing droplet deformation [167]. Electrostatic forces acting on the positive ions lead to the formation of the "Taylor cone", and when this forces exceeds surface tension, a spray of droplets with high charge density is ejected from the tip of the cone to the counter electrode [171]. After the release of the droplets

from the "Taylor cone", they pass through the area between the tip of the capillary and the counter electrode and are undergoing desolvation [167]. As the droplet loses solvent, the charge density increases to a point where the repulsion forces overcome the surface tension and the droplets are released by the fission of the initial drop [164, 171]. The fissions and evaporation of the charged droplets results in the formation of desolvated ions that are transmitted to the opening of the mass spectrometer [164].

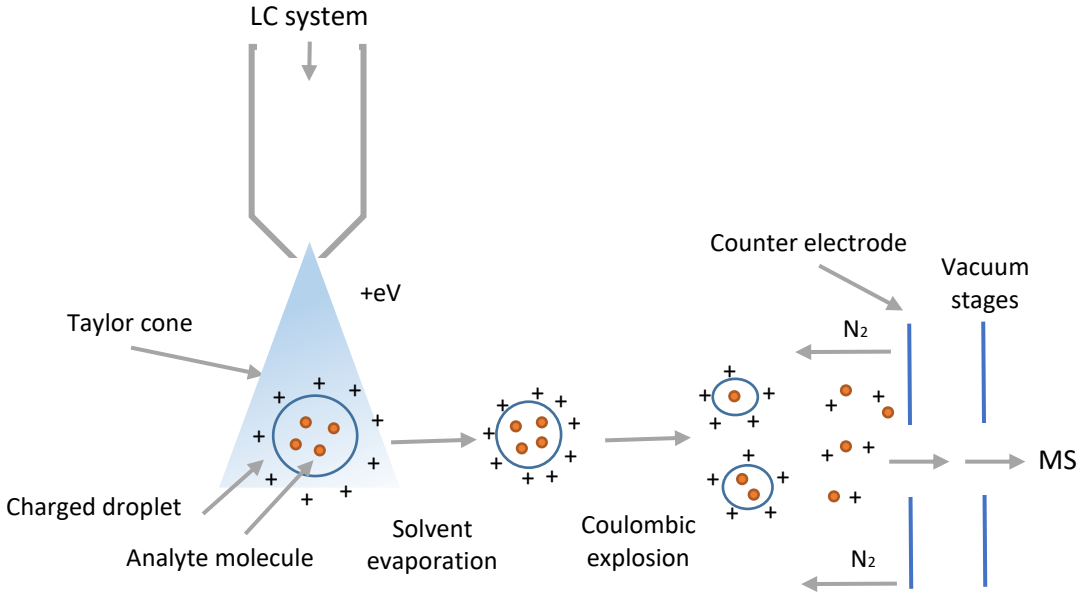

Figure 2.4. Mechanism of ion formation in electrospray ionization (ESI). The sample introduced into the capillary tube is pressurized and subjected to a high potential, giving rise to the Taylor cone. After evaporation of the solvent, the Rayleigh limit is reached, leading to Coulombic explosions, transforming the liquid into small droplets that flow into the mass spectrometer. Adapted from [171].

Once ions are very reactive and short-lived, their formation and analysis must be conducted in a vacuum. Also, this allows ions to reach the detector without undergoing collisions with other gaseous molecules, otherwise there would be a deviation of the ions trajectory and a loss of charge due to collisions against the instrument [168]. Besides separating the ions present in the sample in analysis, mass analyzers can also act as a mass filter and deflect ions with a specific m/z ratio. Among the several mass analyzers available, the most common are time-of-flight (TOF), quadrupole and ion trap, being that each type has its specific characteristics [172].

Using a mass spectrometer as a chromatographic detector presents considerable advantages to the analysis. One advantage is that it can provide an absolute identification, once it offers not only the molecular weight of the analyte but also some structural information [165]. When analyzing complex and/or liquid samples, LC is commonly used for pre-MS complexity reduction. In this analysis, the chromatographic peaks generated by the separated components are individually introduced in the ionization source of the mass spectrometer to generate the ions

that will posteriorly be separated, detected and quantified. While LC-MS is typically applied in the analysis of thermally unstable and nonvolatile molecules, GC-MS is used in the analysis of volatile and semi-volatile samples [173]. However, HPLC is the separation method of choice in the study of biological samples by MS, once most of the biological samples are liquid or nonvolatile and it allows faster analysis.

Given the wide range of sources, there is a large number of mass analyzers that have been developed [168]. From all the different mass analyzers, the quadrupole (Figure 2.5) is the most used. This mass analyzer uses the stability of the trajectories in the electric field to separate the ions according to their m/z ratios [168]. The quadrupole comprises four electrodes arranged in two opposite pairs. One pair of rods is maintained at a positive potential, while the other is kept at a negative potential, and it is applied to the cylinders a combination of continuous and radiofrequency current [169, 170]. The pair of positive cylinder acts as a filter for higher mass, and the negative pair for small masses [169]. Within the quadrupole, ions that do not present the specific m/z ratio, have an unstable trajectory and collides with the walls of the quadrupole, not being detected.

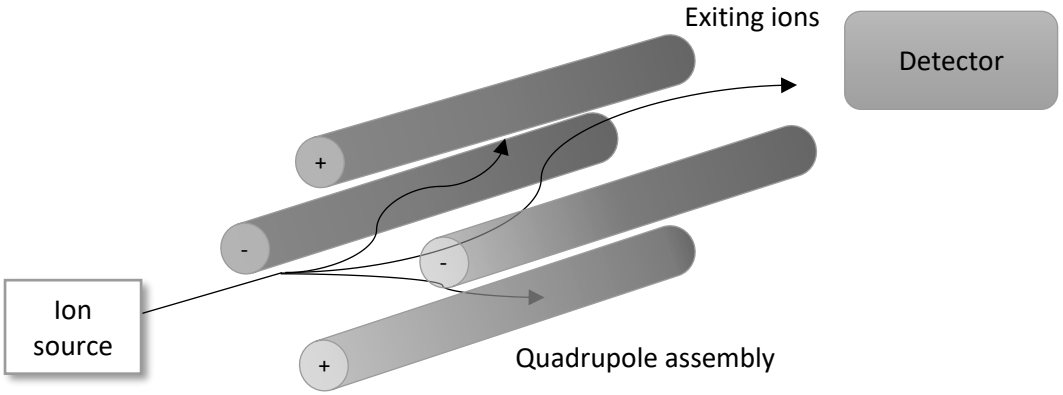

Figure 2.5. Schematic representation of a quadrupole mass analyzer. When inside the quadrupole, ions are subjected to an electric field, and oscillate in different directions. Ions with a specific m/z ratio have stable oscillations, flow through the quadrupole and reach the detector. In turn, the oscillations of ions with other m/z values are unstable, leading them to collide with the rods, not being detected. Adapted from [168].

Tandem mass spectrometry (MS/MS) is related to a group of techniques in which one stage of mass spectrometry is used to isolate a specific ion and a second stage is used to analyze the relationship of the ion with others from which it may have been generated or which it may generate on decomposition [165]. The system is constituted by several mass analyzers, allowing successive analysis in one sample, providing higher selectivity, precision, accuracy and sensitivity over single stage mass analysis [170]. The selectivity is high, once the probability of two different components to originate the same precursor and product ions is very small, and it also increases

with the reduction of interferent signals. Then, this allows a quantification with low detection limits and a greater confidence in the identification and detection of the analytes in study.

When performing tandem mass analysis, usually three quadrupoles are positioned in series. In a triple quadrupole, the three quadrupoles have different functions, the first and the last one (Q1 and Q3) act as mass filters while the central quadrupole (q2) assumes the role of a collisional cell. When the analyte enters the ionization chamber, it is transformed into an ion (known as the principal or precursor ion) which will be selected according to its m/z ratio in the first quadrupole. The ions with the adequate m/z ratio pass through the first quadrupole and enters the collision cell. This second quadrupole has the sole function of accelerating ions which collide with molecules of the inert gas (ex. nitrogen) existing in this region of the mass analyzer (collision-induced dissociation (CID)), leading to its fragmentation [172], in order to obtain structural information. Finally, product ions enter the third quadrupole, which selects them according to their m/z ratio [166].

Triple quadrupoles usually work in multiple reaction monitoring (MRM) mode for targeted quantification (Figure 2.6), allowing to monitor specific CID reactions. In this operation mode, the two quadrupoles (Q1 and Q3) operate in selected ion monitoring (SIM) mode, selecting and focusing specific m/z ratios [174]. It also allows the focus of precursor and product ions for longer periods of time, allowing an increase in sensitivity and selectivity. For a proper identification of the compounds and to ensure specificity in the quantification of analytes in complex mixtures, it should be used at least two MRM transitions, one for quantification and the other for qualitative confirmation of the compound [175].

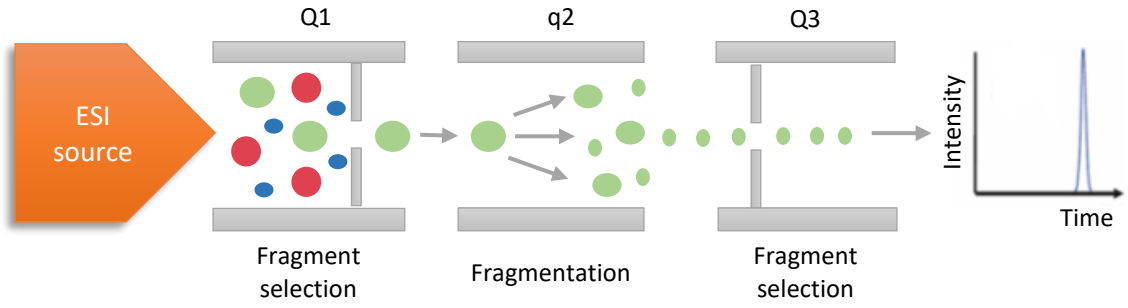

Figure 2.6. Representation of the multiple reaction monitoring (MRM). The source generated ions are separated in the first quadrupole (Q1) and then the selected ions are allowed to pass to the collision cell (q2), where it is fragmented by collision-induced dissociation (CID). Finally, the characteristic fragment ions are selected according to the specific m/z ratios in the third quadrupole (Q3), reaching the detector.

2.2.2.1. Isotopic abundances

It is usual to find most of the elements present in nature as isotope mixtures. An isotope is an atom with the same number of protons of a given element but a different number of neutrons, and, consequently, with a different molecular mass [176]. Since MS has the ability to distinguish elements based on their m/z ratio, isotopes play a vital role in mass spectra, being responsible for the appearance of peaks as isotopic pattern. These isotopic patterns are characteristic of the elements, providing important data about the elemental composition of the compounds [166, 168]. Therefore, through a visual analysis it is possible to identify the isotopic composition and see if the component contains elements like chlorine, bromine or boron, once they have unique isotope patterns (Figure 2.7).

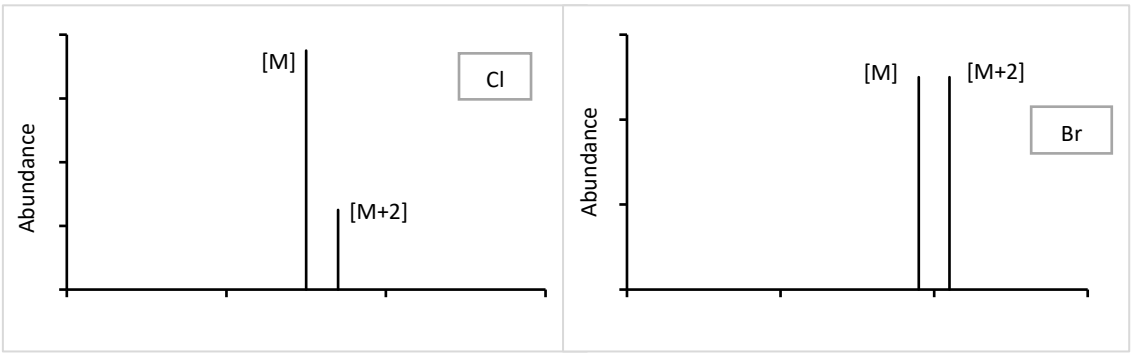

Figure 2.7. Isotopic patterns of chlorine and bromine. Each separate line represents an isotope and the height of each one corresponds to its relative abundance.

Thus, each isotope will appear as a separate line in the mass spectrum and the height of each peak will correspond to the relative abundance of each isotope present in the sample, once elements with high natural abundance will originate a very high peak and, on the other hand, elements with a low natural abundance presents a lower peak. The peak which presents higher intensity is known as the base peak, the largest peak in the spectrum, being labeled M^+ or M^-, while the intensity of every other peak is reported in comparison to this base peak [168]. The pattern peaks are labeled as [M+1], [M+2], and so on, reflecting the natural abundance of the isotopes and the added mass.

2.3. Analytical method validation

One of the main requirements of any process involving chemical analysis is to obtain quality data that meet the proposed objectives and that allows it acceptance in an international level.

This leads to an increase of the need to develop methods that provide reproducible, consistent, valid and reliable results. In this sense, the validation of analytical methods aims to demonstrate, through laboratory studies, that the method is appropriate for the quantification of the analyte in study at a certain concentration level, in a specific biological matrix, with satisfactory accuracy and precision [177]. Once this process aims to demonstrate that the method is reliable for its purpose, any kind of modification in the analytical procedure requires a revalidation process [178].

The validation process provides a quality assurance and analytical performance. Its main purpose is to demonstrate that the analytical method in question is suitable for the analysis of the sample that will be used and that every future measurement in routine analysis will be close enough to the unknown true value for the content of the analyte in the sample [179]. Since the development of a method is a process that involves a series of manipulations of the sample, it is normal that during the process errors are made and, therefore, in the end there is an accumulation of systematic and/or random errors, being able to alter the final result of the analysis [180]. In this way, it is essential to demonstrate, through validation, that the method leads to credible and appropriate results, with the desired quality.

From a scientific point of view, it is essential to obtain reliable analytical data, once the use of wrong results can lead to false interpretation and conclusions [181, 182]. Therefore, this made the certification of the developed methods a subject of growing interest and so, only the validation process can accurately demonstrate the quality of the analytical method through the acceptance of the different parameters and prove its applicability for a certain purpose [181]. Also, for these reasons, judicial authorities require the accreditation of the laboratories who provide results with a legal purpose, to avoid unjustified legal consequences [182].

Despite of the importance of all this validation process, there is no consensus of which parameters should be taken into account and validated to characterize a method and to choose the appropriate decision criteria and statistic test to use. This is due to the fact that there are several guidelines with different criteria, even though none of them is considered the more appropriated. From the international organizations who provide these type of guidelines, there is the International Union of Pure and Applied Chemistry (IUPAC), the International Organization for Standardization (ISO), the United States Food and Drug Administration (FDA), and the European Medicines Agency (EMA), which are the most commonly used guidelines. However, they all differ in the parameters and methodologies used in the validation process.

Method validation studies rely on the determination of the overall method performance parameters and, usually, the minimum requirements evaluated for the quantitative procedures involve: selectivity, calibration model (linearity), stability, precision (repeatability, intermediate

precision), accuracy, limit of detection, limit of quantification and matrix effects. Although, there are other parameters that can be evaluated, such as recovery, reproducibility and robustness [177].

2.3.1. Selectivity

Selectivity refers to the ability of a method to identify and distinguish a particular analyte in a complex mixture without the interference of the other components which are expected to be present in the sample matrix, such as metabolites or degradation products [181]. Therefore, it is necessary to determine the possible interferences of other substances present in the matrix. It is important not to confuse selectivity with specificity, the later one means that it is not supposed to occur any interference, since the method is specific for the analyte [183]. Usually, all guidelines recommend that the validation process starts with the analysis of the method selectivity, because if it is not acceptable there is the need to apply several changes in the developed method [181].

2.3.2. Linearity

The choice of an appropriate calibration model is necessary for a reliable quantification and, so, the relationship between the concentration of analyte in the sample and the corresponding detector response must be studied. Thus, the response function or calibration curve represents the method's ability to provide the analytical signal directly proportional to the concentration of the analyte, within the working range [184, 185]. The function is obtained using calibration standards prepared in the same matrix as the matrix of the intended study samples by spiking the blank matrix with a known concentration of the analyte of interest [177].

2.3.3. Working range

In any quantitative method, there is a range of analyte concentrations (known as working range) that can be defined as the interval between the upper and lower concentration in which the analyte concentration can be determined with precision, accuracy and linearity [183, 186]. Within the range, the sensitivity can be considered constant. The first series of values are usually the values of the limits and the latter depends on the measuring equipment. All the measured values must be within the working range, once extrapolation is not allowed [187].

2.3.4. Limit of detection and limit of quantification

When performing tests on samples with low analyte levels, it is important to know what is the lowest concentration of analyte that can be detected and quantified by the method. The lower limits of the calibration curve are important to indicate the detection and quantitation ability of the analytical method at this level of concentration.

The limit of detection (LOD) corresponds to the beginning of the range in which it is possible to distinguish, with a given statistical confidence, the blank signal from the sample signal and indicate whether the analyte in question is present or absent in the sample. In other words, it is the lowest concentration of analyte that can be detected but not statistically quantified, since the quantification at this level is subject to significant errors [181, 183]. However, a value lower than this does not mean the complete absence of the analyte [180].

For a proper definition of this concept, it is important to include two statistical concepts: type I and type II errors. Type I error (α) is when the null hypothesis is true and it is rejected, while type II (β) error is when the null hypothesis is false and it is accepted. Therefore, for an appropriate analysis of the data, these errors should be minimal (α = β = 5%) [180].

In turn, the LOQ is the lowest concentration of analyte that can be statistically determined with adequate precision and accuracy in certain operational conditions [183]. In practice, when the calibration curve is already well defined, it generally corresponds to the calibration pattern of lower concentration (excluding blank). After determined, it must be tested to ensure that the accuracy and precision are satisfactory [180]. The concentrations below the LOQ should not be quantitatively defined, but they can be reported as only present [188].

2.3.5. Precision

Precision is a measure of the degree of closeness of the values obtained by the analytical method when analyzing, repetitively, the same sample, under specific and controlled conditions. It is expressed as the percentage coefficient of variation ($\%CV$) or the relative standard deviation (R.S.D.) of the replicate measurements [177, 184, 186]. This parameter can be evaluated at three different levels: repeatability, intermediate precision and reproducibility [184].

The repeatability (also known as within-day, within-run or intra-day precision) refers to the dispersion of the results of the method operating in a short time and under the same operating conditions (same sample, equipment, analyst, method, laboratory, etc.) [181, 183, 184].

Intermediate precision (also known as inter-assay, between-run or between-day precision) is related with the dispersion of the results of the method subject to the same procedure and to

random variations within the same laboratory over an extended period of time. The differences represent some alterations that may occur in routine analysis, such as different days, different analysts, different equipment, etc., [183, 184].

Finally, the reproducibility (also known as precision between laboratories) is related to the dispersion of the results obtained from inter-laboratory studies, reflecting the random errors of measurement [184]. It allows to evaluate the correlation of results between dependent and/or independent assays on the same sample in specific operating conditions. This parameter should only be evaluated if a method is supposed to be used in different laboratories [181].

2.3.6. Accuracy

The accuracy of a method is affected by systematic (bias) and random errors, however, it is often used to describe only the systematic error component. Thus, the term is typically used in the sense of bias [184]. Accuracy can be defined as the degree of agreement between individual results found in a particular test and a reference value accepted as true [181, 189]. It is important to notice that an accurate or true value is a value obtained by a perfect measurement, and this value is indeterminate by nature [190].

2.3.7. Carry-over

Carry-over is the appearance of an analyte signal in blank samples after the analysis of samples with a high analyte concentration [177]. Specific measures should be tested during the method development and validation and applied during the analysis of the study samples [187]. This is important to know how much analyte is still retained in the column, since it can affect the signal of the next sample, mainly if the previous injected sample had a higher concentration, as well as the precision and accuracy of the method [191].

2.3.8. Recovery

The absolute recovery of a method is evaluated through the comparison of the response (peak area) of a spiked matrix standard before the extraction procedure with the response of an equal amount of the analyte spiked into a matrix after the sample treatment. This parameter indicates whether the method provides a response for the entire amount of analyte that is present in the sample [186]. Even though recovery is not among the validation parameters regarded as essential for method validation, it is interesting to evaluate if the sample treatment is effective

enough for the study [181]. When performing analytical methods, recovery should also be evaluated for the compounds used as internal standards [192]. In LC-MS analysis, this parameter should be assessed along with the study of matrix effect, once part of the change of the response in prepared samples when compared with their standard solutions might be due to some matrix effects [181].

2.3.9. Matrix effects

The LC-MS is susceptible to matrix effects, a significant source of imprecision, which may have a major impact on the accuracy, precision and robustness of bioanalytical methods and so, when performing LC-MS analysis, the evaluation of this parameter is essential [181, 193]. Matrix effects can be described as the difference between the mass spectrometric response for the analyte in standard solution and the response for the same analyte in a biological matrix, such as the plasma [193]. This effect is due to the presence of unmonitored, co-eluting compounds from the matrix that may affect the detection of the analyte under study and compromise the efficiency of its ionization and causing the suppression or enhancement of the peak abundance [187, 192]. It is important to highlight that matrix effects are analyte specific [193, 194].

3. Objective

Plasma catecholamines, like DA, norepinephrine or epinephrine, provide a reliable biomarker of sympathetic activity. For example, DA, an endogenous neurotransmitter, is known to play a significant role in neurodegenerative disorders, such as Parkinson's disease. The determination of neurotransmitters, their precursors and metabolites facilitates better understanding of complex neurobiology in the central nervous system disorders and has expanding uses in many other fields. Thus, there has been a continuing interest in developing new and better analytical methodology for quantitative determinations of these molecules in a variety of biological materials, including plasma, blood, urine and cerebrospinal fluid.

Despite all the methods proposed for the quantification of DA metabolism, they all present some limitations that affect the reliability of the results and don't allow them to be applied in real plasma samples, with the purpose to a possible application in the scientific field. Among the most common limitations we have insufficient sensitivity, difficulty at sample preparation and potential interferences from structurally similar endogenous compounds (matrix interferences). Also, their low circulating concentration, their instability and the limited volume of blood collected requires a complex sample preparation and an exhaustive and complex method to ensure their accurate quantification.

Moreover, as previously mentioned, some studies showed that sometimes DA metabolites and precursors concentrations in the plasma of patients (for example, HVA and DOPAC) are more useful to study some pathologic changes in DA pathway, like in Parkinson's disease.

Therefore, there is the need to develop a reliable method to quantify DA metabolism, since this analysis can be an important step in a possible precocious diagnosis of this disease. In the experimental part of the current project, the main goal is the development and validation of a high-performance liquid chromatography coupled with tandem mass spectrometry based method for a quantitative determination of DA metabolism. The validation procedure is essential to certify the consistency of the results.

In order to test the developed method, it was applied in a group of plasma samples from Parkinson's disease patients who were already diagnosed with the pathology and are under medication, an important aspect to take into account, since it will influence the levels of some of the metabolites under study.

4. Materials and methods

4.1. Materials

- Micropipettes® Research Plus (Eppendorf®);
- Multipipette® Plus (Eppendorf®);
- PS – Microplate 384 well, 128.0/85 mm (Greiner bio-one);
- Microcentrifuge tubes (0.6 ml, 1.5 ml, 5 ml)
- Vials 500µL (VWR®).

4.2. Equipments

- Components of the liquid chromatography coupled to a mass spectrometer system:
  - Autosampler CTC HTC-xt (Eksingent/PAL);
  - Liquid Chromatography, Nexera system (Shimadzu®);
  - ESI source, turbo V™;
  - Hybrid triple quadrupole/linear ion trap mass spectrometer, 4000 QTRAP® (ABSciex);
  - Analyst® (1.6.2) (ABSciex) for MS system.
- Analytical balance CP 224S (Sartorius);
- Bench-top Centrifuge (Minispin-Eppendorf®);
- Concentrator Plus (Eppendorf®) - “speedvac”;
- Quick spin, model QS 7000 (Edward Instrument Co);
- Thermomixer comfort (Eppendorf®);
- Vortex, model MS3 basic (IKA®).

4.3. Standards and reagents

The list of analytical and internal standards is showed in Table 4.1 and the reagents used in the chromatographic analysis are presented below.

Table 4.1. List of standards used in the development and validation process.

	Name	Molecular weight (g/mol)	Brand
Analytical standards	L-tyrosine	181.19	Santa Cruz Biotechnology
	L-DOPA	197.19	Santa Cruz Biotechnology
	Dopamine hydrochloride	189.64	Sigma-Aldrich-Fluka
	3-Methoxytyramine hydrochloride	203.67	Sigma-Aldrich-Fluka
	3,4-Dihydroxyphenylacetic acid	168.15	Sigma-Aldrich-Fluka
	Homovanillic acid	182.17	Sigma-Aldrich-Fluka
Internal standards	L-tyrosine (d7, 98%)	188.23	Cambridge Isotope Laboratories
	L-DOPA (ring-d3)	200.21	Sigma-Aldrich
	Dopamine-1,1,2,2-d4 hydrochloride	193.66	Sigma-Aldrich
	3-Methoxytyramine hydrochloride (1,1,2,2-d4, 97%)	207.69	Cambridge Isotope Laboratories
	3,4-Dihydroxyphenylacetic acid (Ring-d3, 2,2-d2, 98%)	173.18	Cambridge Isotope Laboratories
	Homovanillic acid - d3	185.19	Santa Cruz Biotechnology

Reagents:

- Acetonitrile (LC Grade, Fisher Chemical™);
- Formic Acid (LC Grade, Amresco®);
- Methanol (LC Grade, Fisher Chemical™);
- Water (LC Grade, Fisher Chemical™).

4.4. Standard solutions

Stock standard solutions were prepared by dissolving ≈2 mg of the pure substance in 2 ml of LC Grade water, in the case of dopamine hydrochloride, 3-methoxytyramine hydrochloride, 3,4-dihydroxyphenylacetic acid, homovanillic acid, 3-methoxytyramine hydrochloride (d4), 3,4-dihydroxyphenylacetic acid (d5). In the case of dopamine-d4, ≈5 mg of the pure substance was dissolved in 2 ml of water, while in homovanillic acid-d3 solution, ≈1 mg was dissolved in 2 ml of water. L-DOPA presented low solubility in water, as well as their respective internal standard solutions. Then, 2 and 2.5 mg was dissolved in 3 ml of water and 1 ml of acetonitrile (ACN), in the case of L-tyrosine and L-tyrosine (d7), respectively, and ≈2.5 and ≈1 mg was dissolved in 3 ml of

methanol and 1 ml of water, for L-DOPA and L-DOPA-d3 standard solutions, respectively. Each mixture was agitated by vortex to obtain a homogeneous solution, at room temperature. L-tyrosine and L-DOPA mixtures were subjected to a heating process in a thermomixer during 10 and 20 minutes, respectively, at 60 °C at 750 rpm. Aliquots of 200 or 300 µL of all stock solutions were prepared and stored at -20°C. For more information about the standard solutions see appendix 8.1.

4.5. Clinical trial protocol

The following research protocol was approved by the Ethical Committee of CHCB. Patients and Healthy controls had given their informed consent to the study.

4.5.1. Parkinson's disease group

The study was carried out with 38 PD patients, of which 21 were males (55.3%) and 17 were females (44.7%), with age between 55 and 86 years. The chosen patients were recruited from appointment list of the neurology sector of Centro Hospitalar Cova da Beira (Covilhã – Portugal), between January 2013 and December 2013.

The patients with clinical diagnosis of PD established by the UKPDBBC and modified Hoehn & Yahr staging scale between 1 and 4 were included. All patients were subjected to an interview that included: questionnaire, neurological examination (performed by a neurologist), laboratory tests and medical record evaluation. The neurologist performed the neurological examination to apply mH&Yss and provide clinical data, through the evaluation of PD cardinal signs[3]. The interview and medical record evaluation allowed to acquire some demographic and medical information, such as, duration of PD, early motor symptoms, actual motor symptoms, presence or absence of non-motor symptoms, copies of brain imaging exams, mean daily dosage of L-DOPA, actual and previous medications, comorbidities (simultaneous presence of two chronic diseases or conditions), additional medications and emergency appointments.

[3] Tremor is involuntary, rhythmic and, mainly, at rest. In limbs, when patient relaxes with hands on the lap it is possible to evaluate the tremor. It could also affect legs, lips, jaw or tongue. The rigidity is characterized by increased resistance to passive movement about a joint, decreased arm swing with walking and the typical stooped posture. Bradykinesia is a generalized slowness of movement or even absence of movement (akinesia). It's evaluated through observation of facial hypomimia and limb movement, including speed, amplitude and rhythm of finger tapping, hand gripping, pronation-supination hand movements and heel or toe taping. Gait freezing and festination may develop in later disease. "Pull" test evaluates postural instability: the examiner stands behind the patients and pulls the patients by his shoulders. Patients with postural instability take multiple steps backwards or could fall (positive "pull" test). Disease progression could lead to a festinant gait or confine the patient in a wheelchair, when postural reflexes are lost

Patients with Diabetes mellitus, hypertension, coronary and heart disease, hyperlipidemia and thyroid disease were also included, when treated with the appropriate medication and if there was no evidence of exacerbations or complications in the clinical records, in the past 6 months.

All documents were properly identified by a study number to maintain confidentiality.

4.5.2. Control group

The control group was constituted by 32 participants, of which 19 were males (59.4%) and 13 were females (40.6%), with age between 55 and 86 years. All the participants were volunteers from CHCB. Most of them were recruited from urology and gynecology sectors.

The volunteers were subjected to an interview that involved a questionnaire, neurological and physical exam, laboratory tests and medical records evaluation. It was also performed a summary neurological examination[4], in order to exclude neurological symptoms, and cardiac and pulmonary evaluations, to provide additional clinical information. Interview and medical record evaluation allowed to obtain comorbidities and actual medications.

All documents were identified by study number to maintain confidentiality.

4.6. Instrumental conditions

During the development of a LC-MS method, experimental conditions must be optimized. The main objective in analytical method optimization is to adjust the several parameters in order to determine the best analysis conditions and enhance the performance characteristics of each analyzed compound.

4.6.1. Liquid chromatography

The chromatographic separation was performed with a Gemini® C18 (3µm, 110Å, 50×2mm) column. It was also used a Security Guard™ cartridges Gemini® C18 (4×2 mm), in order to protect the chromatographic column, since it prevents the contaminants to reach the analytical column. A specific elution gradient (Table 4.2) was developed to allow an efficient separation of the

[4] Cranial nerves number II (visual fields); III, IV and VI (ocular motility); VII-motor (wrinkle forehead, close eyes tight, show teeth); and XII (stick out tongue and move it side to side). Tremor (patient's arms are held outstretched and fingers extended), hand rapid alternating movements (finger tapping), finger-to-nose, muscular tone (elbow, wrist and knee passive movements), diadochokinesia (alternating pronate and supinate movements), osteotendinous reflexes (biceps, finger flexors and patellar) and plantar reflex.

analytes. The flow rate was 250 µL/min and the running time was 7 min for each sample, once the maximum retention time for all the analytes was approximately 4 min. It was injected, between each sample, a blank (solution of 0.1% formic acid (FA) in ACN), with the same elution gradient and program of injection that was used for the samples. The volume that was injected either for plasma samples and for the blanks between samples was 10 µL.

Table 4.2. Elution gradient used in the chromatographic analysis.

Time gradient (min)	Mobile phase (% v/v)	
	0.1% FA in H_2O	0.1% FA in ACN
0	98	2
1	98	2
3	50	50
3.5	5	95
4.0	5	95
4.1	98	2
7.0	98	2

4.6.2. Mass spectrometry

The equipment and data acquisition were assured by the Analyst® 1.6.2 (ABSciex) software. It was performed a direct injection into the mass spectrometer of the analytes and internal standards, using a syringe pump with a flow rate of 10 µL/min, with concentrations of 1 µM for all the molecules, except for DA-d4, DOPAC and DOPAC-d5, in which 5 µM, 10 µM and 10 µM were used, respectively. This process allows to state the ideal conditions to define in the mass spectrometer.

The mass spectrometer was equipped with an ESI source, that operated in the positive and negative ionization mode, where the ion spray voltage was 5500V, the nebulizer gas 1 (GS1) was 30 psi, the entrance potential (EP) was 10V, the curtain gas (CUR) was 30 psi and the temperature source was 450°C. Besides these parameters, there is also the declustering potential (DP), collision energy (CE) and collision exit potential (CXP), which differ amongst each molecule and transition. To monitor the precursor ions of the analytes and internal standards, mass spectrometer was operated in the MRM triple quadrupole scan mode. The monitored transitions of the analytes and the optimized parameters are presented in Table 4.3. The analytical data (peak areas) were processed by Multiquant™ 3.0 (ABSciex) software while compound fragmentation spectra were analyzed by Peak View™ 1.1.1.2 (ABSciex) software.

Table 4.3. Mass spectrometer acquisition parameters optimized to each compound: MRM transitions, declustering potential (DP), collision energy (CE), and collision exit potential (CXP).

Compound	Transitions (m/z)		DP (eV)	CE (eV)	CXP (eV)
	Q1	Q3			
L-tyrosine	182.2	91.1	56.0	41.0	6.0
		136.2		19.0	12.0
		165.1		15.0	12.0
L-DOPA	198.2	135.1	51.0	27.0	8.0
		152.1		19.0	14.0
		181.1		15.0	12.0
DA	154.2	65.0	56.0	49.0	10.0
		91.1		33.0	16.0
		137.2		15.0	12.0
3-MT	168.3	91.0	51.0	35.0	16.0
		119.1		25.0	10.0
		151.1		15.0	14.0
DOPAC	167.0	95.2	-45.0	-28.0	-5.0
		122.2		-30.0	-7.0
		123.2		-12.0	-7.0
HVA	181.0	122.2	-65.0	-22.0	-7.0
		136.7		-12.0	-7.0
		137.2		-12.0	-1.0
L-tyrosine (D7)	189.2	96.1	56.0	41.0	18.0
		143.2		21.0	12.0
		172.2		15.0	14.0
L-DOPA (ring-d3)	201.2	154.1	51.0	19.0	12.0
		155.2		21.0	14.0
		183.2		15.0	16.0
DA (1,1,2,2-d4)	158.3	94.1	51.0	33.0	16.0
		95.1		37.0	16.0
		141.2		15.0	12.0
3-MT (1,1,2,2-d4)	172.3	68.0	51.0	53.0	10.0
		94.0		33.0	16.0
		123.1		27.0	8.0
DOPAC (ring-d3, 2,2-d2)	172.1	100.2	-50.0	-30.0	-5.0
		126.2		-32.0	-7.0
		128.2		-12.0	-7.0
HVA-d3	184.0	122.2	-60.0	-22.0	-7.0
		139.8		-12.0	-1.0
		140.3		-12.0	-1.0

4.7. Extraction procedure - protein precipitation

All samples were subjected to the same analytical procedure for the extraction. To each microcentrifuge tube, containing 100 µl of plasma, three volumes of methanol were added (300 µl). The samples were agitated by vortex and then by continuous agitation for 5 minutes at 800 rpm's in a thermomixer. Then, to promote proteins aggregation, the samples were centrifuged at 14,000×*g* for 10 minutes. The supernatant was collected to a new microcentrifuge tube and 10 µl were injected into the system.

4.8. Analytical method validation

The validation process is required to prove the quality of the analytical method and it is achieved through the fulfillment of minimum acceptance criteria in order to allow its application in numerous fields [181]. Therefore, validation of the developed method was performed and the parameters used to validate the method were: selectivity, linearity, limit of detection, limit of quantification, precision, accuracy, carry-over, recovery and matrix effects.

During the method validation, usually it is used a blank biological matrix spiked with the analyte of interest. Internal standards can also be added during sample processing, in cases of chromatographic methods [177], a compound that can be differentiated from the target analyte by mass spectrometry detection and that can be used to account for the variability during the sample preparation and measurement [181].

The statistical tests and their respective acceptance criteria applied in each parameter are exposed in the following pages. All the calculations were performed with the help of a Microsoft Excel® spreadsheet properly developed for the validation method.

4.8.1. Selectivity

Intrinsic selectivity can be studied using, at least six independent sources of blank matrices, being individually analyzed and evaluated for some possible matrix interference [177]. To prove the selectivity of the method, the blank matrix should not produce a significant interference at the retention time of the analyte of interest [187].

To evaluate the selectivity in plasma, six individual sources of blank plasma were selected and divided into two aliquots with 100 µL of plasma each. One aliquot was spiked with 10 µL of a solution containing the six analytes and the six internal standards (positive samples) and 290 µL

of methanol were added. To the other aliquot no compound was added, and so, 300 µL of methanol were added, to reach the same total volume (negative samples). Then, all the samples were subjected to the same extraction procedure and 10µL of each was injected into the LC-MS/MS system. The selectivity was also assessed in solvent, where three different positive and negative samples were used. The positive samples were prepared with 10 µL of the solution containing the analytes and internal standards and 390 µL of methanol, while negative samples contained 400 µL of methanol. Then, 10 µL of each sample was also injected into the LC-MS/MS system. A blank (ACN:0.1% FA) was injected between samples to reduce the carry-over effect.

After all the analysis, the results of the positive samples were compared with those of the negative samples. The criteria used to evaluate the selectivity were defined by the World Anti-Doping Agency (WADA) for qualitative assays for chromatographic analysis and MS. In LC analysis, the retention time (RT) of the analyte should not differ by more than 2% or ± 0.1 min, whichever is lower, when compared with the RT of the positive control sample.

When MS/MS detection is used, it should be monitored, at least, two precursor-product ions transitions and, in this case, the signal-to-noise (S/N) of the least intense diagnostic ion must be higher than 3:1 [196]. The determination of S/N was performed by the Multiquant™ 3.0 software. The criteria applied to calculate this parameter were defined by one of the positive samples. The maximum tolerance range used for the identification of the compounds was calculated as described in the Table 4.4. The relative abundance is the ratio between the area of a specific ion and the area of the most abundant ion (base peak), being the final value expressed as a percentage [196].

Table 4.4. – Maximum tolerance windows for relative ion intensities to ensure appropriate confidence in identification [196].

Relative abundance (% of base peak)	Maximum tolerance windows (%)
> 50%	± 10 (absolute)
25% to 50%	± 20 (relative)
5% to <25%	± 5 (absolute)
<5%	± 50 (relative)

4.8.2. Linearity

To evaluate linearity, it is necessary to use a sufficient number of calibrators. Although there is no agreement on how many calibrators should be used, it was stated that the calibration curve

must be constructed using at least five to eight different concentration levels (excluding blank samples, due to possible errors) [184, 188]. It is expressed as a mathematical expression (linear regression equation) that will be used to determine the concentration of the analyte in real samples. Each standard is prepared by adding an appropriate and known volume of the stock solutions [188].

The linearity study was performed in solvent and plasma samples. Then, to assess the linearity of the method in solvent, it was prepared one calibration curve with twelve calibrators, which contained 10 µL of a solution containing the six analytes and 390 µL of a solution (0.4 µM) with the six internal standards. The calibration standards were uniformly distributed in a wide range of concentrations: 0.0025, 0.005, 0.010, 0.015, 0.025, 0.05, 0.1, 0.2, 0.3, 0.4, 0.5 and 0.6 µM. In plasma samples, 100 µL of plasma, 20 µL of the mix containing the analytes, 10 µL of the mix containing the internal standards and 270 µL of methanol were used. The concentration range in plasma was: 0.005, 0.01, 0.02, 0.03, 0.05, 0.1, 0.2, 0.4, 0.6, 0.8, 1 and 1.2 µM. The plasma samples were subjected to the extraction procedure explained in section 4.7. After collecting the supernatant, water was added to make up a final volume of 400 µL. Four calibration curves in solvent and plasma were prepared in four different days.

The simplest regression model typically used is the ordinary least squares model [189, 197]. It is used to establish a relation between the two variables under study, the analytical response and the analyte concentration, being mathematically expressed by equation (4.1) [198].

$$y = mx + b \tag{4.1}$$

where the independent variable (x) is the analyte concentration, the dependent variable (y) is the respective response, b is the y-intercept, and m is the slope [198]. Linearity can be confirmed through the coefficient of correlation (R), which reveals the relationship between the measured signal and the concentration of the respective patterns. However, coefficient of determination (R^2) is used to translate the suitability of a linear model to the experimental values [199]. In both cases, the obtained values should be above 0.99 [185]. Additionally, the zero-value should be included within the confidence interval of 95%.

It was also used the standard error of the residuals ($S_{y/x}$) as a measure of the goodness of fit of the model, in order to exclude the absolute residual values higher than the double of $S_{y/x}$. Finally, it was performed a visual inspection of plots for residuals versus concentration and peak area ratio versus concentration [184].

4.8.2.1. Mandel test

Despite being very common to evaluate the calibration model through the coefficient of correlation (R) resultant from the regression analysis, from a statistical point of view it is not acceptable to only use this model, as it is considered a poor test to evaluate the linearity [184]. Therefore, there are other statistical tests and quality parameters that are suggested to evaluate the goodness of fit of the model [200].

Therefore, the Mandel's fitting test was used to verify if the data had a linear or non-linear (quadratic) behavior [200]. From the calibration curve, it was calculated the difference between the variance of the linear and the quadratic correlation [180, 201-203], as presented in equation (4.2).

$$\mathrm{D}S^2 = (N-2)\ x\ S^2_{y/x}\ x\ (N-3)\ x\ S^2_y \tag{4.2}$$

$$S^2_{y/x} = \frac{\sum_{i=1}^{n}(y_i - \hat{x}_i)^2}{N-2} \tag{4.3}$$

$$S^2_y = \frac{\sum_{i=1}^{n}(y_i - \hat{y}_i)^2}{N-3} \tag{4.4}$$

where $S^2_{y/x}$ and S^2_y correspond to the predicted values by the polynomial fit of first (linear fit) and second (quadratic fit) degree, respectively, and N is the number of calibration standards used to make the calibration curve [201].

The TV is calculated through equation (4.5) [180, 200, 201] and compared with the F_{crit} at the (N-1; N-1; α) confidence level of 95% (α=0.95), allowing to accomplish if the calibration function is linear or nonlinear.

$$TV = \frac{DS^2}{S^2_{y_2}} \tag{4.5}$$

To evaluate if the calibration curve follows a linear or a quadratic behavior it should be considered the following criteria [180]:

✓ If $TV \leq F_{crit}$ - the difference between the variances is not statistically significant, and so, the calibration curve has a linear behavior;

✓ If $TV > F_{crit}$ - the difference between the variances is statistically significant, and so, the calibration curve has a quadratic behavior. In this case, it should be analyzed the possibility of reducing the working range.

4.8.3. Working range

When using a method that involves performing a calibration curve, the working range can be evaluated through the homogeneity of variance test (or F test) [182] or the visual evaluation of residuals versus concentration plots [198]. The homogeneity of variance test allows to verify if the error is the same in every value of the independent variable, otherwise there is a violation of the homoscedasticity.

To appraise the homogeneity of variance, ten different replicates of the lowest and highest concentrations levels were used, which corresponded to 0.015, 0.6 µM in solvent and 0.30, 1.2 µM in plasma. To each calibrator, a solution (0.4 µM) containing the six internal standards was added.

This test is applied in accordance with the following equation (4.6).

$$TV = \frac{S_2^2}{S_1^2} \quad (4.6)$$

where S_2^2 and S_1^2 are the variances obtained for the highest and lowest concentration levels of the working range, respectively, and TV is the test value. The TV follows a F-distribution and it is compared with the tabulated value of the unilateral Fisher-Snedecor distribution (F_{crit}) (N-1; N-1; α) at a confidence level of 95% (α = 5%) [198]. It is important to highlight that the numerator is always the highest variance value. The variances of first and last calibrator were calculated according to equation (4.7) [180].

$$S_i^2 = \frac{\sum_{j=1}^{n}(y_i - \bar{y}_i)^2}{n_i - 1} \quad (4.7)$$

where S_i^2 is the variance, i ($i = 1$ and $i = 2$) is the number of the calibrator, j is the number of replicates made for every calibrator ($j = 1$ to 10); n is the number of results; y_i is the result and $\bar{y}_i$ is the mean of results obtained [180].

As hypothesis, it is assumed as null hypothesis (H_0) that there is no significant difference between the variances, being a purely random difference, while the alternative hypothesis (H_1) assumes that there is a significant difference, the numerator variance exceeds the denominator.

Therefore, to evaluate if the calibration curve follows a homoscedastic or heteroscedastic behavior we should considerer the following criteria [180]:

- ✓ If $TV \leq F_{crit}$, the difference between the variances is not statistically significant, and so, the working range follows a homoscedastic behavior;
- ✓ If $TV > F_{crit}$, the difference between the variances is statistically significant, and so, the working range follows a heteroscedastic behavior.

After this analysis, it was performed a visual inspection of residuals versus concentration plots to evaluate the distribution of the residuals around the x-axis. If it is verified that the variance is constant along the whole working range, residuals will be randomly around the x-axis and TV will be lower than F_{crit}.

If in the study of homogeneity of variances, there is heteroscedasticity in data, it is possible to reduce the working range and repeat the verification of the homogeneity of variances until $TV \leq F_{crit}$ is reached, or weighted least squares linear regression should be used to find the straight line for calibration. This test consists in choosing the appropriate weighting factor (w_i) [198]. In the latter case, this non-homogeneity of variances can also be tested by using the Cochran criterion, when the number of observations is the same for all concentration levels [179].

4.8.3.1. Weighted least squares linear regression

As mentioned, ordinary least squares regression models are only applied when there is a homogeneity of the data. Therefore, when data is heteroscedastic, weighted least squares linear regression is used to find a straight line for calibration and a weighting factor (w_i) is necessary [179, 181, 182]. These empirical weights describe the speed of the rise of the signal when the concentration increases [186, 204]. The empirical weights that are usually studied include: $\frac{1}{x}$; $\frac{1}{x^2}$; $\frac{1}{\sqrt{x}}$; $\frac{1}{y}$; $\frac{1}{y^2}$; $\frac{1}{\sqrt{y}}$, where x is the concentration and y is the detector response [204]. Therefore, w_i can be obtained through the equation (4.8) [205].

$$w_i = \frac{1/S_{yi}^2}{(\sum_i^p 1/S_{yi}^2)/p} \tag{4.8}$$

where w_i is the weighting factor; S_{yi}^2 is the appropriate empirical weight for the data, and p is the number of calibration standards.

The best weighting factor is chosen according to a percentage relative error ($\%RE$), which compares the regressed concentration (C_{found}) with the nominal standard concentration in the sample (C_{nom}), as expressed in equation (4.9). This value is useful as an indicator of goodness of fit in the evaluation of the weighting factor [198].

$$\%RE = \frac{C_{found} - C_{nom}}{C_{nom}} x\ 100 \quad (4.9)$$

Thus, plots of $\%RE$ versus concentration and the sum of $\%RE$ ($\sum \%RE$) were performed in order to evaluate the $\%RE$ [198]. The best w_i is the one that leads to a narrow horizontal band of randomly distributed $\%RE$ around the concentration axis and has the smallest value of $\Sigma\ \%RE$ across the concentration range [198]. Also, if this difference falls within 15 or 20% for the limit of quantification (LOQ) the model is accepted [182].

When using weighted least squares linear regression, the model parameters (m and b) for each w_i is converted into its weighted equivalent by adding the term w_i into the equation and the estimated values are calculated by equations (4.10), (4.11) and (4.12) [198].

$$m = \frac{\sum w_i x \sum w_i y_i x \sum w_i x_i x \sum w_i x_i y_i}{\sum w_i x \sum w_i x_i^2 - (\sum w_i x_i)^2} \quad (4.10)$$

$$b = \frac{\sum w_i x_i^2 x \sum w_i y_i x \sum w_i x_i x \sum w_i y_i x_i}{\sum w_i x \sum w_i x_i^2 - (\sum w_i x_i)^2} \quad (4.11)$$

where x_i and y_i are the i[th] data pair of n total data pairs and w_i is the chosen weighting factor.

The correlation coefficient (r-value), that expresses the dependence established between the two variables, can be calculated by equation (4.12) [198].

$$r = \frac{\sum w_i x \sum w_i x_i y_i - \sum w_i x_i x \sum w_i y_i}{\sqrt{\sum w_i x \sum w_i x_i^2 - (\sum w_i x_i)^2} x \sqrt{\sum w_i x \sum w_i y_i^2 - (\sum w_i y_i)^2}} \quad (4.12)$$

To evaluate this parameter four different calibration curves were performed, with twelve calibrators each, which were uniformly distributed within the calibration range: 0.0025, 0.005, 0.010, 0.015, 0.025, 0.05, 0.1, 0.2, 0.3, 0.4, 0.5 and 0.6 µM in solvent; 0.005, 0.01, 0.02, 0.03, 0.05, 0.1, 0.2, 0.4, 0.6, 0.8, 1 and 1.2 µM in plasma samples. To each calibrator, a 0.4 µM solution containing the six internal standards was added.

4.8.4. Limit of detection and limit of quantification

There are different criteria that can be used to determine the LOD and LOQ [183, 189, 201]. One of the methods is their determination through the standard deviation of the response and the slope, which allows to determine this value from the standard deviation of the blank. The LOD is expressed as a mean sample blank value plus two or three times the standard deviations of the blank samples [183, 189].

Despite all the different approaches that can be used to determine the limits, there is no preference on the existent guidelines for which one to choose. Therefore, LOD and LOQ were calculated based on the standard error of the response and the slope, through equations (4.13) and (4.14) [180, 204]:

$$LOD = \frac{3.3 \; x \; S_{y/x}}{m} \tag{4.13}$$

$$LOQ = \frac{10 \; x \; S_{y/x}}{m} \tag{4.14}$$

where $S_{y/x}$ is the standard error of the response and m is the slope of the calibration curve [180, 189]. The standard error of the response can be calculated through equation (4.15) [205, 206].

$$S_{y/x} = \sqrt{\frac{\sum (y_i - \hat{y}_i)^2}{n-2}} \tag{4.15}$$

where $S_{y/x}$ is the residual standard deviation; y_i is the analytical signal measured, $\hat{y}_i$ is the estimated value of y_i and n is the number of experimental points.

In cases where the data is heteroscedastic, the previous equation must be modified, since it is only applicable in homoscedastic data (linear models). Thus, the relative standard deviation of the weighted correlation ($S_{\left(\frac{y}{x}\right)w}$) is calculated by equation (4.16) [205].

$$S_{\left(\frac{y}{x}\right)w} = \sqrt{\frac{\sum w_i (y_i - \hat{y}_i)^2}{n-2}} \tag{4.16}$$

where $S_{\left(\frac{y}{x}\right)w}$ is the residual standard deviation of weighted regression; w_i is the weight factor used; y_i is the analytical signal measured and $\hat{y}_i$ is the estimated value of y_i.

The assessment of limits (LOD and LOQ) was performed along with the linearity study. The parameters of the calibration curves of each analyte, namely the standard error of the response and the slope, were used to calculate these limits through the previous equations.

4.8.5. Precision

Both precision and accuracy (presented in section 4.8.6) are usually estimated through the analysis of quality control (QC) samples, under well-established conditions [184]. Since they both vary over the working range, usually they are evaluated at three different concentration levels (low, medium and high) [181, 184, 187]. Each concentration level must be prepared in triplicate, with a total of 9 determinations [183], and this study should be performed on several separate days [182]. After the analysis, using an ANOVA calculation, both repeatability and intermediate precision can be determined (see appendix 8.15) [182, 207].

Usually, the analysis of repeatability and intermediate precision consists in the analysis of a test sample in *p* different runs, being that in each run the sample should be analyzed *n* times under the same repeatability conditions. It is also important to vary the main sources of variation between each run [207].

Then, to evaluate precision, QCs were prepared, along with the different calibration curves, at two concentration levels: 0.15 (medium) and 0.35 (high) µM in solvent and 0.3 (medium) and 0.7 (high) µM in plasma. In solvent and plasma, 390 µL and 10 µL of internal standard solution were added, respectively. Each QC was prepared in triplicate.

The intermediate precision and repeatability, expressed by $\%CV$, were calculated through equations (4.17) and (4.18) [182, 192, 207].

$$\%CV\ Repeatability\ within = \frac{\sqrt{s^2_{within}}}{\bar{x}} x\ 100 \quad (4.17)$$

$$\%CV\ Intermediate\ precision = \frac{\sqrt{s^2_{between} + s^2_{within}}}{\bar{X}} x\ 100 \quad (4.18)$$

where s^2_{within} and $s^2_{between}$ are the variance within groups and between groups, respectively, and $\bar{x}$ is the mean value of concentrations.

The acceptance criteria for the precision determined at each concentration level that was set was that the coefficient of variation ($\%CV$) should not exceed 15% for all the concentrations, except near the LOQ, where it should be lower than 20% [177, 181, 182].

4.8.6. Accuracy

The accuracy of a measurement can be described by the absolute error, corresponding to the difference between the obtained value and the correct value. On the other hand, it can be also obtained by the relative error, which is the ratio of the absolute error and the correct value, being only an indication of the percentage deviation obtained. However, a good accuracy is not always synonymous of a good precision.

The experimental procedure used to evaluate the accuracy of the method was similar to the one used in the analysis of the precision. Accuracy, expressed in percentage of relative error ($\%RE$), can be calculated through equation (4.19) [192].

$$\%RE\ Accuracy = \frac{C_{obs} - C_{nom}}{C_{nom}} x\ 100 \quad (4.19)$$

where C_{obs} is the mean of experimental concentrations and C_{nom} is the nominal concentration.

Recovery of the QCs analysis can also be calculated, being defined as a ratio between the observed and the nominal concentrations, and it is expressed by equation (4.20) [200].

$$\%Recovery = \frac{C_{obs}}{C_{nom}} x\ 100 \quad (4.20)$$

The defined acceptance criteria for the accuracy determined at each concentration level was that the mean concentrations should be within 15% of the nominal values, except for the LOQ, where it should be within ±20% [177, 181].

4.8.7. Carry-over

Carry-over study allow to know how much analyte is retained in the column after the analysis of a sample with a high analyte concentration. Therefore, this should be assessed by analyzing blank samples after the injection of high concentration samples at upper limit of quantification and analyzing if signal of the previously analyzed sample is present [177].

To evaluate the carry-over effect, five blank samples were analyzed after the injection of the highest level of concentration standard, 0.60 µM for solvent and 12.04 µM for plasma samples. It was used as blank methanol and 75% methanol for solvent and plasma, respectively. This procedure was repeated in three different days.

As an acceptance criteria, the carry-over of the blank sample following a high concentration standard should not be greater than 20% of the LOQ and 5% for the internal standard [177, 182].

4.8.8. Recovery

This analysis should be performed by comparing the analytical response obtained for the analyte added in the biological matrix before the sample clean-up procedure, at three different concentration levels, with the response obtained in the analysis of samples that were spiked with the analyte, at a known concentration, after the extraction method, which represents 100% of recovery [181]. Thus, to evaluate the recovery, three levels of concentration were selected (low, medium and high), corresponding to 0.07, 0.5 and 0.8 µM, each one prepared in triplicate. The plasma was used from a pool of different aliquots since these sample were collected with different collection tubes who contained different coagulants. For each level of concentration, two aliquots were set. One contained 100 µL of plasma, to which 10 µL of a mix solution with the six analytes and internal standards were added, followed by 290 µL of methanol and then subjected to the extraction method. In turn, the other aliquot contained 100 µL of plasma and 300 µL of methanol and was first subjected to the extraction procedure, being then added 10 µL of the mix solution to the supernatant.

The determination of the recovery, in percentage, was performed through equation (4.21) [186, 193].

$$\%Recovery = \frac{A_{ab}/A_{ISb}}{A_a/A_{IS}} x\ 100 \qquad (4.21)$$

where A_{ab} and A_{ISb} are the response of the analyte and internal standard spiked into the matrix before the extraction procedure, while A_a and A_{IS} are the response of the analyte and internal standard spiked into the matrix, at the same concentration level, after the extraction procedure, respectively.

Although high recovery values are desirable to maximize the sensitivity of the method, it does not need to be 100%, but it should be consistent, accurate, and reproducible [192]. Despite there are no specific criteria to evaluate this parameter, some guidelines specify that it should be greater than 50% [181]. When analyzing the internal standard, its recovery should be within 15% of the value determined for the analyte [186].

4.8.9. Matrix effects

The principal approach of this experiment is to compare the peak area of the analyte spiked in blank matrix extracts from different origins with pure solutions containing equivalent amounts of the analyte [182, 193]. This should be performed using at least six blank samples from different origins and for three concentration levels [177, 182, 187, 192]. However, as mentioned, the plasma was used from a pool, due the difference between the collection tubes on which the samples were collected.

To evaluate the matrix effect, three levels of concentration were selected (low, medium and high), corresponding to 0.07, 0.5 and 0.8 µM, and prepared in triplicate. In plasma samples, 100 µL of plasma were subjected to the extraction procedure and to the collected supernatant 10 µL of a mix solution containing the analytes and internal standards were added. It was prepared a standard solution in methanol which was spiked with 10 µL of the same mix solution. This was also prepared at the same levels of concentration used in the plasma samples.

Matrix effect can be expressed in terms of matrix influence factor (f) and calculated through equation (4.22) [182].

$$f = \frac{A_{\,post-extracted\ spiked\ sample} - A_{standard\ solution}}{A_{standard\ solution}} \qquad (4.22)$$

where f is the matrix effect, $A_{\,post-extracted\ spiked\ sample}$ is the peak area of the compound of interest spiked in the sample after the extraction procedure and $A_{standard\ solution}$ is the peak area of the compound of interest at the same concentration but in a pure standard solution.

Matrix factor can be defined as the ratio between the peak response in the presence of matrix ions and the peak response in the absence of matrix ions, where peak response is defined as the peak area or peak area ratio (ratio of the peak area of the analyte vs that of the internal standard) of chromatographic peaks. Because of the similarities in chemical properties and elution times of the stable-isotope labeled internal standard and the analytes, the matrix factors for an analyte and its stable-isotope labeled internal standard are usually similar [187].

When using the previous equation, negative results indicate suppression, while positive results may indicate ion enhancement. A value equal to zero would represent no matrix effect [182, 192, 194]. As criteria to evaluate matrix effect, the variability in matrix factors, measured by the coefficient of variation (CV), should be lower than 15% [187, 192], since it indicates that changes in the matrix will not significantly influence the results [182]. The value of %CV may be assessed through equation (4.23) [186].

$$\%CV = \frac{S}{\bar{X}} x\ 100 \qquad (4.23)$$

where $\%CV$ is the coefficient of variation of the matrix effects, S is the standard deviation and $\bar{X}$ is the mean value.

4.9. Application of the analytical method to biological samples

After the validation procedure, the developed method was applied in biological samples, which included three different groups: negative control, positive control and PD patients. This application is essential to prove the reliability of the method.

Eight, seven and seven samples were selected from the negative control group, PD patients' group and positive control group, respectively. In the selection of plasma samples from patients and positive control group, its was taken into account the dose of medication that the patients were taking, in order to have a great variability of samples. Therefore, samples from patients which have been prescribed with low, medium and high doses of L-DOPA were chosen, in positive control samples and PD patients' samples. In the control group, the criteria taken into account was the age, since samples from patients with similar age to those selected from the other groups were preferred.

All plasma samples were processed according with the extraction protocol stated in section 4.7. To each plasma aliquot (100 µL), 10 µL of a mix containing the six internal standards were added. Then, 10 µL of each sample were injected into the LC-MS/MS system. The samples were processed in a specific order: negative control samples, PD patients' samples, positive control samples.

5. Results and discussion

5.1. Method development

In this project, the method development and validation involved the analysis of six analytes (L-tyrosine, L-DOPA, DA, 3-MT, DOPAC and HVA). The results obtained during this process and used to determine which parameters to use in the spectrometric settings are presented in this section. The optimization of these parameters is essential to establish the optimal conditions for each one of the analytes, namely the best ionization conditions to reduce the fragmentation and achieve the maximum abundance of the protonated molecules.

5.1.1. Fragmentation spectra

During the method development, the fragmentation spectra of each one of the analytes were obtained to determine the transitions to monitor throughout the validation process. The fragmentation spectra are representative of the fragments formed in the collision cell due to the dissociation of energetically unstable molecular ions. Thus, to obtain these spectra with the possible fragments formed by each analyte, it is applied a gradual increase in the CE applied to the analyte. This allows to select the ion to monitor, once the product ions are generated at different collision energies, and to find the optimum CE for each product ion. In Figure 5.1 it is presented an example of the CE values corresponding to three different fragments of DA, where it is possible to notice that the smaller fragment (p. e. m/z of 65.0) need higher collision energies, while the largest fragment (p. e. m/z of 137.2) require lower collision energies. This represents the quantity of energy that the precursor ion receives, being accelerated in the collision cell, where it collides with gas molecules and then fragments.

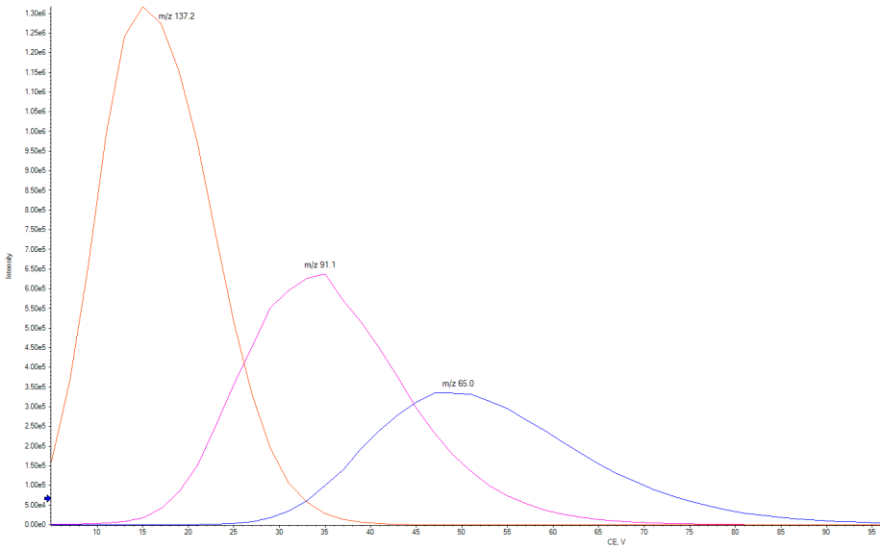

Figure 5.1. Collision energy ramping values for three fragments of dopamine. Each peak is signaled with the corresponding fragment. It is possible to notice that smaller fragments will need higher collision energies, while the largest fragments are produced with lower energies.

Besides the CE, there is another parameter which also should be optimized, namely the DP. This parameter is important to minimize solvent cluster ions that may attach to the analyte. The DP is adjusted by raising it high enough so that adduct peaks are eliminated but not so high that the analytes begin to fragment. When performing the optimization of this parameter, as seen in Figure 5.2, the maximum height of the peak will correspond to the best value of DP.

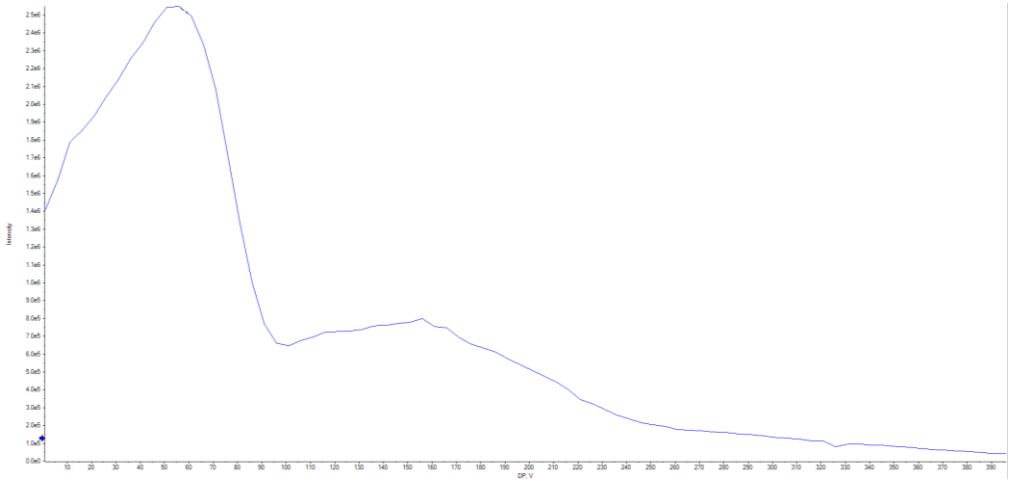

Figure 5.2. Declustering potential ramping for dopamine. Results show a maximum intensity at 56V for this molecule.

After the optimization of the indicated parameters, the fragmentation spectra of each one of the studied analytes can be found, presenting all the fragments obtained in CID conditions. These spectra allow to determine which transitions to monitor during the method development. In MRM

detection, product ions with lower m/z values are problematic, once the chemical noise (background) is more intense at these values. Then, the ideal product ion to monitor when using MRM detection is the one observed at a good relative abundance in the spectrum.

The fragmentation spectrum of DA (Figure 5.3) presents a peak with m/z of 154.20, which corresponds to the intact molecule and three other intense fragments with m/z of 65.07, 91.09 and 137.18, which were chosen to monitor the analyte. The peak with m/z of 154.20 is obtained when the least amount of collision energy was applied, since that energy was not enough to fragment the analyte. The energy necessary to obtain the remaining fragments is the determinant factor when choosing the fragments to monitor, since the fragments that require higher CE are less likely to be produced, while the other fragments are more sensitive and easily formed.

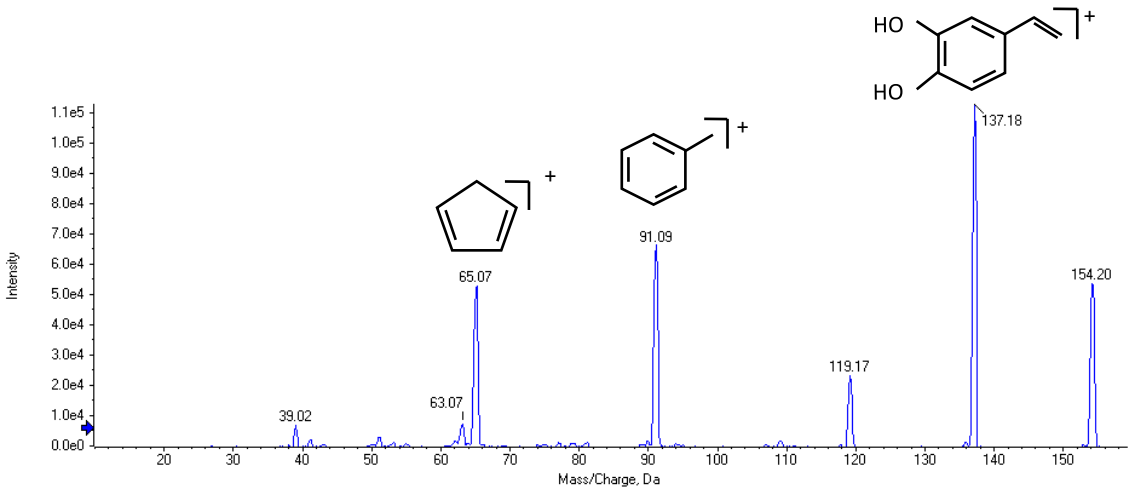

Figure 5.3. Average fragmentation spectrum of dopamine, with m/z of 154.20 $[M+H]^+$. The fragments were obtained by ESI in positive ionization mode and varying the collision energy from 5V to 130V by direct infusion at 10 µL/min of a 1 µM dopamine hydrochloride solution. The main peaks are illustrated with the respective fragment.

The fragments present in the average fragmentation spectrum of DA are characteristic of the molecule and are due to the loss of parts of the intact molecule, as illustrated in Figure 5.4. The fragment with higher intensity (m/z of 137.18) corresponds to $[M+H-NH_3]^+$, the second most intense (m/z of 119.17) corresponds to $[M+H-NH_3-OH]^+$ and the last (m/z of 65.07) corresponds to $C_5H_5^+$. The represented fragments are the ones illustrates in Figure 5.3.

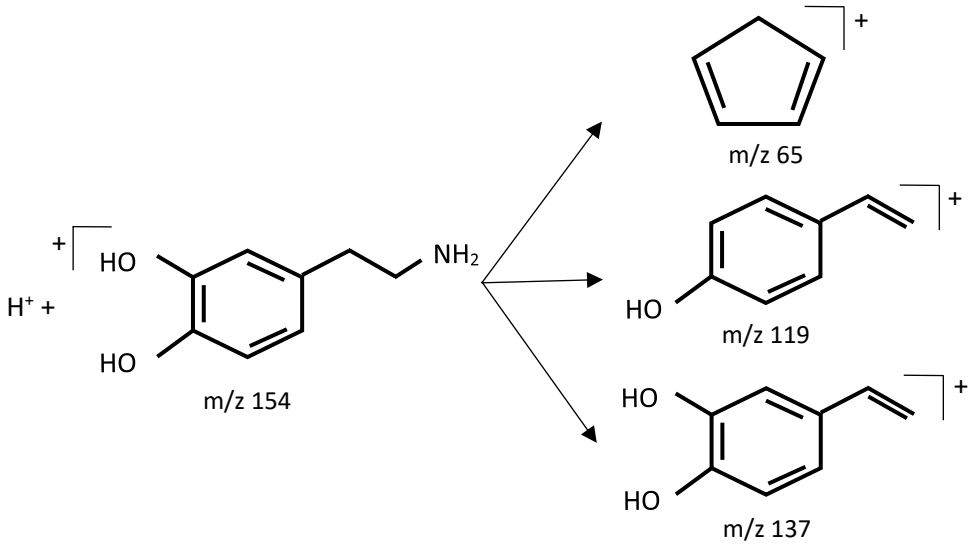

Figure 5.4. Characteristic fragments observed in mass spectrometry for dopamine $[M+H]^+$, with m/z of 154,20. Adapted from: [208, 209].

When it comes to the internal standard (Figure 5.5), the peak with m/z of 158 corresponds to the intact analyte, as it is a tetra deuterated molecule (DA-d4). The fragments to monitor in the internal standard analysis are 95.06, 123.08 and 141.09. It is important to notice that the fragmentation of DA-1,1,2,2-d4 is similar to the fragmentation of DA hydrochloride, since the difference between them only relies on the substitution of four hydrogens by four deuteriums.

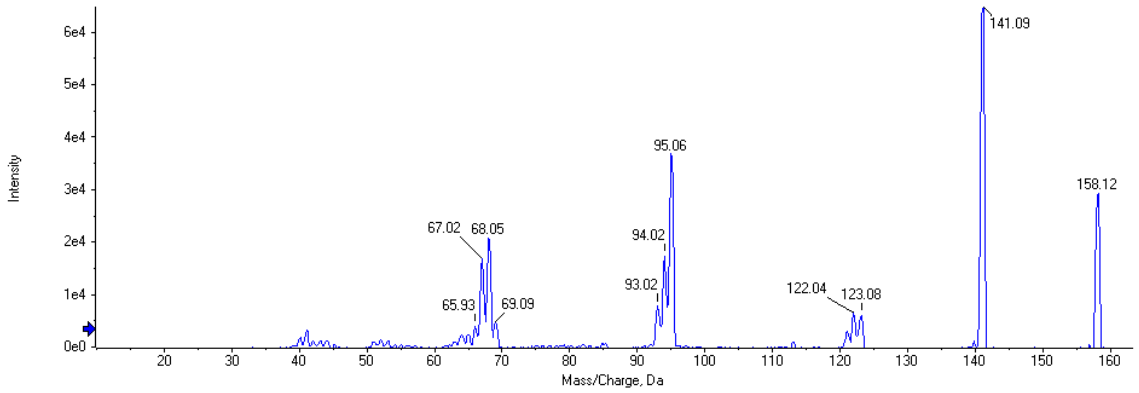

Figure 5.5. Average fragmentation spectrum of dopamine-1,1,2,2-d4, with m/z of 158.12 $[M+H]^+$. The fragments were obtained by ESI in positive ionization mode and varying the collision energy from 5V to 130V by direct infusion at 10 µL/min of a 5 µM dopamine-1,1,2,2-d4 solution.

It was also performed an analysis of DA using the MRM triple quadrupole operating in the negative mode. In this analysis, the m/z corresponding to the entire analyte was 152.20, once the analyte was in the deprotonated state. However, the peaks intensity was lower than the one

obtained in the positive mode. Then, for this reason, it was stated that the analysis of DA would be performed using the MRM triple quadrupole operating in the positive mode.

The same approach was used with L-tyrosine (Figure 5.6). The analyte was clearly identified by MS/MS fragmentation of the precursor ion $[M+H]^+$, which corresponds to the peak with m/z of 182.19, when lower CE was applied. It can also be observed in the fragmentation spectrum three other intense peaks, corresponding to the fragments with m/z of 91.06, 136.18 e 165.13, which were chosen to be monitored. The first fragment results from cleavage of the ammonia unit, the second is produced by the consecutive loss of water and a carbonyl group, and the last results from the consequent loss of the ammonia, a water molecule and a carbon group.

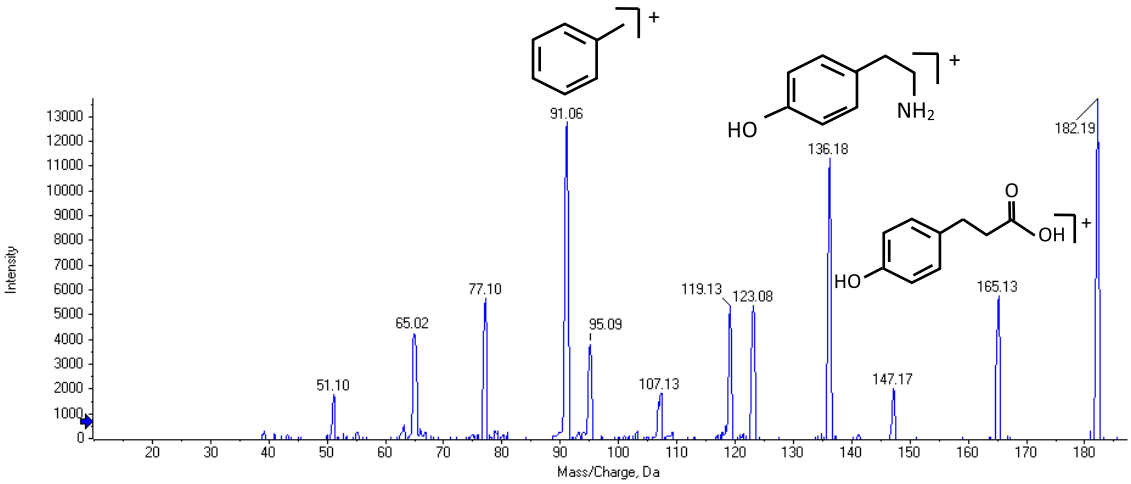

Figure 5.6. Average fragmentation spectrum of L-tyrosine, with m/z of 182.19 $[M+H]^+$. The fragments were obtained by ESI in positive ionization mode and varying the collision energy from 5V to 130V by direct infusion at 10 µL/min of a 1 µM L-tyrosine solution. The main peaks are illustrated with the respective fragment.

In the fragmentation spectrum of the internal standard (Figure 5.7), it is possible to see, once again, a similarity with the spectra of the analyte, since the only difference existing between them arises from the substitution of the hydrogens for deuterium. Then, in this spectrum, the peak with m/z of 189.07 corresponds to the intact molecule and the fragments that were chosen to be monitored were 96.07, 143.09 e 172.02, since they are those with higher intensity.

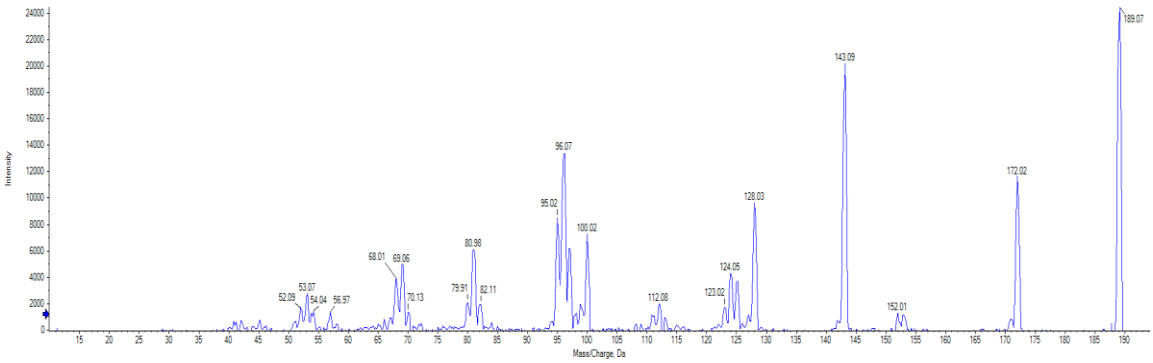

Figure 5.7. Average fragmentation spectrum of L-tyrosine (d7), with m/z of 189.07 $[M+H]^+$. The fragments were obtained by ESI in positive ionization mode and varying the collision energy from 5V to 130V by direct infusion at 10 µL/min of a 1 µM L-tyrosine (d7) solution.

In the fragmentation spectrum of L-DOPA (Figure 5.8), the peak with m/z of 198.03 corresponds to the intact molecule, since it required less energy to be formed. The fragments with m/z of 181.00, 152.01 and 135.01 were chosen to be monitored in the posterior analysis of this analyte.

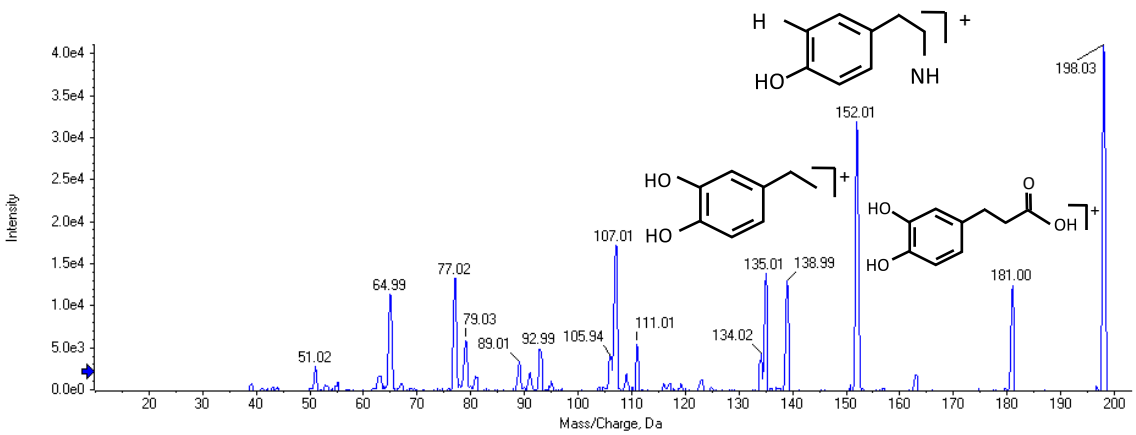

Figure 5.8. Average fragmentation spectrum of levodopa, with m/z of 198.03 $[M+H]^+$. The fragments were obtained by ESI in positive ionization mode and varying the collision energy from 5V to 130V by direct infusion at 10 µL/min of a 1 µM levodopa solution. The main peaks are illustrated with the respective fragment.

When it comes to the internal standard (Figure 5.9), the peak with m/z of 201.25 refers to the intact analyte and the fragments with m/z of 183.15, 154.18 and 137.15 were chosen to be monitored.

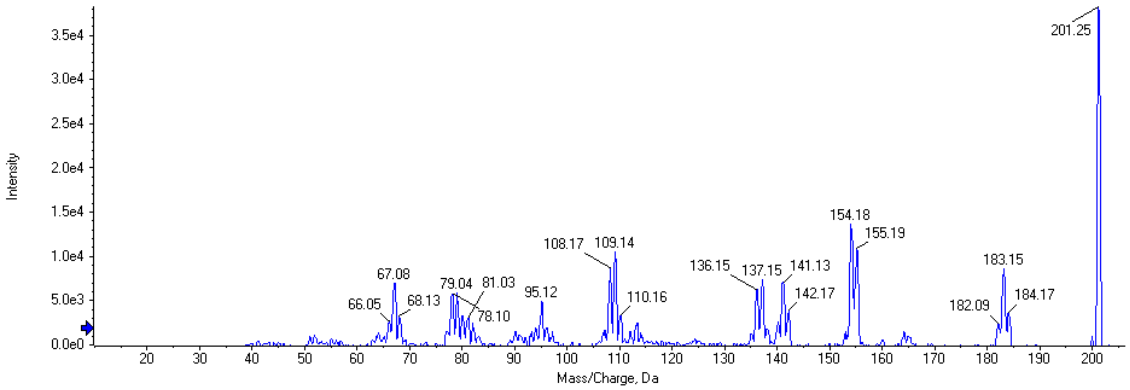

Figure 5.9. Average fragmentation spectrum of levodopa (ring-d3), with m/z of 201.25 $[M+H]^+$. The fragments were obtained by ESI in positive ionization mode and varying the collision energy from 5V to 130V by direct infusion at 10 µL/min of a 1 µM levodopa (ring-d3) solution.

In the spectrometric analysis of 3-MT (Figure 5.10) it is possible to find a peak with a m/z of 168.17, which is represented with the intact molecule. As seen in the spectrum, the fragments with m/z of 151.13, 119.11 and 91.02 are three of the most intense fragments, and, consequently, these were chosen to monitor the analyte.

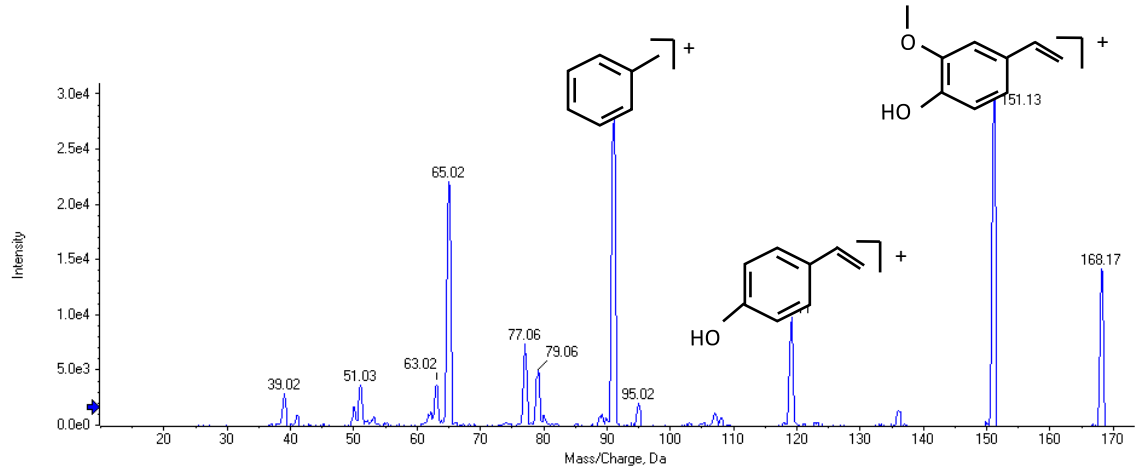

Figure 5.10. Average fragmentation spectrum of 3-methoxytyramine, with m/z of 168.17 $[M+H]^+$. The fragments were obtained by ESI in positive ionization mode and varying the collision energy from 5V to 130V by direct infusion at 10 µL/min of a 1 µM 3-methoxytyramine solution. The main peaks are illustrated with the respective fragment.

In the spectrum of the internal standard (Figure 5.11), the peak with a m/z of 172.11 corresponds to the molecule and the fragments with m/z of 155.09, 123.08 and 95.07 were chosen to the posterior analysis.

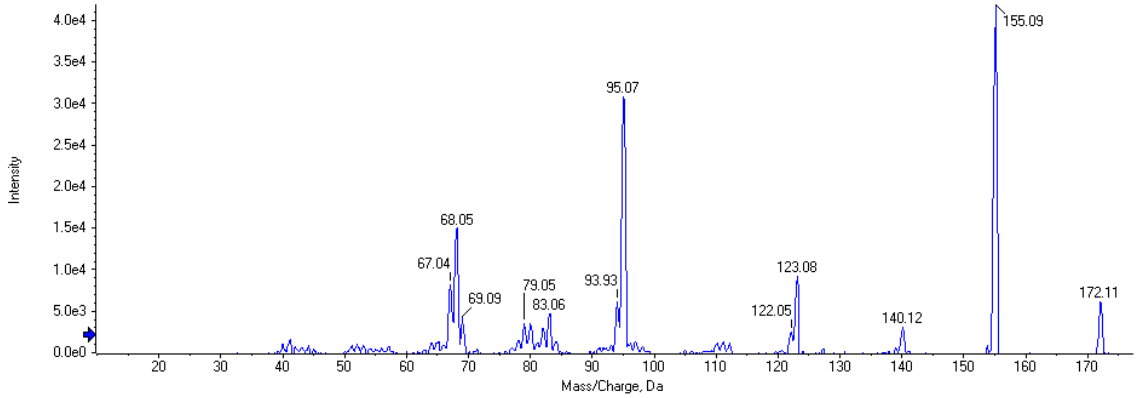

Figure 5.11. Average fragmentation spectrum of 3-methoxytyramine (1,1,2,2-d4), with m/z of 172.11 $[M+H]^+$. The fragments were obtained by ESI in positive ionization mode and varying the collision energy from 5V to 130V by direct infusion at 10 µL/min of a 1 µM 3-methoxytyramine (1,1,2,2-d4) solution.

The fragmentation spectra of DOPAC and its internal standard were acquired in negative ionization mode. In the DOPAC spectrum (Figure 5.12), the peak with m/z of 167.11 corresponds to the intact molecule and the peak with m/z of 123.10 matches with a characteristic fragment of this analyte. The intensity of the remaining fragments is lower when compared with the most intense peak, which difficult their identification within the spectrum. However, two other transitions were chosen, which were used as qualifiers. Then, the fragments with m/z of 123.10, 122.20 and 95.20 were chosen to monitor the analyte.

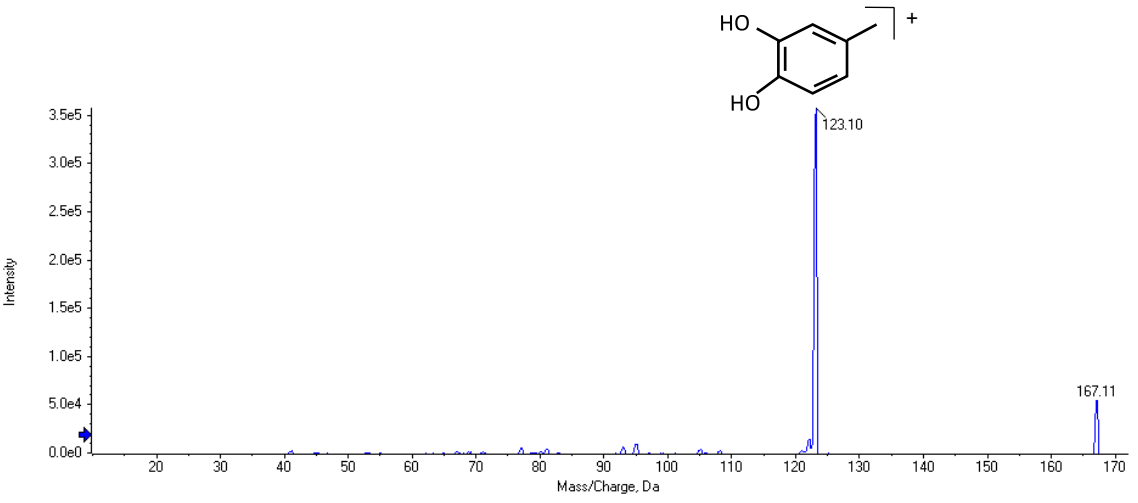

Figure 5.12. Average fragmentation spectrum of 3,4-dihydroxyphenylacetic acid, with m/z of 167.11 $[M+H]^+$. The fragments were obtained by ESI in negative ionization mode and varying the collision energy from -130V to -5V by direct infusion at 10 µL/min of a 10 µM 3,4-dihydroxyphenylacetic acid solution. The main peaks are illustrated with the respective fragment.

In what concerns to the internal standard (Figure 5.13), only one characteristic fragment is clearly visible in the spectrum, since the other fragments also present a very low intensity. In this

case, the fragments with m/z of 128.22, 126.20 and 100.20 were chosen for the analysis of the molecule.

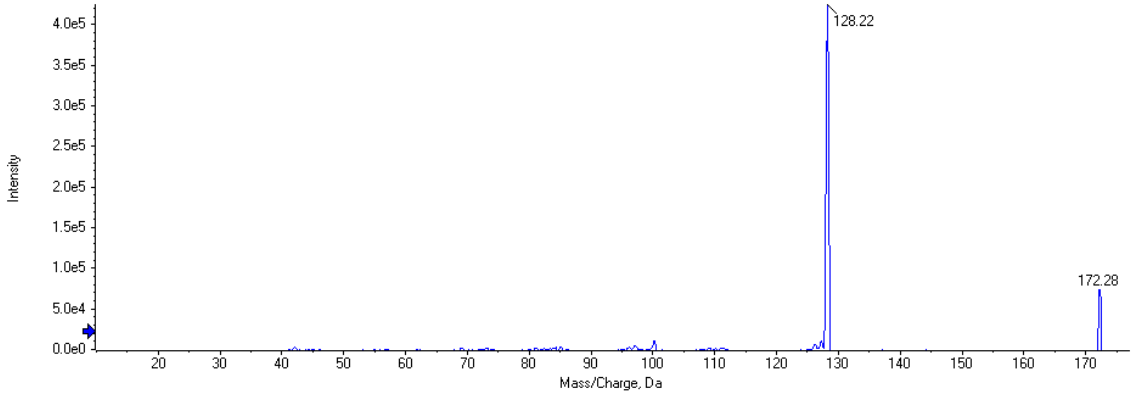

Figure 5.13. Average fragmentation spectrum of 3,4-dihydroxyphenylacetic acid (Ring-d3, 2,2-d2), with m/z of 172.29 $[M+H]^+$. The fragments were obtained by ESI in negative ionization mode and varying the collision energy from -130V to -5V by direct infusion at 10 µL/min of a 10 µM 3,4-dihydroxyphenylacetic acid (Ring-d3, 2,2-d2) solution.

In the analysis of HVA and its internal standard, the mass spectrometer was also operated in negative ionization mode. In Figure 5.14 it is possible to see that, as in DOPAC analysis, not all the fragments are clearly visible in the fragmentation spectrum, even though in this case it can be seen quite well two fragments. For HVA, fragments with m/z of 137.25, 136.7 and 122.18 were chosen to monitor this molecule.

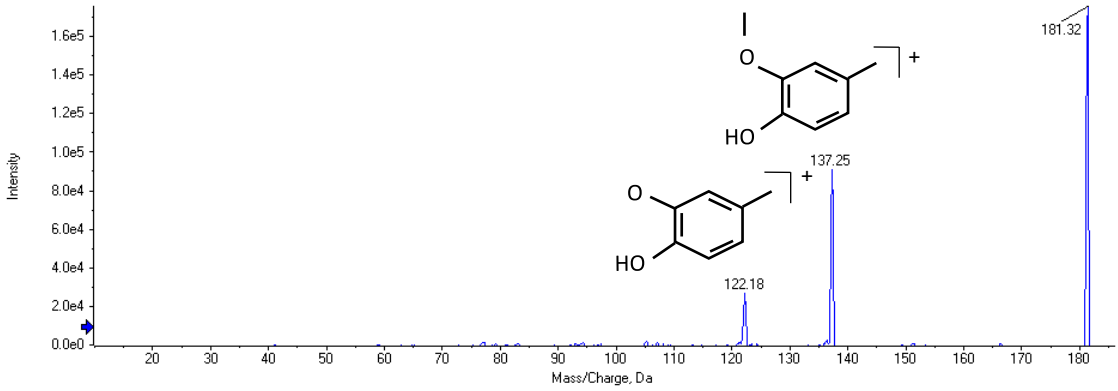

Figure 5.14. Average fragmentation spectrum of homovanillic acid, with m/z of 181.32 $[M+H]^+$. The fragments were obtained by ESI in negative ionization mode and varying the collision energy from -130V to -5V by direct infusion at 10 µL/min of a 1 µM homovanillic acid solution. The main peaks are illustrated with the respective fragment.

The internal standard spectrum also presents two of the characteristic fragments of the molecule with higher intensity, being that the fragments with m/z of 140.26, 139.80 and 122.19 were chosen to identify this analyte in the following analysis.

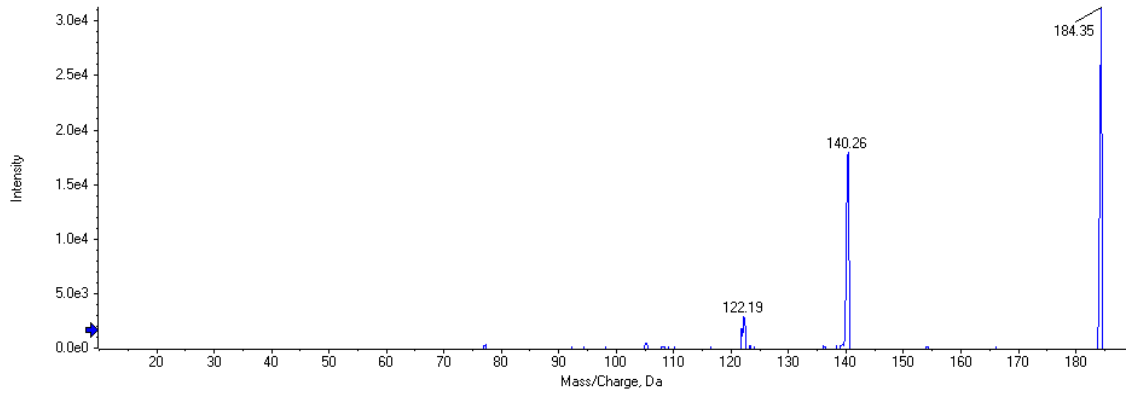

Figure 5.15. Average fragmentation spectrum of homovanillic acid (d3), with m/z of 184.35 $[M+H]^+$. The fragments were obtained by ESI in positive ionization mode and varying the collision energy from -130V to -5V by direct infusion at 10 µL/min of a 1 µM homovanillic acid (d3) solution.

5.1.2. Compound identification

The previous data allows to choose the ion transitions (m/z) that will be monitored in the MRM mode to each analyte and internal standard. The selected transitions are presented in Tables 5.1 and 5.2.

Table 5.1. MRM transitions and respective retention time (RT) used in the identification of the studied analytes.

Compound	Transitions (m/z)		RT (min)
	Q1	Q3	
L-tyrosine	182.2	91.1 136.2 165.1	0.68
L-DOPA	198.2	135.1 152.1 181.1	0.68
DA	154.2	65.0 91.1 137.2	0.71
3-MT	168.3	91.0 119.1 151.1	0.71
DOPAC	167.0	95.2 122.2 123.2	3.38
HVA	181.0	122.2 136.7 137.2	3.68

Table 5.2. MRM transitions and respective retention time (RT) used in the identification of the studied internal standards.

Compound	Transitions (m/z)		RT (min)
	Q1	Q3	
L-tyrosine_d7	188.2	96.1 143.2 172.2	0.68
L-DOPA_d3	200.2	154.1 155.2 183.2	0.68
DA_d4	157.1	94.1 95.1 141.2	0.71
3-MT_d4	171.1	68.0 94.0 123.1	0.71
DOPAC_d5	173.2	100.2 126.2 128.2	3.38
HVA_d3	185.2	122.2 139.8 140.3	3.68

To accommodate possible changes that occur at the level of the sample preparation process, it is important to use an internal standard. However, the choice of an adequate internal standard relies on some specific criteria. The internal standard is a compound that should not be present in the samples that will be analyzed, it should be chemically and physically similar to the analyte under study (usually, a stable-isotope-labelled internal standard), it should elute in a similar retention time to the analyte and present a similar signal intensity [165].

It is often used as stable-isotope the deuterium. In this case, the molecular weight of the compound is higher than the unlabeled precursor, which ensures that the ions in the molecular ion region of the unlabeled compound does not occur in the same m/z region as those from the labeled molecule [165].

Therefore, for these reasons, it was stated that the deuterated compounds of each analyte would be used as its respective internal standards.

5.1.3. Plasma analysis

As a first step prior to the validation procedure, several analyzes in solvent were performed to discover the working range that should be used during the development and validation of the current method. Before evaluating if the working range was adequate to perform the validation in plasma samples, some preliminary tests in matrix were required.

Human plasma samples were fortified with the analytes under study to verify if all of them could be properly detected in the matrix. Then, three different aliquots containing 80 µL of plasma were prepared. The first aliquot was spiked with 10 µL of a mix containing the six analytes and 10 µL of a mix containing the six internal standards before the extraction procedure. The second aliquot was spiked with 10 µL of the mix with the internal standards before the extraction and with 10 µL of the mix with the analytes after the extraction. Finally, the third aliquot was only spiked with 10 µL of the internal standard mix but not with the analytes, which allowed us to analyze this aliquot as a "blank" matrix. The plasma samples were all subjected to the same extraction procedure (section 4.7).

In this analysis, samples which were evaporated and resuspended after the extraction were compared with samples which were not subjected to the evaporation step (the supernatant was placed in a vial and analyzed), to define the proper extraction method to apply to plasma samples. This allowed to conclude that, in overall, better results were obtained in the samples that were not evaporated. An example of that is presented in Figure 5.16, where it is possible to see that the intensity of DA is higher when no evaporation is performed.

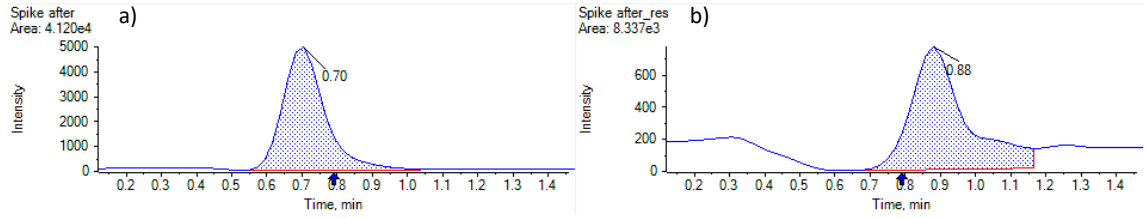

Figure 5.16. Chromatogram of the fragment with m/z 91.1 of dopamine in a sample that was not evaporated and resuspended, being the supernatant injected into the LC-MS/MS system (a) and in a sample that was evaporated and resuspended (b).

The results also allowed to conclude that only one analyte (HVA) could be properly detected in the "blank" matrix, since the remaining analytes did not produce any peak response (see appendix 8.2). In Figure 5.17 there is an example of one of DA fragments, were it is possible to see a lack of response in the matrix (Figure 5.17 a)). Moreover, it was also possible to see that there

were several losses during the extraction procedure, by comparing the samples who were spiked before and after the extraction procedure (Figure 5.17 b) and c), respectively).

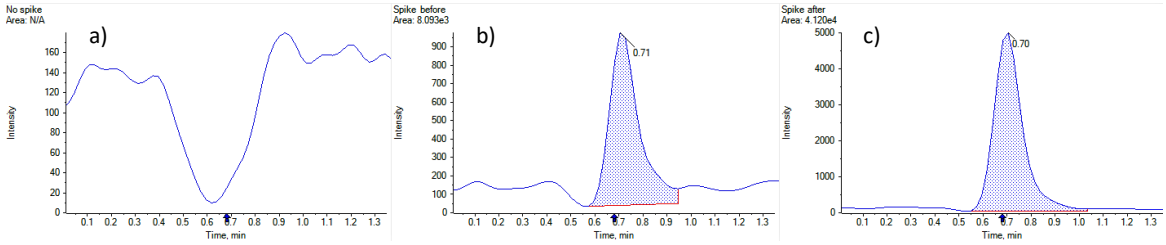

Figure 5.17. Analysis of the fragment with m/z 91.1 of dopamine in a "blank" plasma sample (a), in a plasma sample that was spiked with 10 µL of a mix containing the six analytes and the six internal standards before the extraction procedure (b), and in a plasma sample that was spiked with 10 µL of a mix containing the six analytes and the six internal standards after the extraction procedure (c).

Since it was notice that in "blank" plasma sample any endogenous analyte was detected, it was performed a study using different amounts of plasma, to analyze if the lack of response could be due to the small amount of plasma used in the previous analysis (80 µL). Therefore, 200 µL, 300 µL and 400 µL of plasma were tested. However, no peak response was obtained to the same analytes (see appendix 8.3). An example of one of DA fragments is presented in Figure 5.18, were it is possible to see an apparent signal suppression at the expected retention time.

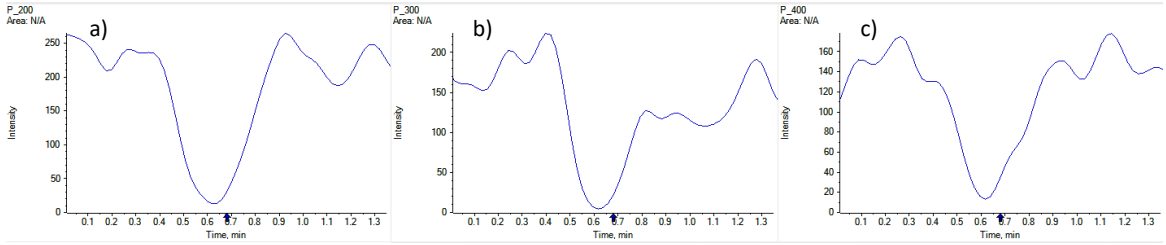

Figure 5.18. Chromatogram of the fragment with m/z 91.1 of dopamine in 200 µL (a), 300 µL (b) and 400 µL (c) of plasma.

In what concerns to detection of endogenous L-tyrosine in plasma, it was possible to observe a peak in the expected retention time of L-tyrosine, however, its intensity was constant, independently of the amount of plasma used. This raised some doubts about the reliability of the data and it was considered that maybe this peak did not correspond to L-tyrosine and was an artifact of the matrix, making its detection in plasma samples doubtful.

Nevertheless, before proceeding with the validation methodology, the working range used in the analysis in solvent was evaluated in plasma. This allowed to test the lowest concentrations that could be detected in plasma samples and choose the concentration range to be used in the

linearity study. It was stated that the concentration range in plasma would be the double of the one used in the solvent, since the results showed that the values used in solvent were too low to detect in plasma and that higher concentrations could be achieved with a linear behavior. Even though DA and L-DOPA were detected in spiked samples in the previous analysis, in the calibration curve both analytes were not properly detected, which may indicate that the peaks that had been identified could not correspond to the analytes.

Taking into account the difficulties found in the detection of L-tyrosine, L-DOPA and DA in plasma samples, it was stated that the validation procedure would be performed in solvent and plasma. Therefore, all DA metabolism was analyzed in solvent while in plasma only 3-MT, DOPAC and HVA were considered. However, it is important to highlight that not all the validation parameters were evaluated in solvent, for instance the recovery and matrix effects, since these can only be studied in matrix samples.

This analysis was important to highlight the difficulties faced during a method development and that this process is hard-working and time-consuming. Taking into account the amount of time available to perform the current work, it was not possible to perform more tests in order to improve the chromatographic analysis and detect all the analytes in plasma samples.

5.2. Analytical method validation

The data that is presented in this section was analyzed through an Excel® spreadsheet that was specifically developed for the analysis of analytical method validation, which applies all the criteria presented in section 3.9. Due to the wide results obtained for each validation parameter, only the main results and some examples of the application of the criteria are expressed in this section. The remaining results are presented in the appendices.

5.2.1. Selectivity

During the method development and validation, it is essential to prove that the method is capable of measure the intended analyte(s) and that their quantification is not affected by the presence of other endogenous compounds existing in the biological matrix [187]. Then, evidence should be provided that the substance quantified is the intended analyte, being very important to obtain a signal free from the influence of any other specie present in the sample matrix [210].

A common approach to establish the method selectivity is to demonstrate lack of response in blank matrices, in order to prove that there are no signals interfering with the signal of the

analyte and/or the internal standard [181, 184, 211]. This approach has become state of the art, and the requirement that was established was that it should be analyzed, at least, six different sources of blank plasma [184, 211]. Once interferences, even if present in small quantities, can affect the quantification of unknown samples with concentrations near the LOQ, the selectivity should be established with respect to interferences from endogenous substances [212]. The blank matrix, if not containing the potential interfering compounds, are spiked with the pure substance of interest, and its signal is compared with the signal obtained with blank matrices, processed without the analyte [204].

Thus, in plasma analysis, six independent sources of blank matrix were divided into two aliquots. One aliquot was spiked with the analytes and internal standards (positive samples) and the other was not spiked with any compound (negative samples). In solvent, three positive and negative samples were used, being that positive aliquots were spiked with the compounds and negative aliquots were not spiked with anything.

Examples of the results obtained in the analysis of selectivity in solvent and plasma are presented in Figure 5.19 and Figure 5.20, for both positive and negative samples. Through the visual evaluation of the obtained chromatograms we can verify that in the negative samples there is no peak with the same RT as the analytes.

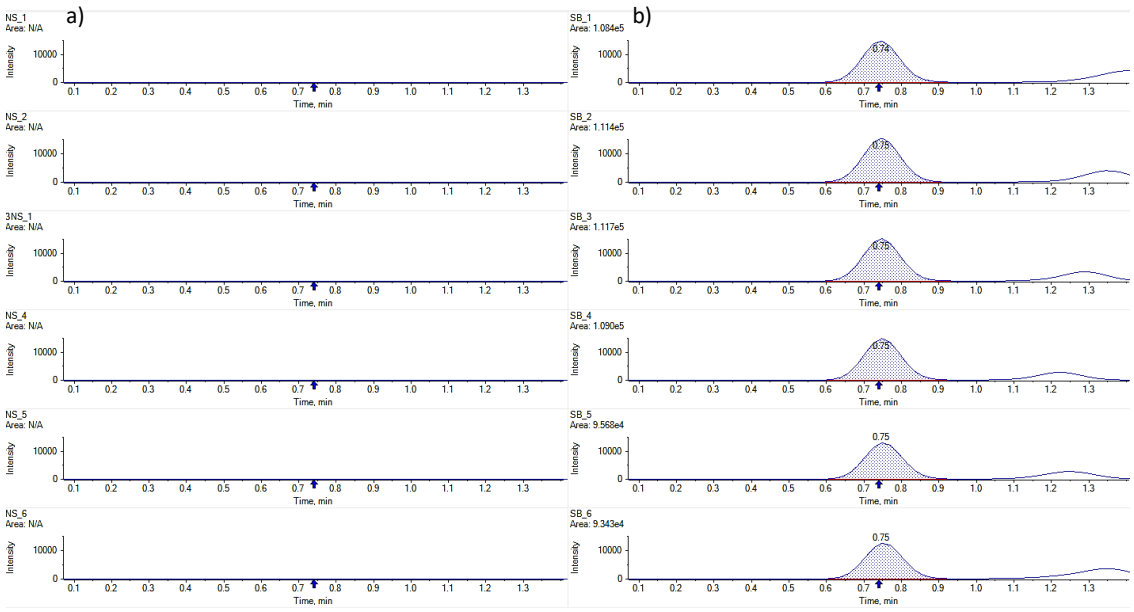

Figure 5.19. Chromatographic spectra of the fragment with m/z 91.0 of 3-methoxytyramine for the selectivity in plasma. a) Six different sources of blank plasma samples that were not spiked with any compound (negative samples). b) Six blank plasma samples spiked with a mix containing the analytes and the internal standards (positive samples).

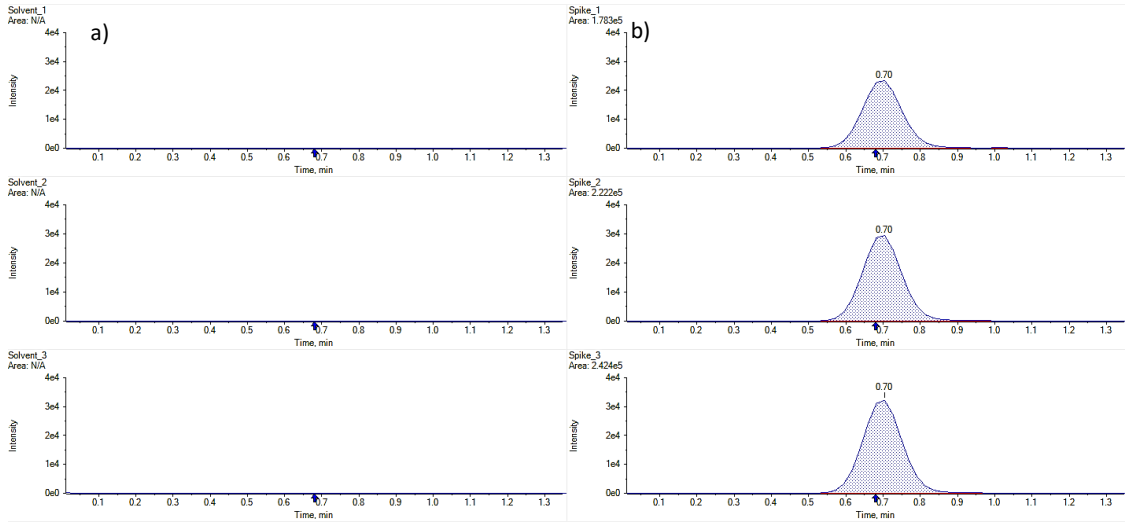

Figure 5.20. Chromatographic spectra of the fragment with m/z 91.1 of dopamine for the selectivity in solvent. a) Three different solutions constituted by methanol that were not spiked with any compound (negative samples). b) Three solvent solutions spiked with a mix containing the analytes and the internal standards (positive samples).

For a proper identification of the analytes under study, the WADA criteria were applied, as established in section 4.8.1 [196]. The data obtained for both positive and negative samples was analyzed through a specific excel spreadsheet, properly developed for the analysis of analytical method validation data. The criteria applied in the negative samples were the opposite of the positive ones.

According to the WADA criteria, when analyzing the performance of the chromatographic separation, both RT and RT_{ratio} can be used to assess this parameter, being usually chosen the smaller value [196]. Then, in the present study, it was decided to use the RT of the analyte, since the use of the RT_{ratio} did not allowed to validate this parameter, because most values did not fulfill the established criteria.

In Table 5.3 there is an example of one of the three solvent samples that were used to study the selectivity of DA in solvent. The values of all the transitions were within the criteria in positive and negative samples. The remaining positive and negative samples also fulfil the WADA criteria (Table 8.3, appendix 8.4). Since the negative samples did not present any interference, the method proved to be selective for DA in solvent.

Table 5.3. Application of the acceptance WADA criteria for the identification of dopamine in solvent.

	Transition	Relative abundance		S/N		ΔRT	
Criteria	154.2/65.0	8.999	18.999	>3		0.684	0.711
	154.2/91.1	26.485	39.727			0.683	0.711
	154.2/137.2	90.000	110.000			0.680	0.708
	Transition	**Absolute area**	**Relative area**	**S/N**	**RT_A**	**RT_{IS}**	**RT_{ratio}**
Positive #1	154.2/65.0	75383.131	13.999	1014.081	0.697	0.689	1.013
	154.2/91.1	178276.702	33.106	1497.620	0.697	0.689	1.013
	154.2/137.2	538499.379	100.000	1858.686	0.694	0.689	1.008
	Transition	**Absolute area**	**Relative area**	**S/N**	**RT_A**	**RT_{IS}**	**RT_{ratio}**
Negative #1	154.2/65.0	-	-	-	-	-	-
	154.2/91.1	-	-	-	-	-	-
	154.2/137.2	-	-	-	-	-	-

In Table 5.4 there is an example of one of the six plasma samples that were used to study the selectivity of 3-MT in plasma. In the analysis of 3-MT, the third fragment (151.1) did not allowed to validate the obtained data, since it would not fulfil the criteria applied in the study. Moreover, there were some doubts about the reliability of the chromatograms of this fragment due to the differences obtained when compared with the other two. Then, this fragment was not used in the evaluation of any validation parameter of 3-MT in solvent and plasma samples.

Table 5.4. Application of the acceptance WADA criteria for the identification of 3-methoxytyramine in plasma.

	Transition	Relative abundance		S/N		ΔRT	
Criteria	168.3/91.0	1.279	3.837	>3		0.730	0.760
	168.3/119.1	90.000	110.000			0.728	0.758
	Transition	**Absolute area**	**Relative area**	**S/N**	**RT_A**	**RT_{IS}**	**RT_{ratio}**
Positive #1	168.3/91.0	108406.439	100.000	528.002	0.745	0.737	1.010
	168.3/119.1	65814.452	60.711	482.206	0.743	0.737	1.008
	Transition	**Absolute area**	**Relative area**	**S/N**	**RT_A**	**RT_{IS}**	**RT_{ratio}**
Negative #1	168.3/91.0	-	-	-	-	-	-
	168.3/119.1	-	-	-	-	-	-

From the analysis of the table, it is possible to conclude that positive and negative samples are within the WADA criteria. Moreover, the remaining five positive and negative samples were also in accordance with the criteria used (see Table 8.9, appendix 8.4), which demonstrates that the developed method is selective for 3-MT in plasma samples.

In solvent, DOPAC and HVA data were within the criteria (see Tables 8.7 and 8.8, appendix 8.4) and the method proved to be selective for these molecules in solvent. In turn, some values of RT_A of L-tyrosine, L-DOPA and 3-MT did not fulfil the criteria (see Tables 8.4-8.6, appendix 8.4), however, it is possible to see through visual evaluation of the chromatographic spectra of the molecules that there is no peak in the negative samples (see Figure 8.10-8.17, appendix 8.4), which means that no interferences occur at the same retention time of the analytes. Then, the method is also selective for these two molecules.

In plasma samples, the method proved to be selective for DOPAC and HVA in plasma (see Tables 8.10 and 8.11, appendix 8.4), since both positive and negative samples were within the criteria.

5.2.2. Linearity

After being known the selectivity of the method it is important to evaluate the relationship between the concentration of the analyte and the respective detector response, throughout the working range [184]. The evaluation of this parameter is essential to prove that the developed method leads to results that are directly proportional to the concentration of the analyte under study in the analyzed samples. This can be achieved by analyzing spiked calibration samples and plotting the respective responses versus the concentrations.

Then, to perform the linearity study, it was assumed that the obtained results followed the simplest linear regression model. Due to the difficulties encountered in the detection of DA, L-DOPA and L-tyrosine in plasma samples during the method development, linearity was studied in both solvent and plasma samples. The calibration curve of the fragment with m/z 91.1 of DA is represented in Figure 5.21.

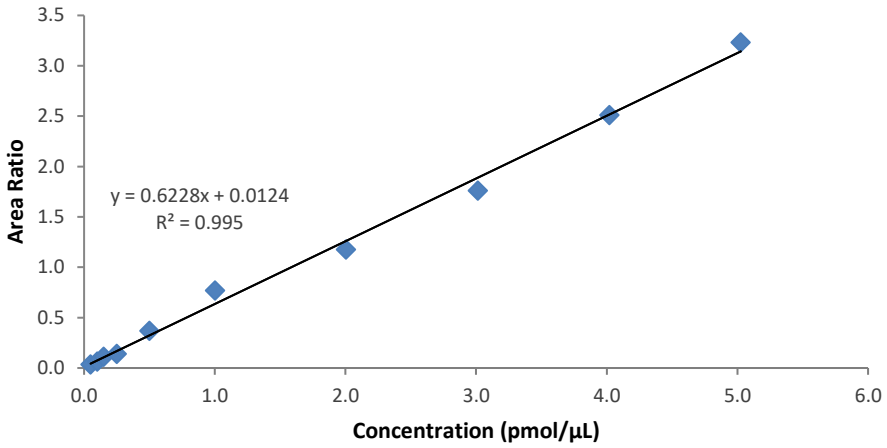

Figure 5.21. Calibration curve for the fragment with m/z 91.1 of dopamine in solvent.

The model appears to be linear for all the molecules, either in solvent and plasma samples, within the working range. In concern with the criteria applied in the classical linear regression, all the molecules were in accordance with the criteria, presenting R^2>0.99 (Tables 5.5 and 5.6) and the confidence interval containing zero. However, since the use of this parameter is not sufficient to prove the linearity of the method, other parameters, for instance the double of the standard error of the regression ($S_{y/x}$) and a visual inspection of residuals versus concentration were used to evaluate the method. Even though visually all the molecules present a randomly distribution around the x axis in the residual evaluation, some of the absolute values of residuals did not fulfil the criteria of being less than the double of $S_{y/x}$ (see appendix 8.5 to appendix 8.13).

Table 5.5. Results obtained in the study of the simple linear regression model for each analyte in solvent.

Compound	Transition[1]	Working range (pmol/µL)	Calibration curve	R^2	$S_{y/x}$
L-tyrosine	182.2/136.2	0.005-0.5	y = 0.2564x + 0.0164	0.997	0.029
L-DOPA	198.2/152.1	0.01-0.6	y = 0.3087x + 0.0045	0.996	0.043
DA	154.2/91.1	0.005-0.5	y = 0.6228x + 0.0124	0.995	0.081
3-MT	168.3/119.1	0.003-0.5	y = 0.3524x + 0.0211	0.997	0.039
DOPAC	167.0/123.2	0.01-0.6	y = 0.2542x + 0.0129	0.999	0.023
HVA	181.0/137.2	0.003-0.5	y = 0.1407x + 0.0069	0.997	0.015

[1]Transition used in quantification

Table 5.6. Results obtained in the study of the simple linear regression model for each analyte in plasma.

Compound	Transition[1]	Working range (pmol/µL)	Calibration curve	R^2	$S_{y/x}$
3-MT	168.3/119.1	0.005-1.0	y = 0.3106x + 0.0546	0.995	0.082
DOPAC	167.0/123.2	0.005-1.0	y = 0.2372x + 0.0239	0.995	0.066
HVA	181.0/137.2	0.005-1.2	y = 0.1293x + 0.0532	0.996	0.036

[1]Transition used in quantification

5.2.2.1. Mandel test

The Mandel's fitting test was used to evaluate the linearity of the calibration curves and which regression model better fits the data [200, 202].

All F_{cal} values showed to be less than the value of F_{crit}, meaning that there is no significant difference between the variances and that the linear adjustment is the more appropriate for the calibration curves of the analytes (Tables 5.7 and 5.8).

Table 5.7. Results obtained from the Mandel test for each molecule in solvent.

Compound	Transition[1]	Mandel test (F_{cal})	F_{crit} (N-1; N-1; 0.95)
L-tyrosine	182.2/136.2	0.36	12.246
L-DOPA	198.2/152.1	2.17	12.246
DA	154.2/91.1	3.97	12.246
3-MT	168.3/119.1	-0.75	12.246
DOPAC	167.0/123.2	2.16	12.246
HVA	181.0/137.2	-1.32	11.259

[1]Transition used in quantification

Table 5.8. Results obtained from the Mandel test for each molecule in plasma.

Compound	Transition[1]	Mandel test (F_{cal})	F_{crit} (N-1; N-1; 0.95)
3-MT	168.3/119.1	-6.11	11.259
DOPAC	167.0/123.2	-3.77	11.259
HVA	181.0/137.2	3.52	11.259

[1]Transition used in quantification

5.2.3. Working range

When using linear regression model, it is assumed that the variances of measured values are constant over the working range (homoscedastic data) [184] and that the residuals are randomly distributed along the x-axis [198]. However, in analytical methodologies it is essential to confirm if there is a significant difference between the variances within the limits of the range [198].

Usually, when the concentration range is large it is expected that there is a difference in the variances and that higher concentrations present larger deviations, which may influence the regression line more than deviations associated with smaller concentrations [198]. Then, plots of residuals versus concentration were obtained to all the analytes, being presented an example of the fragment with m/z 91.1 of DA in Figure 5.22. It is possible to verify that there is an increase of the variances as a function of concentration, which leads to the hypothesis of heteroscedastic data. Nevertheless, a test of homogeneity of variances (F-test) should be performed in order to confirm the results.

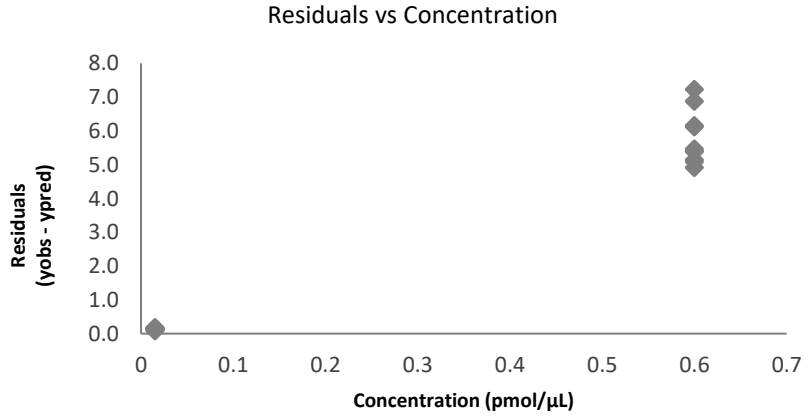

Figure 5.22. Plot of the residuals versus concentration used in the homoscedasticity study of the fragment with m/z 91.1 of dopamine. Ten replicates of the lowest and highest calibrant were analyzed to evaluate their variance.

The test used to evaluate the variances allowed to observe differences between the values of the variances within the limits of the working range (0.015-0.6 µM in solvent and 0.03-1.2 µM in plasma samples).

The results obtained in the homogeneity test (Tables 5.9 and 5.10) show that values of F_{cal} are higher than the tabled value of F_{crit} for every molecule, in solvent and plasma. Then, there is a significant difference between the variances, which means that there is a heteroscedasticity in the data for all the studied compounds.

Table 5.9. Results obtained from the homoscedasticity test for each analyte in solvent.

Compound	Transition[1]	Test of homogeneity of variances (F_{cal})	Criteria $F_{cal} \leq$ Fcrit (N-1; N-1; 0.95)
L-tyrosine	182.2/136.2	4918.647	$F_{cal} \leq 6.541$ *F* (9; 9; 0.95)
L-DOPA	198.2/152.1	3435.369	
DA	154.2/91.1	871.316	
3-MT	168.3/119.1	4886.444	
DOPAC	167.0/123.2	4034.076	
HVA	181.0/137.2	521.171	

[1]Transition used in quantification

Table 5.10. Results obtained from the homoscedasticity test for each analyte in plasma.

Compound	Transition[1]	Test of homogeneity of variances (F_{cal})	Criteria $F_{cal} \leq$ Fcrit (N-1; N-1; 0.95)
3-MT	168.3/119.1	250.035	$F_{cal} \leq 6.541$ *F* (9; 9; 0.95)
DOPAC	167.0/123.2	774.573	
HVA	181.0/137.2	44.136	

[1]Transition used in quantification

5.2.3.1. Weighted least squares linear regression

Once heteroscedasticity was proven through the homoscedasticity test, the choice of an appropriate regression model is requested [184]. When using heteroscedastic data, there are different approaches that can be followed. It is possible to reduce the working range until reach

the homoscedasticity ($F_{cal} \leq F_{crit}$) [180], to use the inverse of variance ($\frac{1}{S^2}$) in each point of the calibration curve or to use weighted least squares linear regression, choosing the appropriated weighting factor [198]. Due to the influence of higher concentrations being different from those of smaller concentrations, it was used the weighted least squares linear regression to compensate these deviations. The empirical weights $\frac{1}{x}$; $\frac{1}{x^2}$; $\frac{1}{\sqrt{x}}$; $\frac{1}{y}$; $\frac{1}{y^2}$; $\frac{1}{\sqrt{y}}$ were studied in order to find the best regression model for each compound [198, 204], through the evaluation of the %RE and R^2.

In order to choose the weighting factor, it was used the percentage of the relative error (%RE), which compares the estimated concentration, from the regression equation obtained for each w_i, with nominal standard concentration in the sample [198]. The best weighting factor is the one that presents the lower value of the sum of the relative errors ($\sum |\%RE|$) in the working range [198, 213].

In Table 5.11 is presented the data of the %RE for the fragment with m/z 91.1 of DA, in order to determine the best fitting model for the calibration curve.

Table 5.11. Relative errors ($\%RE$) and respective sum of the relative errors ($\sum |\%RE|$) calculated by the simplest linear regression and weighted linear regression for each weighting factor (w_i), for the fragment with m/z 91.1 of dopamine in solvent.

Nominal concentration (µM)	Model 1 Unweighted (w_i=1)	Model 2 $\frac{1}{x}$	Model 3 $\frac{1}{x^2}$	Model 4 $\frac{1}{y}$	Model 5 $\frac{1}{y^2}$	Model 6 $\frac{1}{\sqrt{x}}$	Model 7 $\frac{1}{\sqrt{y}}$
0.025	194.51	102.64	39.75	134.14	81.04	161.92	181.92
0.05	38.29	67.63	78.93	64.35	63.98	70.92	68.48
0.1	59.09	49.74	52.65	39.70	39.59	51.27	46.42
0.15	28.51	21.30	21.04	27.50	28.00	24.76	29.05
0.25	37.75	38.30	35.41	34.28	30.54	35.90	33.50
0.5	32.46	33.93	31.75	34.63	33.51	32.25	32.48
1.0	58.79	59.21	56.85	59.63	57.66	58.92	59.01
2.0	30.66	30.64	23.38	29.40	21.31	30.67	30.09
3.0	28.88	28.64	31.11	29.20	32.12	28.50	28.79
4.0	10.27	9.92	17.44	10.44	18.33	9.76	10.03
5.0	14.43	15.21	29.14	15.91	27.26	14.37	14.71
6.0	13.23	12.84	11.18	12.87	9.27	13.61	13.53
$\sum \|\%RE\|$	546.87	469.99	428.63	492.07	442.61	532.84	548.01
R^2	0.99522	0.99520	0.97982	0.99530	0.98558	0.99611	0.99605

To choose the best model, it should present the lowest error and the R^2 should be higher than 0.99. According to what has been established, the $\sum |\%RE|$ of the different weighting factors was compared. The analysis of these values allowed to verify that the models with the lowest relative error were model 2 ($\frac{1}{x}$), model 3 ($\frac{1}{x^2}$) and model 5 ($\frac{1}{y^2}$). When analyzing the second criteria, the value of R^2, it was possible to conclude that, from the previous models, model 2 ($\frac{1}{x}$) was the best model to express the calibration curve behavior, since the other two models did not fulfil the criteria.

When evaluating the data of %RE for the remaining analytes, some variation among the chosen model was observed. For L-tyrosine, L-DOPA, 3-MT and DOPAC in solvent (Tables 8.12 to 8.15, appendix 8.14), the results were similar to the ones found for dopamine, were model 2 ($\frac{1}{x}$) was found to be the best fitting model. For HVA in solvent and 3-MT in plasma (Tables 8.16 and 8.17, appendix 8.14), model 4 ($\frac{1}{y}$) presented the best results, being choose as the best fitting model. In turn, for DOPAC and HVA in plasma (see Tables 8.18 and 8.19, appendix 8.14), model 6 ($\frac{1}{\sqrt{x}}$) was the one that fulfilled the criteria, being the chosen model.

5.2.4. Limit of detection and limit of quantification

As already mentioned, there are three different approaches to determine the LOD and LOQ, namely the visual inspection, the S/N method, and the use of the analytical curve parameters [183, 201]. Although not established which method should preferably be used, since they all present advantages and disadvantages, in the current project it was used the method based in the analytical curve parameters (slope and standard error). This approach has the advantage of presenting higher statistical reliability, once it takes into account the confidence interval of the regression.

Thus, the LOD and LOQ were calculated through equations (4.13) and (4.14) (Section 4.8.3). After the choice of the best calibration model for all the molecules, the standard deviations were recalculated, using equation (4.16).

A summary of the results obtained for the LOD and LOQ calculations are presented on Table 5.12 and 5.13.

Table 5.12. Results obtained for LOD and LOQ for each analyte in solvent.

Compound	Transition[1]	LOD (pmol/µL)	LOQ (pmol/µL)
L-tyrosine	182.2/136.2	0.38	1.15
L-DOPA	198.2/152.1	0.43	1.29
DA	154.2/91.1	0.42	1.28
3-MT	168.3/119.1	0.38	1.14
DOPAC	167.0/123.2	0.26	0.79
HVA	181.0/137.2	0.24	0.71

[1]Transition used in quantification

Table 5.13. Results obtained for LOD and LOQ for each analyte in plasma.

Compound	Transition[1]	LOD (pmol/µL)	LOQ (pmol/µL)
3-MT	168.3/119.1	0.85	2.58
DOPAC	167.0/123.2	0.96	2.92
HVA	181.0/137.2	1.02	3.08

[1]Transition used in quantification

From the obtained results, it was possible to see that, in solvent, DOPAC and HVA are the analytes that present lower limits, when compared with the remaining. In turn, in plasma, 3-MT is the analyte with lower limits. This proved the difficulty in detection and quantification of these type of molecules, which is the main drawback encountered during the development of methods for their quantitative detection.

5.2.5. Precision and accuracy

The analysis of precision can be divided into i) repeatability, ii) intermediate precision and iii) reproducibility. In the current study, only repeatability and intermediate precision were studied, once reproducibility must only be evaluated when the method is used by different laboratories. The precision was characterized in terms of percentage of coefficient of variation (%CV) and the

limits of acceptance were set at 15% of the CV for all concentration, except for the LLOQ, which should not exceed 20% [177, 210].

When it comes to the analysis of accuracy, it was expressed in terms of mean relative error (%MRE) between the measured and the nominal concentration of each calibrator and the limits of acceptance were set to be within 15% of the nominal value, except at the LLOQ, were it should not exceed 20% [177, 210]. Along with the accuracy, it was also determined the recovery for each analyte, which corresponds to the detector response when compared with the nominal response.

Then, in order to evaluate the precision of the study, QCs samples with concentrations of 0.15 µM, 0.35 µM for solvent and 0.3 µM, 0.7 µM for plasma were used as the medium and high concentration, respectively.

The results obtained in the assessment of precision and accuracy in solvent and plasma are presented in Table 5.14 and 5.15, respectively. The values were estimated through a one-way ANOVA analysis (see tables 8.18 and 8.19, appendix 8.15) and through equations (4.17) and (4.18) for precision and (4.19) and (4.20) for accuracy (sections 4.8.4 and 4.8.5). The values that do not follow the criteria are highlighted.

By the analysis of the data it is possible to conclude that the results obtained in repeatability study were within the acceptance criteria. In turn, the data of intermediate precision, the results were not in accordance with the established criteria, for all the analytes, in solvent and plasma, with values that ranged from 26.37% to 32.80%. In terms of accuracy of the method, the results were within the acceptance criteria, which allows to conclude that the method is accurate for the quantification of these molecules.

This analysis allowed to conclude that the current method is accurate for the quantification of all the analytes, however, some improvements must be performed in order to improve the precision of the method.

Table 5.14. Results obtained for the precision (repeatability and intermediate precision), accuracy (%MRE) and recovery at three different levels of concentration, in solvent. Values that do not fulfill the criteria are highlighted.

Compound	Nominal concentration (µM)	Repeatability (%CV_R)	Intermediate precision (%CV_I)	Accuracy (%MRE)	Estimated concentration (µM)
L-tyrosine	1.5	9.14	27.73	9.29	1.64
	3.5	5.87	26.71	5.58	3.70
L-DOPA	1.5	5.25	26.47	-1.73	1.47
	3.5	5.24	26.49	-3.62	3.37
DA	1.5	6.87	27.16	11.64	1.68
	3.5	8.03	27.53	12.36	3.93
3-MT	1.5	5.81	30.19	-0.13	1.50
	3.5	6.16	29.67	-3.76	3.37
DOPAC	1.5	4.03	28.21	5.75	1.59
	3.5	3.55	27.65	0.94	3.53
HVA	1.5	10.45	27.98	-9.33	1.36
	3.5	4.44	26.37	-10.25	3.14

Table 5.15. Results obtained for the precision (repeatability and intermediate precision), accuracy (%MRE) and recovery at three different levels of concentration, in plasma. Values that do not fulfill the criteria are highlighted.

Compound	Nominal concentration (µM)	Repeatability (%CV_R)	Intermediate precision (%CV_I)	Accuracy (%MRE)	Estimated concentration (µM)
3-MT	3.0	8.64	32.80	-4.77	2.86
	7.0	8.85	30.82	-5.60	6.61
DOPAC	3.0	9.75	29.98	1.19	3.04
	7.0	11.50	30.90	-5.06	6.65
HVA	3.0	19.04	31.80	-10.95	2.67
	7.0	10.69	27.93	-10.78	6.25

5.2.6. Carry-over

When performing chromatographic analysis, it is important to verify if there is any analyte retained in the LC system from the preceding injection that can affect the posterior injections, once it can be detected a signal of the previous compound along with the signal of the analyte. Then, in order to evaluate the carry-over effect, it should be analyzed the peak response of a blank matrix sample after the injection of a sample with an expected high concentration [187].

Usually, the approach used in this analysis is the injection of a blank matrix sample after the injection of a high concentration sample, then, five blank samples were injected after the highest calibrator analysis, which was 0.6 µM in solvent and 1.2 µM in plasma samples.

In terms of the acceptance criteria used to evaluate this phenomenon, it was stated that the carry-over should be less than 20% of the peak area of the LLOQ for the analytes and 5% for the internal standard [177].

To demonstrate if there is carry-over effect, in Figure 5.23 there is an example of the visual evaluation performed in this parameter, which represents the chromatograms obtained for the high concentration and the respective five blank samples for the fragment with m/z 91.1 of DA in solvent and for the fragment with m/z 91.0 of 3-MT in plasma. In order to conclude that there is no carry-over, the chromatograms of the blank samples should not present any chromatographic signal.

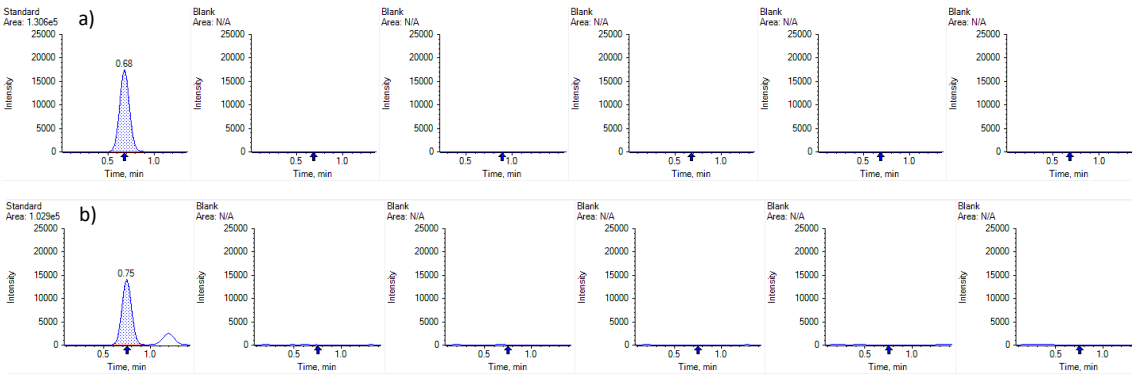

Figure 5.23. Representation of the chromatograms of highest calibrator and the respective five blank injections. a) 0.6 µM calibrator and five blanks of the fragment with m/z 91.1 of DA in solvent; b) 1.2 µM calibrator and five blanks of the fragment with m/z 91.0 of 3-MT in plasma samples.

The results obtained in the analysis of carry-over phenomenon (see Tables 8.20 to 8.37, appendix 8.16) demonstrated that, for all the analytes under study, the established criteria were fulfilled, which demonstrates that no significant carry-over effect was observed, except for L-tyrosine, since the values did not fulfill the criteria (see table 8.22, appendix 8.13). However, since there are some doubts about the reliability of these peaks, as previously mentioned, these values can be uncertain, then, the analysis was carried out taking into account some precautions.

The peaks that were present in blank samples are mainly caused by some analyte retention in previous injections of samples with higher concentrations of the analytes [214].

Carry-over is a major problem in HPLC analysis, since it can influence accuracy and precision of the developed method [215], then, there is the need to minimize this effect. In the current project, several precautions were taken into account to avoid this phenomenon, such as the

injection of a blank between each sample to assure that the analysis were not affected and in the linearity study the calibrators were analyzed from the lower to the highest concentration.

5.2.7. Recovery

The recovery of a method is a measure of the extraction efficiency used during the sample treatment, and it is expressed as a percentage [192]. This parameter is evaluated through the comparison of the response of blank matrix spiked before extraction with the response of blank matrix to which the analyte was added, at the same concentration, after the extraction [192, 212].

Even though, according to some guidelines, this is not considered an essential parameter to be evaluated during a method validation, in this project it was evaluated using the procedure described in section 3.8.6. Besides the study of the recovery of the analytes under study, it was also performed an analysis of the recovery of the internal standards, which is usually stated to be determined independently at the same concentration level used in the method [186]. It is important to notice that this approach was performed along with the matrix effect analysis, as recommended for LC-MS/MS analysis [181].

When it comes to the acceptance criteria that should be applied in the recovery study, there is no consensus about the ideal value. Although some authors recommend that recovery should be close to 100%, other stated that the value is not that important, as long as precision, accuracy, LOD and LOQ are satisfactory [184]. Also, there are authors that consider that it is unlikely that values of 50% or less can compromise the integrity of the method [186].

Then, recovery was calculated at 3 concentration levels, namely 0.7 µM, 5.0 µM and 8.0 µM, which corresponds to low, medium and high concentrations, respectively, with three replicates each (Table 5.16).

Table 5.16. Recovery, in percentage, of the extraction of the plasma for each compound at the three different levels of concentration.

Analyte	Transition[1]	Recovery		
		Low concentration (0.7 µM)	Medium concentration (5.0 µM)	High concentration (8.0 µM)
3-MT	168.3/119.1	102.6	78.0	76.5
DOPAC	167.0/123.2	39.3	40.6	40.6
HVA	181.0/137.2	87.4	85.0	81.7
3-MT-d4	172.3/123.1	91.8	79.3	71.9
DOPAC-d5	172.1/128.2	34.2	39.5	41.2
HVA-d3	184.0/139.8	103.6	103.0	88.1

[1]Transition used in quantification

From the analysis of Table 5.16, it is possible to conclude that recovery ranges from 71.9% to 103.6% for 3-MT, HVA and its corresponding internal standards. The high levels of recovery for these molecules indicates that there is not a considerable loss of analyte during the extraction procedure in most of samples. However, values obtained for DOPAC and DOPAC-d5 were the least satisfactory, even though there is a consistency of results between the samples of the three different concentrations, as well as between the analyte and internal standard results.

5.2.8. Matrix effects

There are matrix components that might affect the ion intensity, either by suppression or enhancement, and the reproducibility and accuracy of the method [216]. This phenomenon is known as matrix effects and its evaluation is obligatory when performing LC-MS analysis [182].

This effect can lead to a difference between the analyte's response when analyzed in the biological matrix or in a standard solution and then it is essential to analyze these differences. Thus, matrix effect was studied on samples spiked after the extraction and in standard solutions in pure solvent. This analysis was performed at three concentration levels (0.7 µM, 5.0 µM and 8.0 µM), with three replicates each (the same used in the recovery study). The matrix factor (f) was calculated through equation (4.22) and the results are present in Table 5.17.

Table 5.17. Matrix effect for each compound at three levels of concentration in plasma. f value was calculated for each transition at three different concentrations.

Analyte	Transition[1]	Matrix factor (f)		
		Low concentration (0.7 µM)	Medium concentration (5.0 µM)	High concentration (8.0 µM)
3-MT	168.3/119.1	-0.838	-0.817	-0.767
DOPAC	167.0/123.2	-0.750	-0.571	-0.289
HVA	181.0/137.2	-0.126	-0.254	-0.006
3-MT-d4	172.3/123.1	-0.829	-0.814	-0.761
DOPAC-d5	172.1/128.2	-0.638	-0.546	-0.271
HVA-d3	184.0/139.8	-0.275	-0.307	-0.063

[1]Transition to be used in quantification

By using equation (4.22) to evaluate the matrix effect, an f value equal to zero represents no matrix effect, a positive value indicates ion enhancement and, in turn, a negative value would indicate ion suppression [182]. The absolute matrix factors were mostly negative, indicating ion suppression. Since the matrix effect observed for the analytes is similar to the matrix effect of its correspondent internal standard, it is possible to conclude that the ion suppression does not affect the previous analysis.

It was also calculated the relative matrix effects for each analyte, expressed as %CV, and the results are present in Table 5.18. Even though f values were not high, some of the %CV values did not fulfil the criteria (%CV ≤ 15%), being that the variability is higher in the standard solutions when compared with the samples that were spiked after the extraction. The data indicates that the matrix effect varies among the samples, another reason to add internal standard in the analysis of this type of samples, since it compensates the variations. This happens because the expected matrix effect observed in the analyte will be similar to the matrix effect in the internal standard.

Table 5.18. Relative matrix effects (expressed as %CV) in plasma for the standard solution and blank matrix samples spiked after extraction. %CV was calculated for each transition at three different concentrations.

Compound	Transition	Relative matrix effects (%CV)					
		Spike after			Standard solution		
		0.7 µM	5.0 µM	8.0 µM	0.7 µM	5.0 µM	8.0 µM
3-MT	168.3/119.1	21.24	8.84	27.52	33.70	17.56	22.03
DOPAC	167.0/123.2	5.95	9.93	23.38	21.47	12.29	17.25
HVA	181.0/137.2	2.39	8.67	22.87	13.09	10.07	19.48
3-MT-d4	172.3/123.1	11.18	12.83	27.79	33.31	20.72	24.74
DOPAC-d5	172.1/128.2	12.02	10.54	24.06	19.57	8.65	16.80
HVA-d3	184.0/139.8	8.39	5.78	20.40	14.38	10.39	25.52

[1]Transition used in quantification

Despite the fact that matrix effect cannot be totally avoided, there are some procedures to reduce this factor. Among the hypothesis, there is the use of a proper sample clean-up method, the use of smaller volumes of analysis or diluted samples, or the use of an internal standard to compensate some losses, which was taken into account in the current project [217]. Moreover, it is also important to notice that the matrix effects are independent of the origin of the matrix, which means that if different pools of matrix are used, it will not affect the matrix effect [182].

5.3. Application of the analytical method to biological samples

After the validation procedure, it is essential to apply the developed method to biological samples, in order to evaluate the veracity of the method, since this type of samples reflect real samples. Therefore, the method was applied in a group of plasma samples from different individuals. The study group was constituted by plasma samples from a positive control group and a patients' group. The control group involved plasma samples from individuals who had another pathology other than PD, as long as they did not present any neurological symptom.

Some complementary information about the patients is synthetized in Table 5.19.

Table 5.19. Complementary information about each individual.

Label	Age (at the collection)	Gender	Daily dose of L-DOPA (mg/day)
CN 6	65	F	NA
CN 8	83	M	NA
CN 11	81	M	NA
CN 15	64	M	NA
CN 28	77	M	NA
CN 29	55	M	NA
CN 30	77	M	NA
CN 35	78	M	NA
DP 11	64	M	300
DP 15	74	F	300
DP 17	76	F	700
DP 18	75	M	50
DP 21	79	M	0
DP 29	72	F	150
DP 33	70	M	0
DP 7	77	M	700
DP 20	86	F	0
DP 23	71	M	300
DP 26	80	F	300
DP 31	77	M	150
DP 35	63	F	300
DP 36	77	M	1000

CN – negative control; DP – Parkinson's disease patient; F – female; M – male; NA – Not applied

For detection and quantification of biological samples, calibration curves were prepared as described on section 4.8.2. Since heteroscedastic data was obtained, the respective weighted least squares regression model was applied to each calibration curve.

The plasma samples were analyzed in a specific order: negative control samples, patients' samples and positive control samples.

The results obtained in the quantification of DA metabolism in the three groups of analysis are expressed in Tables 5.20 to 5.22. In negative control samples, no compound was detected, except for CN 11, where HVA was found. In turn, in the patients and positive control groups, L-DOPA was detected in most of the samples, which was already expected, since the individuals are

under medication (L-DOPA). In concern with DOPAC and HVA, they were also detected in some of the patients and positive control samples. However, some samples were quantified under its LOQ, and so, it is not possible to say if this value corresponds to reality.

Table 5.20. Quantification of dopamine metabolism in negative control samples.

Label	L-DOPA (ng/mL)	DOPAC (ng/mL)	HVA (ng/mL)
CN 6	ND	ND	ND
CN 8	ND	ND	ND
CN 11	ND	ND	0.3*
CN 15	ND	ND	ND
CN 28	ND	ND	ND
CN 29	ND	ND	ND
CN 30	ND	ND	ND
CN 35	ND	ND	ND

ND - Not detected; * - quantified under its limit of quantification

Table 5.21. Quantification of dopamine metabolism in PD patients' samples.

Label	L-DOPA (ng/mL)	DOPAC (ng/mL)	HVA (ng/mL)
DP 11	92.6	4.4*	60.6
DP 15	ND	ND	5.0*
DP 17	593	70.1	281
DP 18	50.1	6.3*	21.4
DP 21	ND	ND	ND
DP 29	28.9	ND	26.4
DP 33	ND	ND	0.98*

ND - Not detected; * - quantified under its limit of quantification

Table 5.22. Quantification of dopamine metabolism in positive control samples.

Label	L-DOPA (ng/mL)	DOPAC (ng/mL)	HVA (ng/mL)
DP 7	398.4	29.6	50.4
DP 20	ND	ND	ND
DP 23	38.9	ND	32.5
DP 26	ND	ND	27.1
DP 31	44.6	ND	10.2*
DP 35	3.03	1.7*	9.5*
DP 36	101.7	1.5*	10.5*

ND - Not detected; * - quantified under its limit of quantification

In order to compare the differences of the values found in the different groups, and try to find a characteristic pattern, plots with the results were performed. Then, in Figures 5.24 to 5.26 plots of the results obtained for the three groups are presented.

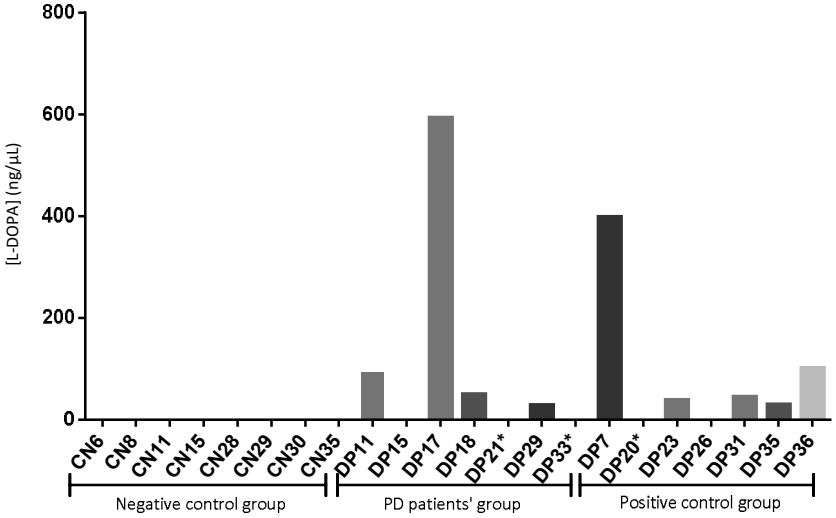

Figure 5.24. Plots of the results of quantification of L-DOPA in the three groups. * - individuals that are not under medication (L-DOPA).

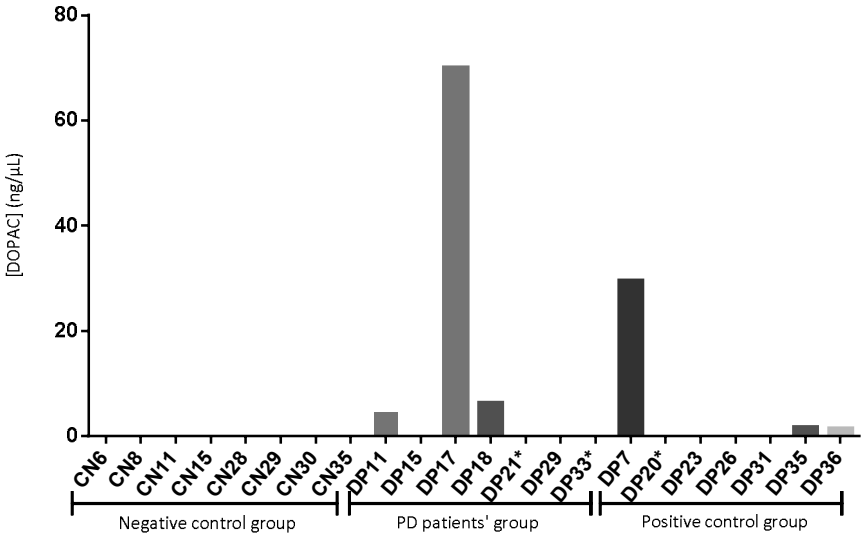

Figure 5.25. Plots of the results of quantification of DOPAC in the three groups. * - individuals that are not under medication (L-DOPA).

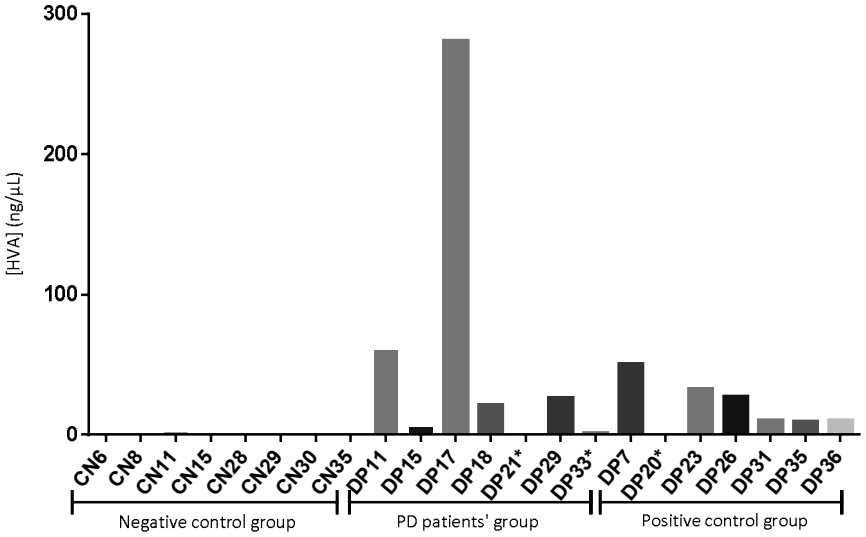

Figure 5.26. Plots of the results of quantification of HVA in the three groups. * - individuals that are not under medication (L-DOPA).

Crossing the results with the information about the daily dose of L-DOPA of each patient, it was attempted to establish a pattern between the dose and the concentration of L-DOPA. It was not possible to establish any correlation, which may indicate that these two parameters are not directly connected. This may be due to the fact that each patient responds to the therapy in a different way and some may need higher doses to get the same effects. When it takes to DOPAC and HVA, metabolites of DA metabolism, it was also not possible to establish a correlation between the samples, probably by the same reason of L-DOPA.

Another possibility to the lack of correlation between the two factors (daily dose of L-DOPA and L-DOPA concentration in plasma) is the difference between the moment of the sample collection and the last dose of medication. When analyzing the kinetics of oral administration of L-DOPA (Figure 5.27), it is possible to see that L-DOPA concentration reaches its maximum in less than an hour and, after that, the levels of L-DOPA in plasma decreases, returning to their baseline values [218, 219]. Therefore, if the sample collection was performed shortly after the last dose of medication, the plasma levels of L-DOPA would be high, reflecting the dose, however, if the collection occurred long after the medication, plasma levels of L-DOPA would be lower (basal levels of L-DOPA). Since there is no information about the time difference between the dose medication and the sample collection, this is just a possibility that could explain the differences found in the plasma samples of the three groups.

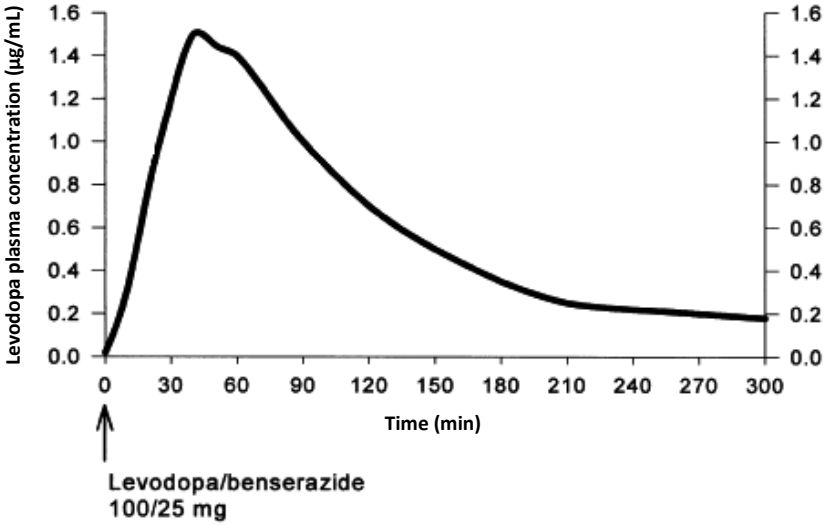

Figure 5.27. Mean levodopa plasma concentration profile after the intake of a test dose of levodopa and benserazide (100/25 mg). Adapted from: [219]

In concern with DOPAC and HVA no correlation was found either.

Even though the developed method did not allow to properly detect all the molecules, and a correlation between the medication and the concentration of the metabolites was not found, this study was important to have an idea of what it is expected to find in this type of samples, which is important to consider in future analysis.

6. Conclusion and future perspectives

The current project had the main purpose of developing a method for the quantitative determination of dopamine metabolism in plasma samples by LC-MS/MS. Besides the method development, it was also performed a validation procedure, in order to prove that the data was reliable. The analytical parameters that were evaluated included: selectivity, linearity, limit of detection and quantification, precision, accuracy, recovery and matrix effects. This method was developed and validated, proving to be selective and efficient.

The chromatographic conditions allowed an efficient separation within a running time of 10 minutes, for each sample. The mass spectrometer operated in MRM mode, in both positive and negative ionization mode, and the optimization of its conditions allowed the choice of the transitions to monitor for each molecule during the validation procedure. From the application of the WADA criteria for evaluation of selectivity it was possible to conclude that the method allowed an unequivocal identification of every transition, since no matrix interferences appear on the expect retention time of each analyte.

The validation procedure was assessed in solvent and plasma samples, because not all the molecules could be detected in the plasma. Then, in the future, it would be important to improve the sample preparation and the chromatographic analysis in order to evaluate the possibility to properly detect all the dopamine metabolism in plasma samples.

The current methodology proved to be linear for all the molecules over the working range, presenting $R^2 > 0.99$ and with satisfactory residuals values (Residuals $< 2x|S_{y/x}|$). The linearity in solvent was proved in the following intervals: 0.05-5.0 pmol/µL for L-tyrosine and DA; 0.03-5.0 pmol/µL for 3-MT and HVA; 0.1-6.0 pmol/µL for L-DOPA; and 0.1-5.0 pmol/µL for DOPAC. In plasma samples, the method was linear in the intervals: 0.5-10.0 pmol/µL for 3-MT and DOPAC; and 0.05-12.0 for HVA. However, a heteroscedastic distribution of the residuals was confirmed for all the molecules, being used a weighted linear regression with empirical weighting factors of 1/x for L-tyrosine, L-DOPA, DA, 3-MT and DOPAC in solvent, 1/y for HVA in solvent and 3-MT in plasma, and $1/x^{1/2}$ for DOPAC and HVA in plasma samples.

In solvent, the limits of detection were: 0.381, 0.426, 0.424, 0.377, 0.260 and 0.235 pmol/µL for L-tyrosine, L-DOPA, DA, 3-MT, DOPAC and HVA, respectively. The limits of quantification were: 1.154, 1.290, 1.284, 1.143, 0.787 and 0.714 pmol/µL for L-tyrosine, L-DOPA, DA, 3-MT, DOPAC and HVA, respectively. In turn, in plasma samples, the limits of detection were 0.852, 0.963 and 1.015 pmol/µL and the limits of quantification were 2.581, 2.617 and 3.077 pmol/µL for 3-MT, DOPAC and HVA, respectively.

In the precision analysis, repeatability and intermediate precision were evaluated. For the repeatability, the results were in accordance with the acceptance criteria. In turn, in intermediate precision analysis, the results were higher and did not fulfil the acceptance criteria, in solvent and plasma, presenting values from 26.37% to 32.80%. Thus, it is essential to re-evaluate this parameter to obtain more precise values that fulfil the criteria, to improve the precision of the method. In what concerns to the accuracy of the method, it proved to be accurate for all the molecules.

In line with the accuracy analysis, carry-over effect was also evaluated from all the analytes. This phenomenon is related with the retention of molecules in the chromatographic column that can affect the posterior analysis. However, no carry-over effect was found, except for L-tyrosine, even though there are some doubts about the reliability of the obtained peaks. To minimize this effect, some precautions were taken into account to avoid possible contaminations between samples, namely, the injection of a blank (ACN: 0.1%FA) between each sample and the injection of samples from the lowest to the highest concentration level.

In the study of recovery, which was performed at three concentration levels (low, medium and high), good recovery values were obtained in plasma, with values which ranged from 71.9% and 103.6% for 3-MT, HVA and its corresponding internal standards. However, low values were obtained for DOPAC and DOPAC-d5.

When using complex matrix, there are some endogenous compounds that might affect the ion intensity, either by suppression or enhancement. Then, the matrix effects were evaluated and negative values were obtained for plasma, which indicates that ion suppression occurs.

Hereupon, it is essential to re-evaluate the validation parameters that were not successfully validated and assess the analysis of all the dopamine metabolism in plasma samples.

After the validation procedure, the developed method was applied in biological samples. Two groups of study and a control group of samples were used to test the method. In the control group, no compound was detected, except for one sample, which presented HVA. In the other two groups, L-DOPA was detected in almost every samples, which was already excepted since the individuals were under medication of L-DOPA. Moreover, DOPAC and HVA were also detected in most of these samples. A correlation between the daily dose of each individual and the concentration of L-DOPA in the plasma was evaluated, however, no relation between these two factors was found. The same was analyzed for DOPAC and HVA, once again no relation was found for these compounds.

Due to the lack of diagnostic test to properly diagnose PD in its initial stage, and due to the relationship between the disease and an impaired dopamine metabolism, the development of a

diagnostic test that would allow to detect variations in dopamine metabolism is vital. Then, the current study proved to be of great interest in a clinical point of view, being a first step to the development of a precocious diagnosis that would rely on the analysis of plasma samples. This is very important since, usually, when PD patients are diagnosed the loss of dopaminergic neurons in the substantia nigra pars compacta is already around 50% and the loss of striatal DA reaches 70 to 80%.

7. References

1. Manyam, B.V., *Paralysis Agitans and Levodopa in "Ayurveda' ' : Ancient Indian Medical Treatise.* Movement disorders, 1990. **5**(1): p. 47-48.
2. Goetz, C.G., *The history of Parkinson's disease: early clinical descriptions and neurological therapies.* Cold Spring Harb Perspect Med, 2011. **1**(1): p. a008862.
3. Dauer, W.P., S., *Parkinson's disease: mechanisms and models.* Neurons, 2003. **39**(6): p. 889-909.
4. Hurwitz, B., *Urban Observation and Sentiment in James Parkinson's Essay on the Shaking Palsy (1817).* Literature and medicine, 2014: p. 74-104.
5. Goetz, C.G., *Charcot on Parkinson's disease.* Movement Disorders, 1986. **1**(1): p. 27-32.
6. Goetz, C.G., *Charcot and Parkinson's Disease*, in *Parkinson's Disease: Diagnosis & Clinical Management*, S.A. Factor and W.J. Weiner, Editors. 2008, Demos Medical Publishing.
7. Mizuno, Y., et al., *Progress in the pathogenesis and genetics of Parkinson's disease.* Philos Trans R Soc Lond B Biol Sci, 2008. **363**(1500): p. 2215-27.
8. Litteljohn, D., et al., *Inflammatory mechanisms of neurodegeneration in toxin-based models of Parkinson's disease.* Parkinsons Dis, 2010. **2011**: p. 713517.
9. Pereira, C., Macedo, P., and Madeira, R.N., *Mobile Integrated Assistance to Empower People Coping with Parkinson's Disease.* Proceedings of the 17th International ACM SIGACCESS Conference on Computers & Accessibility, 2015: p. 409-410.
10. Van Den Eeden, S.K., et al., *Incidence of Parkinson's Disease: Variation by Age, Gender, and Race/Ethnicity.* American Journal of Epidemiology, 2003. **157**(11): p. 1015-1022.
11. Maruyama, M., et al., *Novel mutations, pseudo-dominant inheritance, and possible familial affects in patients with autosomal recessive juvenile parkinsonism.* Annals of neurology, 2000. **48**(2): p. 245-250.
12. Park, A. and Stacy, M., *Non-motor symptoms in Parkinson's disease.* J Neurol, 2009. **256 Suppl 3**: p. 293-8.
13. Kaasinen, V., et al., *Increased frontal [18F] fluorodopa uptake in early Parkinson's disease: sex differences in the prefrontal cortex.* Brain, 2001. **124**(6): p. 1125-1130.
14. Dunnett, S.B. and Björklund, A., *Prospects for new restorative and neuroprotective treatments in Parkinson's disease.* Nature, 1999. **399**: p. A32-A39.
15. Golbe, L.I., Mark, M.H., and Sage, J.I., *Parkinson's disease handbook*. 1 ed. 2009: The American Parkinson Disease Association, Inc.
16. Uitti, R.J., et al., *Defining the Parkinson's disease phenotype: initial symptoms and baseline characteristics in a clinical cohort.* Parkinsonism Relat Disord, 2005. **11**(3): p. 139-45.
17. Lanciego, J.L., Luquin, N., and Obeso, J.A., *Functional neuroanatomy of the basal ganglia.* Cold Spring Harb Perspect Med, 2012. **2**(12): p. a009621.
18. Mathai, A. and Smith, Y., *The corticostriatal and corticosubthalamic pathways: two entries, one target. So what?* Front Syst Neurosci, 2011. **5**: p. 64.
19. Galvan, A. and Wichmann, T., *Pathophysiology of parkinsonism.* Clin Neurophysiol, 2008. **119**(7): p. 1459-74.
20. Goldenberg, M.M., *Medical management of Parkinson's disease. .* Phar Ther, 2008. **33**(10): p. 590-606.

21. Tomlinson, C.L., et al., *Systematic review of levodopa dose equivalency reporting in Parkinson's disease.* Mov Disord, 2010. **25**(15): p. 2649-53.

22. Ferrara, J.M.S., M., *Impulse control disorders in Parkinson's disease.* CNS Spectr, 2008. **13**(8): p. 690-8.

23. Kummer, A. and Teixeira, A.L., *Neuropsychiatry of Parkinson's disease.* Arquivos de neuropsiquiatria, 2009. **67**(3B): p. 930-939.

24. Ushe, M.P., J. S., *Sex, drugs and Parkinson's disease.* Brain, 2013. **136**: p. 368–373.

25. Cannas, A., et al., *Hypersexual behaviour, frotteurism and delusional jealousy in a young parkinsonian patient during dopaminergic therapy with pergolide: A rare case of iatrogenic paraphilia.* Prog Neuropsychopharmacol Biol Psychiatry, 2006. **30**(8): p. 1539-41.

26. Wu, K., Politis, M., and Piccini, P., *Parkinson disease and impulse control disorders: a review of clinical features, pathophysiology and management.* Postgrad Med J, 2009. **85**(1009): p. 590-596.

27. Evans, A.H., et al., *Impulsive and compulsive behaviors in Parkinson's disease.* Mov Disord, 2009. **24**(11): p. 1561-70.

28. Cannas, A., et al., *Aberrant sexual behaviours in Parkinson's disease during dopaminergic treatment.* J Neurol, 2007. **254**(1): p. 110-2.

29. Vilas, D., Pont-Sunyer, C., and Tolosa, E., *Impulse control disorders in Parkinson's disease.* Parkinsonism & Related Disorders, 2012. **18**: p. S80-S84.

30. Mamikonyan, E., et al., *Long-term follow-up of impulse control disorders in Parkinson's disease.* Mov Disord, 2008. **23**(1): p. 75-80.

31. Okun, M.S., *Deep-brain stimulation for Parkinson's disease.* N Engl J Med, 2012. **367**(16): p. 1529-38.

32. Bernheimer, H., et al., *Brain dopamine and the syndromes of Parkinson and Huntington Clinical, morphological and neurochemical correlations.* Journal of the neurological sciences, 1973. **20**(4): p. 415-455.

33. Hornykiewicz, O., *Chemical neuroanatomy of the basal ganglia—normal and in Parkinson's disease.* Journal of chemical neuroanatomy, 2001. **22**(1): p. 3-12.

34. Hornykiewicz, O., *Biochemical aspects of Parkinson's disease.* Neurology, 1998. **51**(Suppl 2): p. S2-S9.

35. Zarow, C., et al., *Neuronal loss is greater in the locus coeruleus than nucleus basalis and substantia nigra in Alzheimer and Parkinson diseases.* Archives of neurology, 2003. **60**(3): p. 337-341.

36. Kuusisto, E., Parkkinen, L., and Alafuzoff, I., *Morphogenesis of Lewy bodies: dissimilar incorporation of α-synuclein, ubiquitin, and p62.* Journal of Neuropathology and Experimental Neurology, 2003. **62**(12): p. 1241-1253.

37. Galvin, J.E., et al., *Monoclonal antibodies to purified cortical Lewy bodies recognize the mid-size neurofilament subunit.* Annals of neurology, 1997. **42**(4): p. 595-603.

38. Pletnikova, O., et al., *Abeta deposition is associated with enhanced cortical alpha-synuclein lesions in Lewy body diseases.* Neurobiol Aging, 2005. **26**(8): p. 1183-92.

39. Goedert, M., *Alpha-synuclein and neurodegenerative diseases.* Nature Reviews Neuroscience, 2001. **2**(7): p. 492-501.

40. Schapira, A.H.V., et al., *Mitochondrial complex I deficiency in Parkinson's disease.* Journal of neurochemistry, 1990. **54**(3): p. 823-827.

41. Parker, W.D., Jr., Parks, J.K., and Swerdlow, R.H., *Complex I deficiency in Parkinson's disease frontal cortex.* Brain Res, 2008. **1189**: p. 215-8.

42. Bowen, B.C., et al., *Proton MR spectroscopy of the brain in 14 patients with Parkinson disease.* American journal of neuroradiology, 1995. **16**(1): p. 61-68.

43. Kish, S.J., Morito, C., and Hornykiewicz, O., *Glutathione peroxidase activity in Parkinson's disease brain.* Neuroscience letters, 1985. **58**(3): p. 343-346.

44. Dexter, D.T., et al., *Basal lipid peroxidation in substantia nigra is increased in Parkinson's disease.* Journal of neurochemistry, 1989. **52**(2): p. 381-389.

45. Dexter, D.T., et al., *Increased levels of lipid hydroperoxides in the parkinsonian substantia nigra: an HPLC and ESR study.* Movement Disorders, 1994. **9**(1): p. 92-97.

46. Floor, E. and Wetzel, M.G., *Increased protein oxidation in human substantia nigra pars compacta in comparison with basal ganglia and prefrontal cortex measured with an improved dinitrophenylhydrazine assay.* Journal of neurochemistry, 1998. **70**(1): p. 268-275.

47. Alam, Z.I., et al., *Oxidative DNA Damage in the Parkinsonian Brain: An Apparent Selective Increase in 8-Hydroxyguanine Levels in Substantia Nigra.* Journal of neurochemistry, 1997. **69**(3): p. 1196-1203.

48. Marttila, R.J., Lorentz, H., and Rinne, U.K., *Oxygen toxicity protecting enzymes in Parkinson's disease: increase of superoxide dismutase-like activity in the substantia nigra and basal nucleus.* Journal of the neurological sciences, 1988. **86**(2): p. 321-331.

49. Ambani, L.M., Van Woert, M.H., and Murphy, S., *Brain peroxidase and catalase in Parkinson disease.* Archives of neurology, 1975. **32**(2): p. 114-118.

50. Meredith, G.E., Sonsalla, P.K., and Chesselet, M.F., *Animal models of Parkinson's disease progression.* Acta Neuropathol, 2008. **115**(4): p. 385-98.

51. Mounsey, R.B. and Teismann, P., *Mitochondrial dysfunction in Parkinson's disease: pathogenesis and neuroprotection.* Parkinsons Dis, 2010. **2011**: p. 617472.

52. Horowitz, M.P. and Greenamyre, J.T., *Gene-environment interactions in Parkinson's disease: the importance of animal modeling.* Clin Pharmacol Ther, 2010. **88**(4): p. 467-74.

53. Halliwell, B., *Oxidative stress and neurodegeneration: where are we now?* J Neurochem, 2006. **97**(6): p. 1634-58.

54. Lochhead, J.J., et al., *Oxidative stress increases blood-brain barrier permeability and induces alterations in occludin during hypoxia-reoxygenation.* J Cereb Blood Flow Metab, 2010. **30**(9): p. 1625-36.

55. Dringen, R., *Metabolism and functions of glutathione in brain.* Progress in neurobiology, 2000. **62**(6): p. 649-671.

56. Rhee, S.G., et al., *Controlled elimination of intracellular H2O2: regulation of peroxiredoxin, catalase, and glutathione peroxidase via post-translational modification.* Antioxidants & redox signaling, 2005. **7**(5-6): p. 619-626.

57. Yoritaka, A., et al., *An immunohistochemical study on manganese superoxide dismutase in Parkinson's disease.* Journal of the neurological sciences, 1997. **148**(2): p. 181-186.

58. Riederer, P., et al., *Transition metals, ferritin, glutathione, and ascorbic acid in parkinsonian brains.* Journal of neurochemistry, 1989. **52**(2): p. 515-520.

59. Arreguin, S., et al., *Dopamine complexes of iron in the etiology and pathogenesis of Parkinson's disease.* J Inorg Biochem, 2009. **103**(1): p. 87-93.

60. Picklo, M.J., et al., *Endogenous catechol thioethers may be pro-oxidant or antioxidant.* Free Radical Biology and Medicine, 1999. **27**(3): p. 271-277.

61. Henchcliffe, C. and Beal, M.F., *Mitochondrial biology and oxidative stress in Parkinson disease pathogenesis.* Nat Clin Pract Neurol, 2008. **4**(11): p. 600-9.

62. Green, D.R. and Kroemer, G., *The pathophysiology of mitochondrial cell death.* Science, 2004. **305**(5684): p. 626-9.

63. Keeney, P.M., et al., *Parkinson's disease brain mitochondrial complex I has oxidatively damaged subunits and is functionally impaired and misassembled.* J Neurosci, 2006. **26**(19): p. 5256-64.

64. McNaught, K.S.P., et al., *Failure of the ubiquitin–proteasome system in Parkinson's disease.* Nature Reviews Neuroscience, 2001. **2**(8): p. 589-594.

65. Schwartz, A.L. and Ciechanover, A., *The ubiquitin-proteasome pathway and pathogenesis of human diseases.* Annual review of medicine, 1999. **50**(1): p. 57-74.

66. McNaught, S.P.K., et al., *Altered Proteasomal Function in Sporadic Parkinson's Disease.* Experimental Neurology, 2003. **179**(1): p. 38-46.

67. McNaught, K.S.P. and Jenner, P., *Proteasomal function is impaired in substantia nigra in Parkinson's disease.* Neuroscience letters, 2001. **297**(3): p. 191-194.

68. Xu, L. and Pu, J., *Alpha-Synuclein in Parkinson's Disease: From Pathogenetic Dysfunction to Potential Clinical Application.* Parkinsons Dis, 2016. **2016**: p. 1720621.

69. Levy, O.A., Malagelada, C., and Greene, L.A., *Cell death pathways in Parkinson's disease: proximal triggers, distal effectors, and final steps.* Apoptosis, 2009. **14**(4): p. 478-500.

70. Hirsch, E.C., Hunot, S., and Hartmann, A., *Neuroinflammatory processes in Parkinson's disease.* Parkinsonism Relat Disord, 2005. **11 Suppl 1**: p. S9-S15.

71. Nagatsu, T. and Sawada, M., *Inflammatory process in Parkinson's disease: role for cytokines.* Current pharmaceutical design, 2005. **11**(8): p. 999-1016.

72. Teismann, P., et al., *Pathogenic role of glial cells in Parkinson's disease.* Movement Disorders, 2003. **18**(2): p. 121-129.

73. Wilms, H., et al., *Activation of microglia by human neuromelanin is NF-κB dependent and involves p38 mitogen-activated protein kinase: implications for Parkinson's disease.* The FASEB journal, 2003. **17**(3): p. 500-502.

74. Wakamatsu, K., et al., *The structure of neuromelanin as studied by chemical degradative methods.* Journal of Neurochemistry, 2003. **86**(4): p. 1015-1023.

75. Zecca, L., et al., *Substantia nigra neuromelanin: structure, synthesis, and molecular behaviour.* Molecular Pathology, 2001. **54**(6): p. 414-418.

76. Kastner, A., et al., *Is the vulnerability of neurons in the substantia nigra of patients with Parkinson's disease related to their neuromelanin content?* Journal of neurochemistry, 1992. **59**(3): p. 1080-1089.

77. Zucca, F.A., et al., *The neuromelanin of human substantia nigra: physiological and pathogenic aspects.* Pigment cell research, 2004. **17**(6): p. 610-617.

78. D'Amato, R.J., Lipman, Z.P., and Snyder, S.H., *Selectivity of the parkinsonian neurotoxin MPTP: toxic metabolite MPP+ binds to neuromelanin.* Science, 1986. **231**(4741): p. 987-989.

79. Lindquist, N.G., Larsson, B.S., and Lyden-Sokolowski, A., *Autoradiography of [14 C] paraquat or [14 C] diquat in frogs and mice: accumulation in neuromelanin.* Neuroscience letters, 1988. **93**(1): p. 1-6.

80. Zecca, L., et al., *The neuromelanin of human substantia nigra and its interaction with metals.* Journal of neural transmission, 2002. **109**(5-6): p. 663-672.

81. Moore, D.J., et al., *Molecular pathophysiology of Parkinson's disease.* Annu. Rev. Neurosci, 2005. **28**: p. 57-87.

82. Polymeropoulos, M.H., et al., *Mapping of a gene for Parkinson's disease to chromosome 4q21-q23.* Science, 1996. **274**(5290): p. 1197.

83. Krüger, R., et al., *AlaSOPro mutation in the gene encoding α-synuclein in Parkinson's disease.* Nature genetics, 1998. **18**(2): p. 106-108.

84. Zarranz, J.J., et al., *The new mutation, E46K, of α-synuclein causes parkinson and Lewy body dementia.* Annals of neurology, 2004. **55**(2): p. 164-173.

85. Singleton, A.B., et al., *α-Synuclein locus triplication causes Parkinson's disease.* Science, 2003. **302**(5646): p. 841-841.

86. Pandey, N., Schmidt, R.E., and Galvin, J.E., *The alpha-synuclein mutation E46K promotes aggregation in cultured cells.* Exp Neurol, 2006. **197**(2): p. 515-20.

87. Conway, K.A., et al., *Acceleration of oligomerization, not fibrillization, is a shared property of both α-synuclein mutations linked to early-onset Parkinson's disease: implications for pathogenesis and therapy.* Proceedings of the National Academy of Sciences, 2000. **97**(2): p. 571-576.

88. Mosharov, E.V., et al., *Alpha-synuclein overexpression increases cytosolic catecholamine concentration.* J Neurosci, 2006. **26**(36): p. 9304-11.

89. Kitada, T., et al., *Mutations in the parkin gene cause autosomal recessive juvenile parkinsonism.* Nature, 1998. **392**(6676): p. 605-608.

90. Itier, J.M., et al., *Parkin gene inactivation alters behaviour and dopamine neurotransmission in the mouse.* Hum Mol Genet, 2003. **12**(18): p. 2277-91.

91. Dodson, M.W. and Guo, M., *Pink1, Parkin, DJ-1 and mitochondrial dysfunction in Parkinson's disease.* Curr Opin Neurobiol, 2007. **17**(3): p. 331-7.

92. Leroy, E., et al., *The ubiquitin pathway in Parkinson's disease.* Nature, 1998. **395**(6701): p. 451-452.

93. Liu, Y., et al., *The UCH-L1 gene encodes two opposing enzymatic activities that affect α-synuclein degradation and Parkinson's disease susceptibility.* Cell, 2002. **111**(2): p. 209-218.

94. Cookson, M.R., *The biochemistry of Parkinson's disease.* Annu Rev Biochem, 2005. **74**: p. 29-52.

95. Petit, A., et al., *Wild-type PINK1 prevents basal and induced neuronal apoptosis, a protective effect abrogated by Parkinson disease-related mutations.* J Biol Chem, 2005. **280**(40): p. 34025-32.

96. Morais, V.A., et al., *Parkinson's disease mutations in PINK1 result in decreased Complex I activity and deficient synaptic function.* EMBO Mol Med, 2009. **1**(2): p. 99-111.

97. Bonifati, V., et al., *Mutations in the DJ-1 gene associated with autosomal recessive early-onset parkinsonism.* Science, 2003. **299**(5604): p. 256-9.

98. Shendelman, S., et al., *DJ-1 is a redox-dependent molecular chaperone that inhibits α-synuclein aggregate formation.* PLoS Biol, 2004. **2**(11): p. 1764-1773.

99. Zimprich, A., et al., *Mutations in LRRK2 cause autosomal-dominant parkinsonism with pleomorphic pathology.* Neuron, 2004. **44**(4): p. 601-7.

100. Hattori, N., et al., *Toxic effects of dopamine metabolism in Parkinson's disease.* Parkinsonism & related disorders, 2009. **15**: p. S35-S38.

101. Carlsson, A., *A Half-Century of Neurotransmitter Research: Impact on Neurology and Psychiatry.* Bioscience Reports, 2001. **21**(6): p. 691-710.

102. Gupta, P.K., *Signal transduction in the nervous system: The 2000 Nobel Prize for physiology or medicine.* Current Science, 2000. **79**(9): p. 1145.

103. Meiser, J., Weindl, D., and Hiller, K., *Complexity of dopamine metabolism.* Cell Communication and Signaling, 2013. **11**(1): p. 34.

104. van Spronsen, F.J., et al., *Phenylketonuria: tyrosine supplementation in phenylalanine-restricted diets.* The American journal of clinical nutrition, 2001. **73**(2): p. 153-157.

105. Wurtman, R.J., et al., *Brain catechol synthesis: control by brain tyrosine concentration.* Science, 1974. **185**(4146): p. 183-184.

106. Gelenberg, A.J., et al., *Tyrosine for the treatment of depression.* The American journal of psychiatry, 1980. **137**(5): p. 622-623.

107. Growdon, J.H., et al., *Effects of oral L-tyrosine administration of CSF tyrosine and homovanillic acid levels in patients with Parkinson's disease.* Life sciences, 1982. **30**(10): p. 827-832.

108. Tyrrell, H.A., *Tyrosine: food supplement or therapeutic agent?* Journal of nutritional & environmental medicine, 1998. **8**(4): p. 349-359.

109. Basheir, B.E.A. and Elbashir, A.A., *Spectrophotometric method for determination of L-DOPA in pharmaceutical formulation using 1,2-naphthoquinone-a-sulphonate as a chromogenic reagent.* European Journal of Pharmaceutical and Medical Research, 2015. **2**(1): p. 304-316.

110. Bortolato, M., Chen, K., and Shih, J.C., *Monoamine oxidase inactivation: from pathophysiology to therapeutics.* Adv Drug Deliv Rev, 2008. **60**(13-14): p. 1527-33.

111. Fornai, F., et al., *Striatal Dopamine Metabolism in Monoamine Oxidase B-Deficient Mice: A Brain Dialysis Study.* Journal of neurochemistry, 1999. **73**(6): p. 2434-2440.

112. Hauptmann, N., et al., *The Metabolism of Tyramine by Monoamine Oxidase A/B Causes Oxidative Damage to Mitochondrial DNA.* Archives of biochemistry and biophysics, 1996. **335**(2): p. 295-304.

113. Antkiewicz-Michaluk, L., et al., *Different action on dopamine catabolic pathways of two endogenous 1, 2, 3, 4-tetrahydroisoquinolines with similar antidopaminergic properties.* Journal of neurochemistry, 2001. **78**(1): p. 100-108.

114. Maurel, A., et al., *Age-dependent increase in hydrogen peroxide production by cardiac monoamine oxidase A in rats.* American Journal of Physiology-Heart and Circulatory Physiology, 2003. **284**(4): p. H1460-H1467.

115. Mallajosyula, J.K., et al., *MAO-B elevation in mouse brain astrocytes results in Parkinson's pathology.* PLoS One, 2008. **3**(2): p. e1616.

116. Lotharius, J. and Brundin, P., *Pathogenesis of Parkinson's disease: dopamine, vesicles and alpha-synuclein.* Nat Rev Neurosci, 2002. **3**(12): p. 932-42.

117. Roth, R.H., Murrin, L.C., and Walters, J.R., *Central dopaminergic neurons: effects of alterations in impulse flow on the accumulation of dihydroxyphenylacetic acid.* European journal of pharmacology, 1976. **36**(1): p. 163-171.

118. Korf, J., Grasdijk, L., and Westerink, B.H.C., *Effects of electrical stimulation of the nigrostriatal pathway of the rat on dopamine metabolism.* Journal of neurochemistry, 1976. **26**(3): p. 579-584.

119. Westerink, B.H. and Korf, J., *Regional rat brain levels of 3, 4-dihydroxyphenylacetic acid and homovanillic acid: concurrent fluorometric measurement and influence of drugs.* European journal of pharmacology, 1976. **38**(2): p. 281-291.

120. Bacopoulos, N.G., Hattox, S.E., and Roth, R.H., *Dihydroxyphenylacetic acid and homovanillic acid in rat plasma: possible indicators of central dopaminergic activity.* European Journal of Pharmacology, 1979. **56**(3): p. 225-236.

121. Zhang, D., et al., *Quantitative determination of dopamine in human plasma by a highly sensitive LC-MS/MS assay: Application in preterm neonates.* J Pharm Biomed Anal, 2016. **117**: p. 227-31.

122. Stefani, A., et al., *Homovanillic acid in CSF of mild stage Parkinson's disease patients correlates with motor impairment.* Neurochemistry International, 2017. **105**: p. 58-63.

123. Eldrup, E., *Significance and origin of DOPA, DOPAC, and dopamine-sulphate in plasma, tissues and cerebrospinal fluid.* Dan Med Bull, 2004. **51**(1): p. 34-62.

124. Chapman, B.J., et al., *The actions of dopamine and of sulpiride on regional blood flows in the rat kidney.* The Journal of physiology, 1980. **298**: p. 437-452.

125. Davis, B.B., Walter, M.J., and Murdaugh, H.V., *The mechanism of the increase in sodium excretion following dopamine infusion. .* Experimental Biology and Medicine, 1968. **129**(1): p. 210-213.

126. Glavin, G.B. and Szabo, S., *Dopamine in gastrointestinal disease.* Digestive diseases and sciences, 1990. **35**(9): p. 1153-1161.

127. Tian, Y.M., et al., *Alteration of dopaminergic markers in gastrointestinal tract of different rodent models of Parkinson's disease.* Neuroscience, 2008. **153**(3): p. 634-44.

128. Goldstein, D.S. and Holmes, C., *Neuronal source of plasma dopamine.* Clin Chem, 2008. **54**(11): p. 1864-71.

129. Chang, M.S., et al., *Historical review of sample preparation for chromatographic bioanalysis: pros and cons.* Drug Development Research, 2007. **68**(3): p. 107-133.

130. Couchman, L. and Morgan, P.E., *LC-MS in analytical toxicology: some practical considerations.* Biomed Chromatogr, 2011. **25**(1-2): p. 100-23.

131. Vogeser, M. and Kirchhoff, F., *Progress in automation of LC-MS in laboratory medicine.* Clin Biochem, 2011. **44**(1): p. 4-13.

132. Bylda, C., et al., *Recent advances in sample preparation techniques to overcome difficulties encountered during quantitative analysis of small molecules from biofluids using LC-MS/MS.* Analyst, 2014. **139**(10): p. 2265-76.

133. Burgess, R., *Protein Precipitation Techniques*, in *Guide to Protein Purification*, R. Burgess and M. Deutscher, Editors. 2009. p. 331-342.

134. Ma, J., et al., *A fully automated plasma protein precipitation sample preparation method for LC-MS/MS bioanalysis.* J Chromatogr B Analyt Technol Biomed Life Sci, 2008. **862**(1-2): p. 219-26.

135. Shakulashvili, N., Finkler, C., and Engelhardt, H., *Separation of catecholamines and serotonin by micellar electrokinetic chromatography with UV detection.* Chromatographia, 1998. **47**(1-2): p. 89-92.

136. Li, W., T., R.D., and Fountain, S.T., *Development and validation of a semi-automated method for L-dopa and dopamine in rat plasma using electrospray LC/MS/MS.* Journal of pharmaceutical and biomedical analysis, 2000. **24**(2): p. 325-333.

137. Dunand, M., et al., *High-throughput and sensitive quantitation of plasma catecholamines by ultraperformance liquid chromatography-tandem mass spectrometry using a solid phase microwell extraction plate.* Anal Chem, 2013. **85**(7): p. 3539-44.

138. Sanchez, A., de Menezes, M.L., and Pereira, O.C.M., *Determinacão de catecolaminas em amostras de plasma de ratos por injeção direta usando CLAE.* Salusvita, 2001. **20**(2): p. 63-81.

139. Kamahori, M., et al., *Analysis of plasma catecholamines by high-performance liquid chromatography with fluorescence detection: simple sample preparation for pre-column fluorescence derivatization.* Journal of Chromatography B: Biomedical Sciences and Applications, 1991. **567**(2): p. 351-358.

140. Mitsui, A., Nohta, H., and Ohkura, Y., *High-performance liquid chromatography of plasma catecholamines using 1, 2-diphenylethylenediamine as precolumn fluorescence derivatization reagent.* Journal of Chromatography B: Biomedical Sciences and Applications, 1985. **344**: p. 61-70.

141. Rao, P.S., et al., *A specific sensitive HPLC method for determination of plasma dopamine.* Chromatographia, 1989. **28**(5-6): p. 307-310.

142. Karimi, M., et al., *Modified high-performance liquid chromatography with electrochemical detection method for plasma measurement of levodopa, 3-O-methyldopa, dopamine, carbidopa and 3,4-dihydroxyphenyl acetic acid.* J Chromatogr B Analyt Technol Biomed Life Sci, 2006. **836**(1-2): p. 120-3.

143. Eisenhofer, G., et al., *Simultaneous liquid-chromatographic determination of 3, 4-dihydroxyphenylglycol, catecholamines, and 3, 4-dihydroxyphenylalanine in plasma, and their responses to inhibition of monoamine oxidase.* Clinical Chemistry, 1986. **32**(11): p. 2030-2033.

144. Wang, Y., Fice, D.S., and Yeung, P.K., *A simple high-performance liquid chromatography assay for simultaneous determination of plasma norepinephrine, epinephrine, dopamine and 3, 4-dihydroxyphenyl acetic acid.* Journal of pharmaceutical and biomedical analysis, 1999. **21**(3): p. 519-525.

145. Rondelli, I., et al., *Simultaneous determination of levodopa methyl ester, levodopa, 3-O-methyldopa and dopamine in plasma by high-performance liquid chromatography with electrochemical detection.* Journal of Chromatography B: Biomedical Sciences and Applications, 1994. **653**(1): p. 17-23.

146. Tolokan, A., et al., *Automated determination of levodopa and carbidopa in plasma by high-performance liquid chromatography-electrochemical detection using an on-line flow injection analysis sample pretreatment unit.* Journal of Chromatography B: Biomedical Sciences and Applications, 1997. **698**(1): p. 201-207.

147. Javidan, S. and Cwik, M.J., *Determination of catecholamines in human plasma by HPLC with electrochemical detection.* Journal of liquid chromatography & related technologies, 1996. **19**(8): p. 1339-1348.

148. Cheng, F.C., et al., *Rapid and reliable high-performance liquid chromatographic method for analysing human plasma serotonin, 5-hydroxyindoleacetic acid, homovanillic acid and 3, 4-dihydroxyphenylacetic acid.* Journal of Chromatography B: Biomedical Sciences and Applications, 1993. **617**(2): p. 227-232.

149. Michotte, Y., et al., *Simultaneous determination of levodopa, carbidopa, 3-O-methyldopa and dopamine in plasma using high-performance liquid chromatography with electrochemical detection.* Journal of pharmaceutical and biomedical analysis, 1987. **5**(7): p. 659-664.

150. Miller, R.B., Dehelean, L., and Belanger, L., *Determination of carbidopa and levodopa in human plasma by high-performance liquid chromatography with electrochemical detection.* Chromatographia, 1993. **35**(9-12): p. 607-612.

151. Zimmermann, J., Dennhardt, R., & Gramm, H. J., *Measurement of plasma catecholamines by high-performance liquid chromatography with electrochemical detection in intensive care patients after dobutamine infusion.* Journal of Chromatography B: Biomedical Sciences and Applications, 1991. **567**(1): p. 240-247.

152. Cai, H.L., Zhu, R.H., and Li, H.D., *Determination of dansylated monoamine and amino acid neurotransmitters and their metabolites in human plasma by liquid chromatography-electrospray ionization tandem mass spectrometry.* Anal Biochem, 2010. **396**(1): p. 103-11.

153. van de Merbel, N.C., et al., *Quantitative determination of free and total dopamine in human plasma by LC-MS/MS: the importance of sample preparation.* Bioanalysis, 2011. **3**(17): p. 1949-1961.

154. Fang, L., et al., *Sensitive, rapid and easy analysis of three catecholamine metabolites in human urine and serum by liquid chromatography tandem mass spectrometry.* J Chromatogr Sci, 2012. **50**(5): p. 450-6.

155. Tsunoda, M., *Recent advances in methods for the analysis of catecholamines and their metabolites.* Anal Bioanal Chem, 2006. **386**(3): p. 506-14.

156. Nohta, H., Yamaguchi, E., Ohkura, Y., & Watanabe, H. , *Measurement of catecholamines, their precursor and metabolites in human urine and plasma by solid-phase extraction followed by high-performance liquid chromatography with fluorescence derivatization.* Journal of Chromatography B: Biomedical Sciences and Applications, 1989. **493**: p. 15-26.

157. Raggi, M.A., et al., *Determination of catecholamines in human plasma by high-performance liquid chromatography with electrochemical detection. .* Journal of Chromatography B: Biomedical Sciences and Applications, 1999. **730**(2): p. 201-211.

158. Raggi, M.A., et al., *Analysis of plasma catecholamines by liquid chromatography with amperometric detection using a novel SPE ion-exchange procedure.* Journal of Separation Science, 2003. **26**(12-13): p. 1141-1146.

159. Takezawa, K., et al., *Automatic semi-microcolumn liquid chromatographic determination of catecholamines in rat plasma utilizing peroxyoxalate chemiluminescence reaction.* The Analyst, 2000. **125**(2): p. 293-296.

160. Scott, R.P., *Principles and practice of chromatography*. Vol. 1. 2003: Chrom-Ed Book Series.

161. Snyder, L.R. and Kirkland, J.J., *Introduction to modern liquid chromatography*. 1979: John Wiley & Sons.

162. Harvey, D., *Modern analytical chemistry*. 2000, McGraw-Hill.

163. Dong, M.W., *Modern HPLC for practicing scientists*. 2006: John Wiley & Sons.

164. Tripathi, A.S., et al., *Liquid Chromatography in conjunction with Mass Spectrometry (LC-MS).* International journal of pharmaceutical and chemical sciences, 2012. **1**(3): p. 1532-1538.

165. Ardrey, R.E., *Liquid chromatography-mass spectrometry: an introduction*, ed. D.J. Ando. 2003: John Wiley & Sons.

166. Kazakevich, Y.V. and Lobrutto, R., *HPLC for pharmaceutical scientists*. 2007: John Wiley & Sons.

167. Fenn, J.B.M., M., et al., *Electrospray ionization for mass spectrometry of large biomolecules.* Science, 1989. **246**(4926): p. 64-71.

168. Hoffmann, E.D. and Stroobant, V., *Mass spectrometry: principles and applications*. 3 ed. 2007: John Wiley & Sons.

169. Lanças, F.M., *A cromatografia líquida moderna e a espectrometria de massas: finalmente "compatíveis"?* Scientia chromatographica, 2009. **1**(2): p. 35-61.

170. Pitt, J.J., *Principles and applications of liquid chromatography-mass spectrometry in clinical biochemistry.* Clin Biochem Rev, 2009. **30**(1): p. 19-34.

171. Banerjee, S. and Mazumdar, S., *Electrospray ionization mass spectrometry: a technique to access the information beyond the molecular weight of the analyte.* Int J Anal Chem, 2012. **2012**: p. 282574.

172. Jickells, S. and Negrusz, A., *Clarke's analytical forensic toxicology*. 2008: Pharmaceutical Press.

173. McEwen, C.N. and McKay, R.G., *A combination atmospheric pressure LC/MS:GC/MS ion source: advantages of dual AP-LC/MS:GC/MS instrumentation.* J Am Soc Mass Spectrom, 2005. **16**(11): p. 1730-8.

174. McMaster, M.C., *LC/MS: a practical user's guide*. 2005: John Wiley & Sons.

175. Wang, E.H., Combe, P.C., and Schug, K.A., *Multiple Reaction Monitoring for Direct Quantitation of Intact Proteins Using a Triple Quadrupole Mass Spectrometer. .* Journal of The American Society for Mass Spectrometry, 2016. **27**(5): p. 886-896.

176. Bocker, S., et al., *SIRIUS: decomposing isotope patterns for metabolite identification.* Bioinformatics, 2009. **25**(2): p. 218-24.

177. (EMA), E.M.A., *Guideline on bioanalytical method validation.* 2011.

178. Shah, V.P., et al., *Analytical methods validation: bioavailability, bioequivalence, and pharmacokinetic studies.* Journal of Pharmaceutical Sciences, 1992. **81**(3): p. 309-312.

179. Gustavo González, A. and Ángeles Herrador, M., *A practical guide to analytical method validation, including measurement uncertainty and accuracy profiles.* TrAC Trends in Analytical Chemistry, 2007. **26**(3): p. 227-238.

180. (Relacre), A.d.L.A.d.P., *Validação de métodos internos de ensaio em análise química.* 2000.

181. Peters, F.T., Drummer, O.H., and Musshoff, F., *Validation of new methods.* Forensic Sci Int, 2007. **165**(2-3): p. 216-24.

182. Wille, S.M.R., et al., *Practical aspects concerning validation and quality control for forensic and clinical bioanalytical quantitative methods.* Accreditation and Quality Assurance, 2011. **16**(6): p. 279-292.

183. Araujo, P., *Key aspects of analytical method validation and linearity evaluation.* J Chromatogr B Analyt Technol Biomed Life Sci, 2009. **877**(23): p. 2224-34.

184. Peters, F.T. and Maurer, H.H., *Bioanalytical method validation and its implications for forensic and clinical toxicology - A review.* Accreditation and Quality Assurance, 2002. **7**(11): p. 441-449.

185. Shabir, G.A., *Validation of high-performance liquid chromatography methods for pharmaceutical analysis: Understanding the differences and similarities between validation*

requirements of the US Food and Drug Administration, the US Pharmacopeia and the International Conference on Harmonization. Journal of chromatography A, 2003. **987**(1): p. 57-66.

186. Causon, R., *Validation of chromatographic methods in biomedical analysis viewpoint and discussion.* Journal of Chromatography B: Biomedical Sciences and Applications, 1997. **689**(1): p. 175-180.

187. Bansal, S. and DeStefano, A., *Key elements of bioanalytical method validation for small molecules.* The AAPS journal, 2007. **9**(1): p. E109-E114.

188. Bressolle, F., Bromet-Petit, M., and Audran, M., *Validation of liquid chromatographic and gas chromatographic methods Applications to pharmacokinetics.* Journal of Chromatography B: Biomedical Sciences and Applications, 1996. **686**(1): p. 3-10.

189. (ICH), I.C.o.H., *Validation of analytical procedures: Text and Methodology, Q2 (R1).* 2005.

190. Ribani, M., et al., *Validação em métodos cromatográficos e eletroforéticos.* Química nova, 2004. **27**(5): p. 771-780.

191. Zeng, W., et al., *A new approach for evaluating carryover and its influence on quantitation in high-performance liquid chromatography and tandem mass spectrometry assay.* Rapid Communications in Mass Spectrometry, 2006. **20**(4): p. 635-640.

192. Cassiano, N.M., et al., *Validação em métodos cromatográficos para análises de pequenas moléculas em matrizes biológicas.* Quim. Nova, 2009. **32**(4): p. 1021-1030.

193. Chambers, E., et al., *Systematic and comprehensive strategy for reducing matrix effects in LC/MS/MS analyses.* J Chromatogr B Analyt Technol Biomed Life Sci, 2007. **852**(1-2): p. 22-34.

194. Taylor, P.J., *Matrix effects: the Achilles heel of quantitative high-performance liquid chromatography-electrospray-tandem mass spectrometry.* Clin Biochem, 2005. **38**(4): p. 328-34.

195. Chou, K.L., Hurtig, H. I., Dashe, J. F. *Clinical manifestations of Parkinson disease.* 2012.

196. (WADA), W.A.-D.A., *Identification criteria for qualitative assays incorporating column chromatography and mass spectrometry.* 2010.

197. Hartmann, C., et al., *Validation of bioanalytical chromatographic methods.* Journal of pharmaceutical and biomedical analysis, 1998. **17**(2): p. 193-218.

198. Almeida, A.M.D., Castel-Branco, M.M., and Falcao, A.C., *Linear regression for calibration lines revisited: weighting schemes for bioanalytical methods.* Journal of Chromatography B, 2002. **774**(2): p. 215-222.

199. Kimanani, E.K., *Bioanalytical calibration curves: proposal for statistical criteria.* Journal of pharmaceutical and biomedical analysis, 1998. **16**(6): p. 1117-1124.

200. Van Loco, J., et al., *Linearity of calibration curves: use and misuse of the correlation coefficient.* Accreditation and Quality Assurance, 2002. **7**(7): p. 281-285.

201. Ribeiro, F.A.D.L., et al., *Planilha de validação: uma nova ferramenta para estimar figuras de mérito na validação de métodos analíticos univariados.* Química Nova, 2008. **31**(1): p. 164-171.

202. Brüggemann, L., Quapp, W., and Wennrich, R., *Test for non-linearity concerning linear calibrated chemical measurements.* Accreditation and Quality Assurance, 2006. **11**(12): p. 625-631.

203. Andrade, J.M. and Gómez-Carracedo, M.P., *Notes on the use of Mandel's test to check for nonlinearity in laboratory calibrations.* Analytical Methods, 2013. **5**(5): p. 1145.

204. Rozet, E., et al., *Advances in validation, risk and uncertainty assessment of bioanalytical methods.* J Pharm Biomed Anal, 2011. **55**(4): p. 848-58.

205. Danzer, K. and Currie, L.A., *Guidelines for calibration in analytical chemistry. Part I. Fundamentals and single component calibration (IUPAC Recommendations 1998).* Pure and Applied Chemistry, 1998. **70**(4): p. 993-1014.

206. Mulholland, M. and Hibbert, D.B., *Linearity and the limitations of least squares calibration.* Journal of Chromatography A, 1997. **762**(1): p. 73-82.

207. Maroto, A., et al., *Estimation of measurement uncertainty by using regression techniques and spiked samples. .* Analytica chimica acta, 2001. **446**(1): p. 131-143.

208. Kushnir, M.M., et al., *Analysis of catecholamines in urine by positive-ion electrospray tandem mass spectrometry.* Clinical chemistry, 2002. **48**(2): p. 323-331.

209. Hao, C., et al., *Study of the neurotransmitter dopamine and the neurotoxin 6-hydroxydopamine by electrospray ionization coupled with tandem mass spectrometry.* Rapid communications in mass spectrometry, 2002. **16**(6): p. 591-599.

210. Administration, U.S.D.o.H.a.H.S.F.a.D., *Bioanalytical Method Validation.* 2013.

211. Karnes, H.T., Shiu, G., and Shah, V.P., *Validation of bioanalytical methods.* Pharmaceutical research, 1991. **8**(4): p. 421-426.

212. Dadgar, D., et al., *Application issues in bioanalytical method validation, sample analysis and data reporting.* Journal of pharmaceutical and biomedical analysis, 1995. **13**(2): p. 89-97.

213. Mansilha, C., et al., *Quantification of endocrine disruptors and pesticides in water by gas chromatography-tandem mass spectrometry. Method validation using weighted linear regression schemes.* J Chromatogr A, 2010. **1217**(43): p. 6681-91.

214. Clouser-Roche, A., et al., *Beyond pass/fail: a procedure for evaluating the effect of carryover in bioanalytical LC/MS/MS methods.* J Pharm Biomed Anal, 2008. **47**(1): p. 146-55.

215. Hughes, N.C., et al., *Determination of carryover and contamination for mass spectrometry-based chromatographic assays.* The AAPS journal, 2007. **9**(3): p. E353-E360.

216. Matuszewski, B.K., Constanzer, M.L., and Chavez-Eng, C.M., *Strategies for the Assessment of Matrix Effect in Quantitative Bioanalytical Methods Based on HPLC-MS/MS.* Analytical chemistry, 2003. **75**(13): p. 3019-3030.

217. Van Eeckhaut, A., et al., *Validation of bioanalytical LC-MS/MS assays: evaluation of matrix effects.* J Chromatogr B Analyt Technol Biomed Life Sci, 2009. **877**(23): p. 2198-207.

218. Contin, M., et al., *Kinetic-dynamic relationship of oral levodopa: Possible biphasic response after sequential doses in Parkinson's disease.* Movement disorders, 1992. **7**(3): p. 244-248.

219. Contin, M., et al., *Levodopa therapy monitoring in patients with Parkinson disease: a kinetic–dynamic approach.* Therapeutic drug monitoring, 2001. **23**(6): p. 621-629.

8. Appendix

Appendix 8.1. Supplementary information about the standard solutions.

	Name	Molecular weight (g/mol)	Mass (mg)	Final volume (mL)	Concentration (mM)
Analytical standards	L-tyrosine	181.19	2.0	4	2.75
	L-DOPA	197.19	2.4	4	3.05
	Dopamine	153.18	2.0	2	6.55
	3-Methoxytyramine	167.21	2.1	2	6.30
	3,4-Dihydroxyphenylacetic acid	168.15	2.2	2	6.54
	Homovanillic acid	182.17	2.0	2	5.49
Internal standards	L-tyrosine (d7, 98%)	188.23	2.5	4	3.30
	L-DOPA (ring-d3)	200.21	1.1	4	1.37
	Dopamine-1,1,2,2-d4	157.12	5.0	2	15.9
	3-Methoxytyramine (1,1,2,2-d4, 97%)	171.11	2.3	2	6.70
	3,4-Dihydroxyphenylacetic acid (Ring-d3, 2,2-d2, 98%)	173.18	1.8	2	5.20
	Homovanillic acid - d3	185.19	1.0	2	2.70

Appendix 8.2. Analysis of plasma samples.

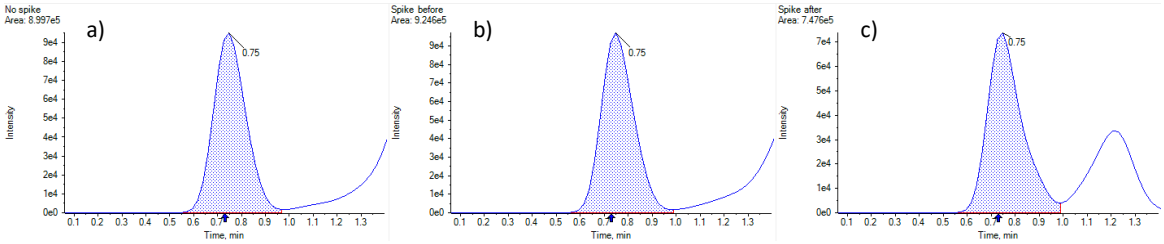

Figure 8.1. Analysis of the fragment with m/z 136.2 of L-tyrosine in a "blank" plasma sample (a), in a plasma sample which was spiked with 10 µL of a mix containing the six analytes and the six internal standards before the extraction procedure (b), and in a plasma sample which was spiked with 10 µL of a mix containing the six analytes and the six internal standards after the extraction procedure (c).

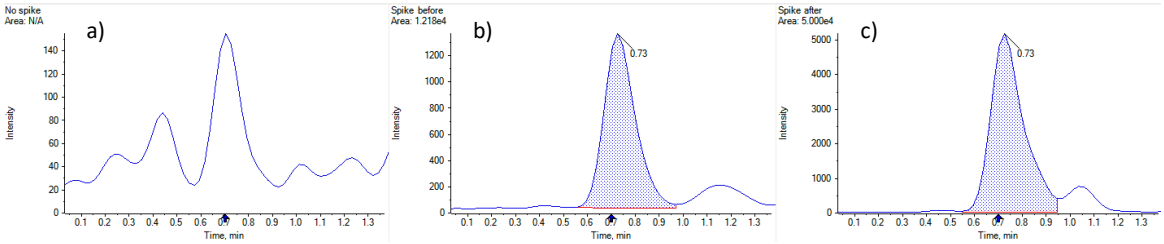

Figure 8.2. Analysis of the fragment with m/z 152.1 of L-ODPA in a "blank" plasma sample (a), in a plasma sample which was spiked with 10 µL of a mix containing the six analytes and the six internal standards before the extraction procedure (b), and in a plasma sample which was spiked with 10 µL of a mix containing the six analytes and the six internal standards after the extraction procedure (c).

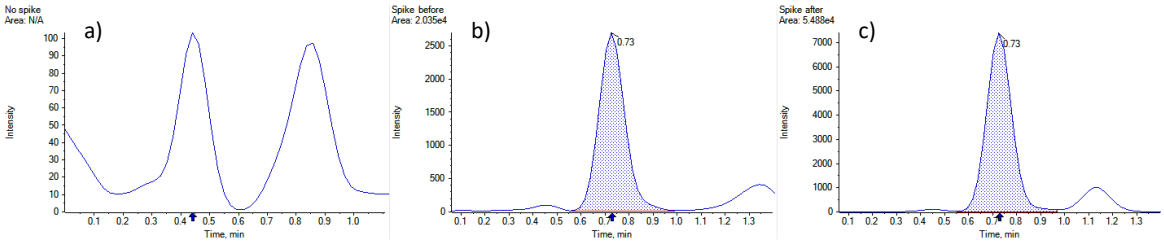

Figure 8.3. Analysis of the fragment with m/z 119.1 of 3-methoxytyramine in a "blank" plasma sample (a), in a plasma sample which was spiked with 10 µL of a mix containing the six analytes and the six internal standards before the extraction procedure (b), and in a plasma sample which was spiked with 10 µL of a mix containing the six analytes and the six internal standards after the extraction procedure (c).

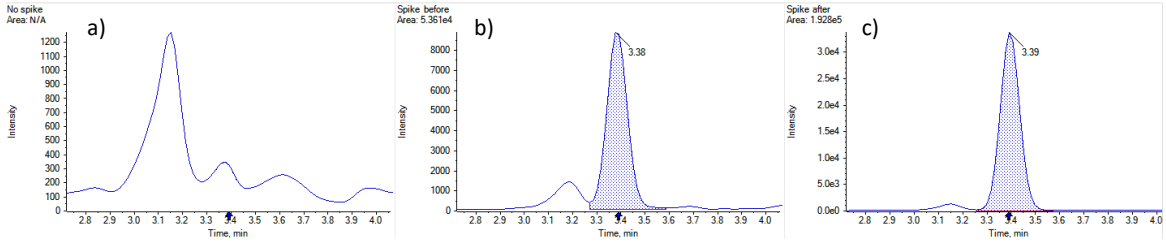

Figure 8.4. Analysis of the fragment with m/z 123.2 of 3,4-dihydroxyphenylacetic acid in a "blank" plasma sample (a), in a plasma sample which was spiked with 10 µL of a mix containing the six analytes and the six internal standards before the extraction procedure (b), and in a plasma sample which was spiked with 10 µL of a mix containing the six analytes and the six internal standards after the extraction procedure (c).

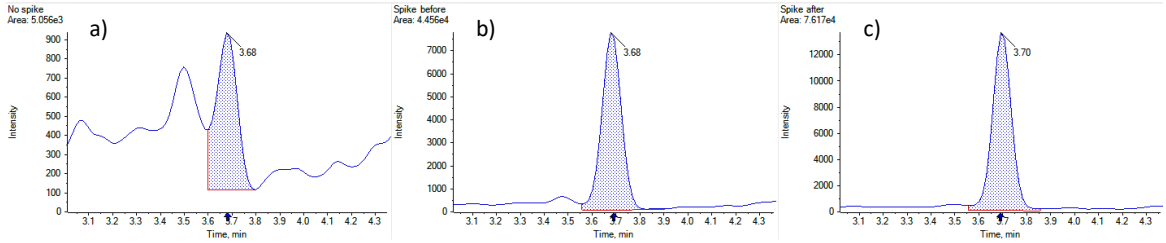

Figure 8.5. Analysis of the fragment with m/z 137.2 of homovanillic acid in a "blank" plasma sample (a), in a plasma sample which was spiked with 10 µL of a mix containing the six analytes and the six internal standards before the extraction procedure (b), and in a plasma sample which was spiked with 10 µL of a mix containing the six analytes and the six internal standards after the extraction procedure (c).

Appendix 8.3. Analysis of different volumes of plasma.

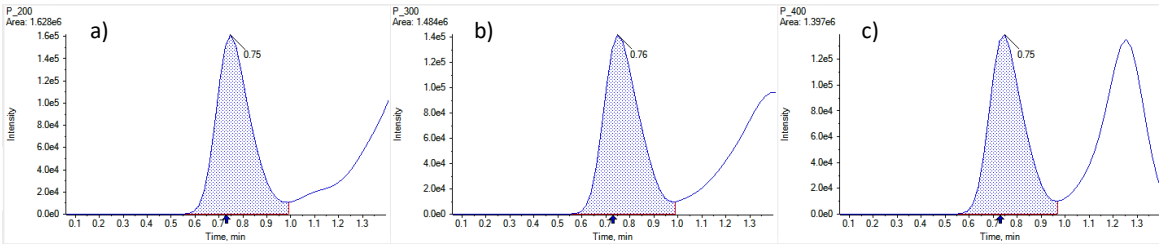

Figure 8.6. Chromatogram of the fragment with m/z 136.2 of L-tyrosine in 200 µL (a), 300 µL (b) and 400 µL (c) of plasma.

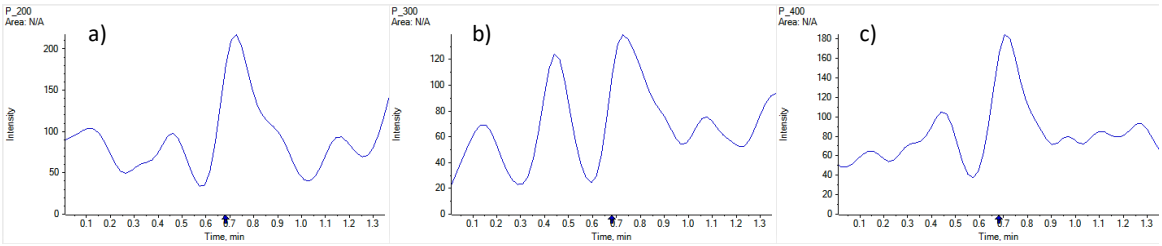

Figure 8.7. Chromatogram of the fragment with m/z 152.1 of L-DOPA in 200 µL (a), 300 µL (b) and 400 µL (c) of plasma.

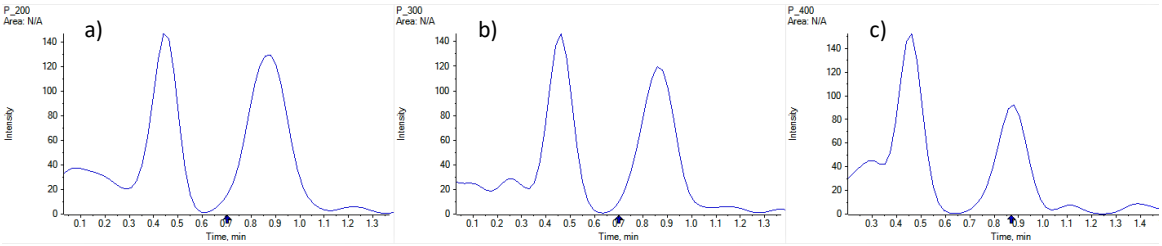

Figure 8.8. Chromatogram of the fragment with m/z 119.1 of 3-methoxytyramine in 200 µL (a), 300 µL (b) and 400 µL (c) of plasma.

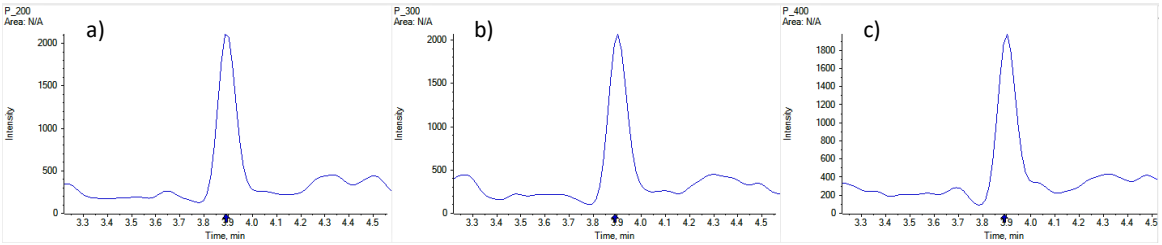

Figure 8.9. Chromatogram of the fragment with m/z 123.2 of 3,4-dihydroxyphenylacetic acid in 200 µL (a), 300 µL (b) and 400 µL (c) of plasma.

Appendix 8.4. Data related to the study of selectivity in solvent and plasma samples.

Table 8.1. Application of the acceptance WADA criteria for the identification of dopamine in solvent.

		Transition	Relative abundance		S/N		ΔRT	
Criteria		154.2/65.0	8.999	18.999			0.684	0.711
		154.2/91.1	26.485	39.727	>3		0.683	0.711
		154.2/137.2	90.000	110.000			0.680	0.708
		Transition	**Absolute area**	**Relative area**	**S/N**	**RT_A**	**RT_{IS}**	**RT_{ratio}**
Positive	#1	154.2/65.0	75383.131	13.999	1014.081	0.697	0.689	1.013
		154.2/91.1	178276.702	33.106	1497.620	0.697	0.689	1.013
		154.2/137.2	538499.379	100.000	1858.686	0.694	0.689	1.008
Negative	#1	154.2/65.0	-	-	-	-	-	-
		154.2/91.1	-	-	-	-	-	-
		154.2/137.2	-	-	-	-	-	-
Positive	#2	154.2/65.0	86990.642	13.696	868.940	0.699	0.690	1.012
		154.2/91.1	222167.316	34.978	1865.882	0.697	0.690	1.010
		154.2/137.2	635170.513	100.000	2027.497	0.697	0.690	1.010
Negative	#2	154.2/65.0	-	-	-	-	-	-
		154.2/91.1	-	-	-	-	-	-
		154.2/137.2	-	-	-	-	-	-
Positive	#3	154.2/65.0	93178.832	13.763	707.214	0.699	0.693	1.009
		154.2/91.1	242449.112	35.811	1907.877	0.698	0.693	1.008
		154.2/137.2	677029.107	100.000	1333.148	0.699	0.693	1.008
Negative	#3	154.2/65.0	-	-	-	-	-	-
		154.2/91.1	-	-	-	-	-	-
		154.2/137.2	-	-	-	-	-	-

Table 8.2. Application of the acceptance WADA criteria for the identification of L-tyrosine in solvent. Values that do not fulfill the criteria are highlighted.

	Transition	Relative abundance		S/N		ΔRT	
Criteria	182.2/91.1	34.727	52.090	>3		0.708	0.737
	182.2/136.2	76.390	96.390			0.709	0.738
	182.2/165.1	90.000	110.000			0.711	0.740
	Transition	**Absolute area**	**Relative area**	**S/N**	**RT_A**	**RT_{IS}**	**RT_{ratio}**
Positive #1	182.2/91.1	80260.780	43.408	651.653	0.723	0.719	1.005
	182.2/136.2	159732.320	86.390	733.440	0.723	0.719	1.005
	182.2/165.1	184896.671	100.000	202.744	0.726	0.719	1.009
Negative #1	182.2/91.1	-	-	-	-	-	-
	182.2/136.2	-	-	-	-	-	-
	182.2/165.1	-	-	-	-	-	-
Positive #2	182.2/91.1	129153.333	43.622	872.526	0.706	0.704	1.004
	182.2/136.2	254944.248	86.107	1001.419	0.705	0.704	1.002
	182.2/165.1	296076.935	100.000	370.402	0.707	0.704	1.005
Negative #2	182.2/91.1	-	-	-	-	-	-
	182.2/136.2	-	-	-	-	-	-
	182.2/165.1	-	-	-	-	-	-
Positive #3	182.2/91.1	128197.465	39.861	863.284	0.708	0.706	1.004
	182.2/136.2	275674.398	85.716	1281.886	0.706	0.706	1.001
	182.2/165.1	321613.572	100.000	439.234	0.708	0.706	1.003
Negative #3	182.2/91.1	-	-	-	-	-	-
	182.2/136.2	-	-	-	-	-	-
	182.2/165.1	-	-	-	-	-	-

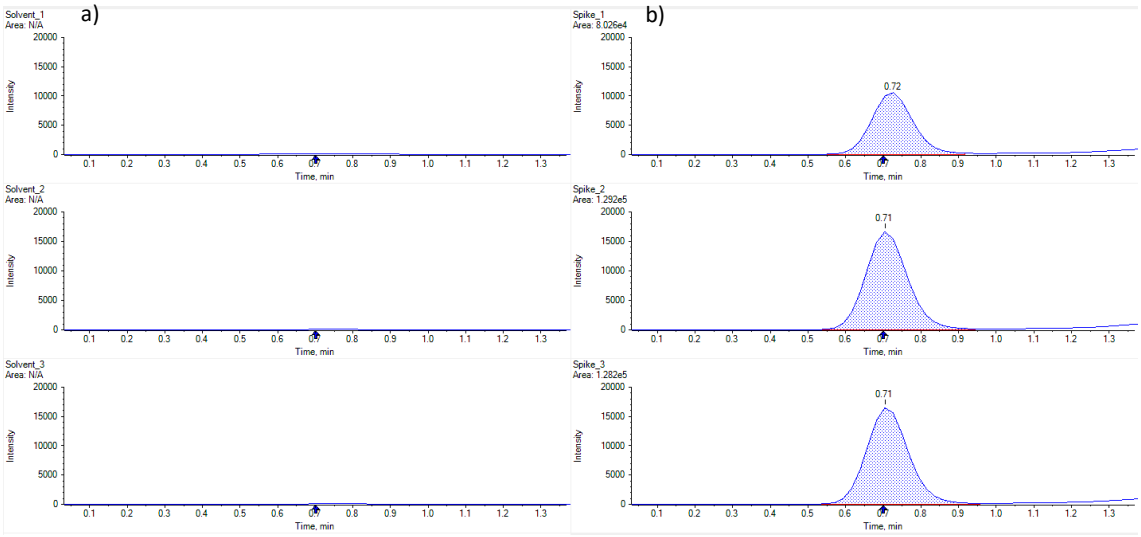

Figure 8.10. Chromatographic spectra of the fragment with m/z 91.1 of tyrosine for the selectivity in solvent. a) Three different solutions constituted by methanol that were not spiked with any compound (negative samples). b) Three solvent solutions spiked with a mix containing the analytes and the internal standards (positive samples).

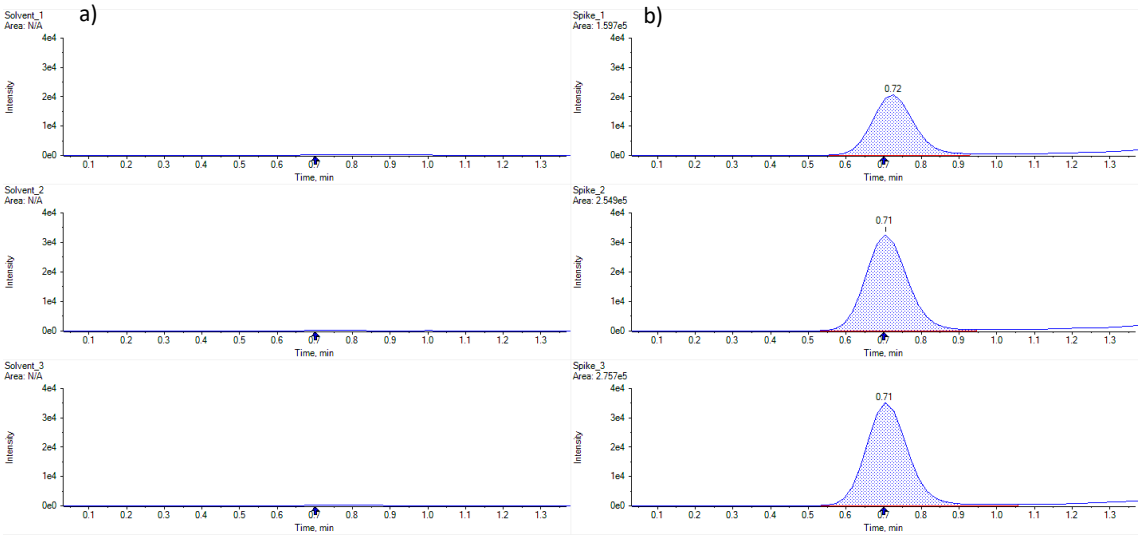

Figure 8.11. Chromatographic spectra of the fragment with m/z 136.2 of tyrosine for the selectivity in solvent. a) Three different solutions constituted by methanol that were not spiked with any compound (negative samples). b) Three solvent solutions spiked with a mix containing the analytes and the internal standards (positive samples).

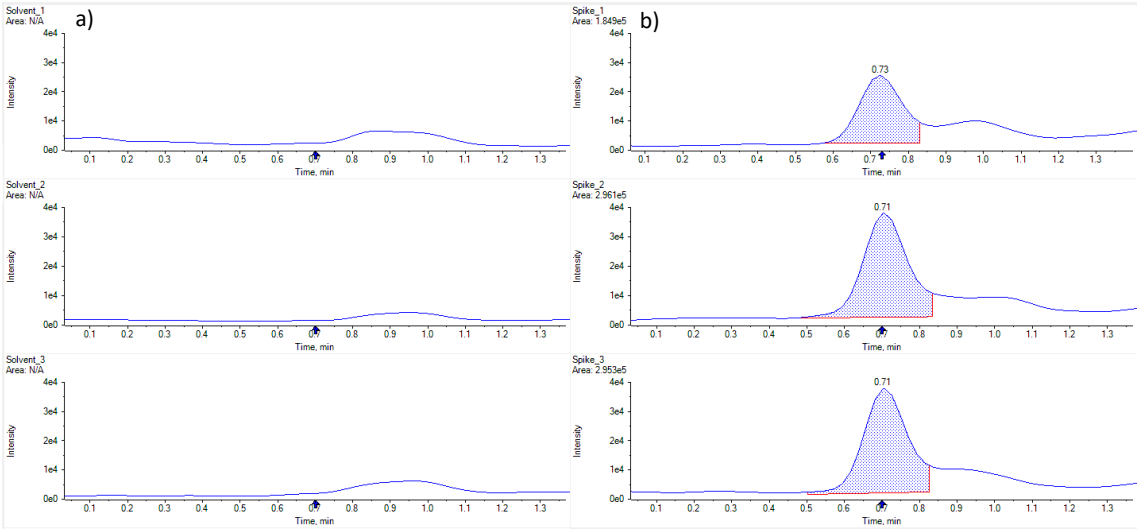

Figure 8.12. Chromatographic spectra of the fragment with m/z 165.1 of tyrosine for the selectivity in solvent. a) Three different solutions constituted by methanol that were not spiked with any compound (negative samples). b) Three solvent solutions spiked with a mix containing the analytes and the internal standards (positive samples).

Table 8.3. Application of the acceptance WADA criteria for the identification of L-DOPA in solvent. Values that do not fulfill the criteria are highlighted.

	Transition	Relative abundance		S/N		ΔRT	
Criteria	198.2/135.1	23.201	34.802	>3		0.706	0.735
	198.2/152.1	90.000	110.000			0.700	0.729
	198.2/181.1	78.551	98.551			0.703	0.731
	Transition	**Absolute area**	**Relative area**	**S/N**	**RT_A**	**RT_{IS}**	**RT_{ratio}**
Positive #1	198.2/135.1	49279.036	29.001	379.192	0.720	0.712	1.012
	198.2/152.1	169919.953	100.000	1085.680	0.715	0.712	1.004
	198.2/181.1	150465.131	88.551	296.397	0.717	0.712	1.007
Negative #1	198.2/135.1	-	-	-	-	-	-
	198.2/152.1	-	-	-	-	-	-
	198.2/181.1	-	-	-	-	-	-
Positive #2	198.2/135.1	73375.810	30.236	476.271	0.699	0.696	1.005
	198.2/152.1	242676.394	100.000	1797.401	0.699	0.696	1.005
	198.2/181.1	194671.930	80.219	382.091	0.700	0.696	1.006
Negative #2	198.2/135.1	-	-	-	-	-	-
	198.2/152.1	-	-	-	-	-	-
	198.2/181.1	-	-	-	-	-	-
Positive #3	198.2/135.1	34.091	566.813	0.703	0.697	1.008	34.091
	198.2/152.1	100.000	1901.794	0.699	0.697	1.003	100.000
	198.2/181.1	88.267	377.409	0.700	0.697	1.005	88.267
Negative #3	198.2/135.1	-	-	-	-	-	-
	198.2/152.1	-	-	-	-	-	-
	198.2/181.1	-	-	-	-	-	-

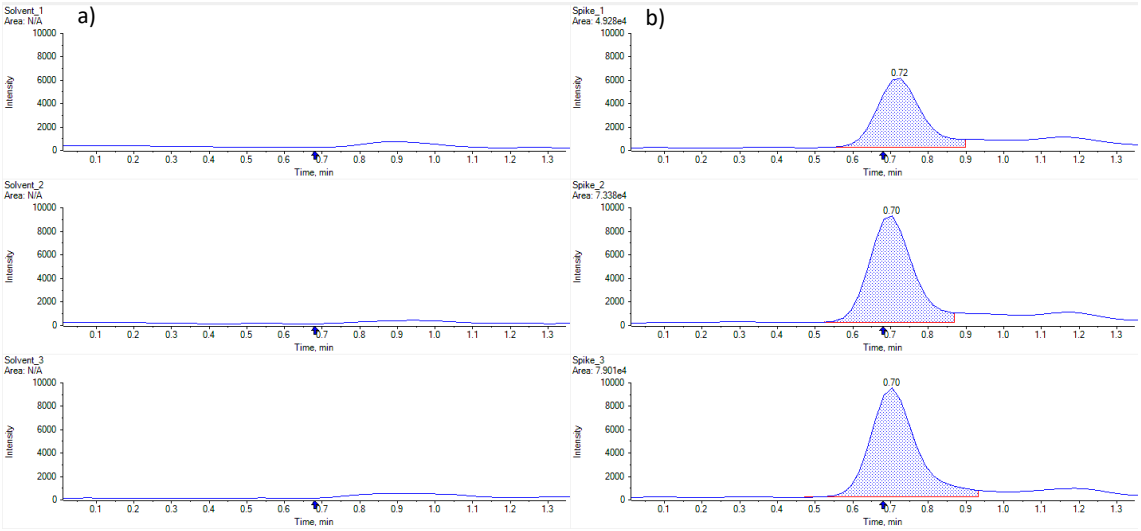

Figure 8.13. Chromatographic spectra of the fragment with m/z 135.1 of L-DOPA for the selectivity in solvent. a) Three different solutions constituted by methanol that were not spiked with any compound (negative samples). b) Three solvent solutions spiked with a mix containing the analytes and the internal standards (positive samples).

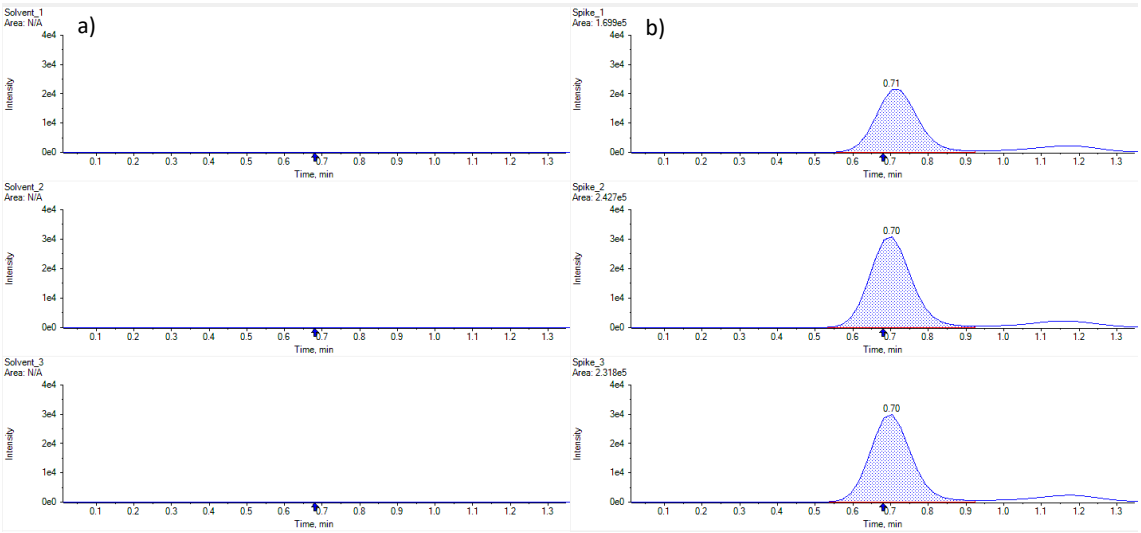

Figure 8.14. Chromatographic spectra of the fragment with m/z 152.1 of L-DOPA for the selectivity in solvent. a) Three different solutions constituted by methanol that were not spiked with any compound (negative samples). b) Three solvent solutions spiked with a mix containing the analytes and the internal standards (positive samples).

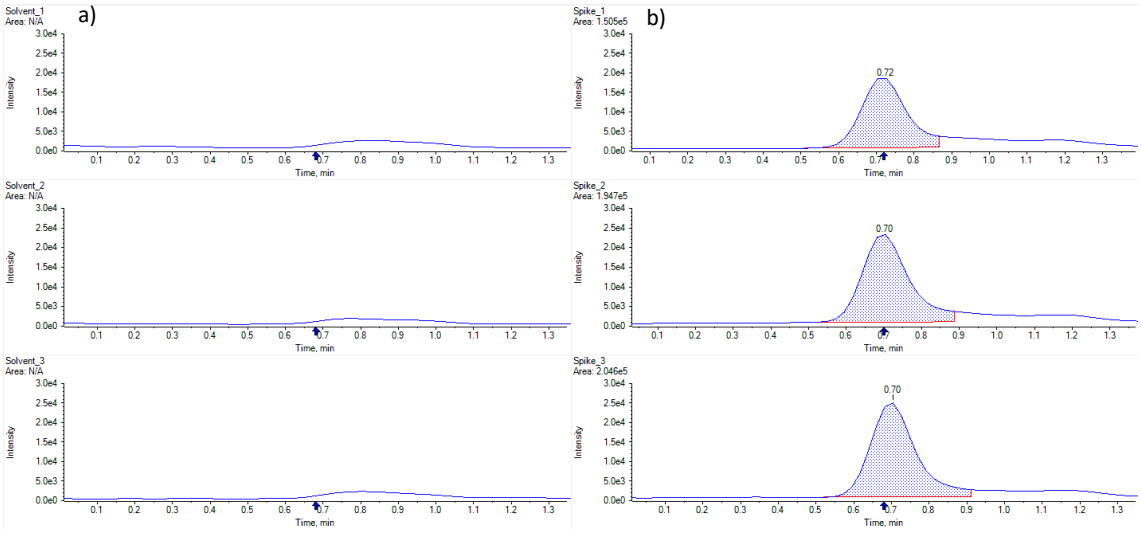

Figure 8.15. Chromatographic spectra of the fragment with m/z 181.1 of L-DOPA for the selectivity in solvent. a) Three different solutions constituted by methanol that were not spiked with any compound (negative samples). b) Three solvent solutions spiked with a mix containing the analytes and the internal standards (positive samples).

Table 8.4. Application of the acceptance WADA criteria for the identification of 3-methoxytyramine in solvent. Values that do not fulfill the criteria are highlighted.

	Transition	Relative abundance		S/N		ΔRT	
Criteria	168.3/91.0	90.000	110.000	>3		0.714	0.743
	168.3/119.1	51.167	71.167			0.713	0.743
	Transition	**Absolute area**	**Relative area**	**S/N**	**RT_A**	**RT_{IS}**	**RT_{ratio}**
Positive #1	168.3/91.0	506040.782	100.000	1188.642	0.728	0.724	1.006
	168.3/119.1	309527.754	61.167	1369.872	0.728	0.724	1.005
Negative #1	168.3/91.0	-	-	-	-	-	-
	168.3/119.1	-	-	-	-	-	-
Positive #2	168.3/91.0	646886.900	100.000	1409.760	0.710	0.708	1.003
	168.3/119.1	382121.081	59.071	1575.927	0.710	0.708	1.004
Negative #2	168.3/91.0	-	-	-	-	-	-
	168.3/119.1	-	-	-	-	-	-
Positive #3	168.3/91.0	679568.151	100.000	2323.955	0.715	0.710	1.008
	168.3/119.1	404846.223	59.574	1982.700	0.712	0.710	1.003
Negative #3	168.3/91.0	-	-	-	-	-	-
	168.3/119.1	-	-	-	-	-	-

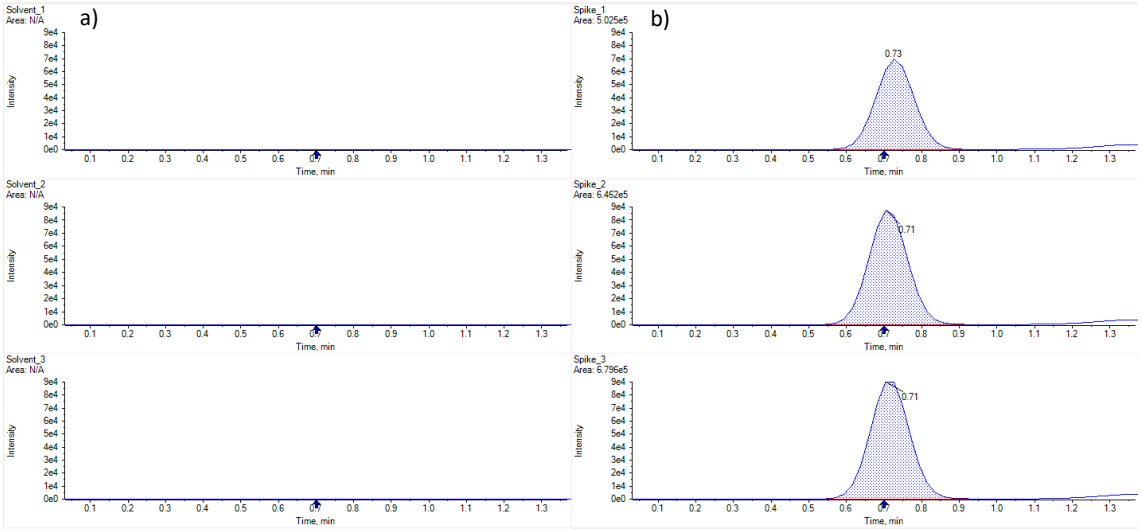

Figure 8.16. Chromatographic spectra of the fragment with m/z 91.0 of 3-methoxytyramine for the selectivity in solvent. a) Three different solutions constituted by methanol that were not spiked with any compound (negative samples). b) Three solvent solutions spiked with a mix containing the analytes and the internal standards (positive samples).

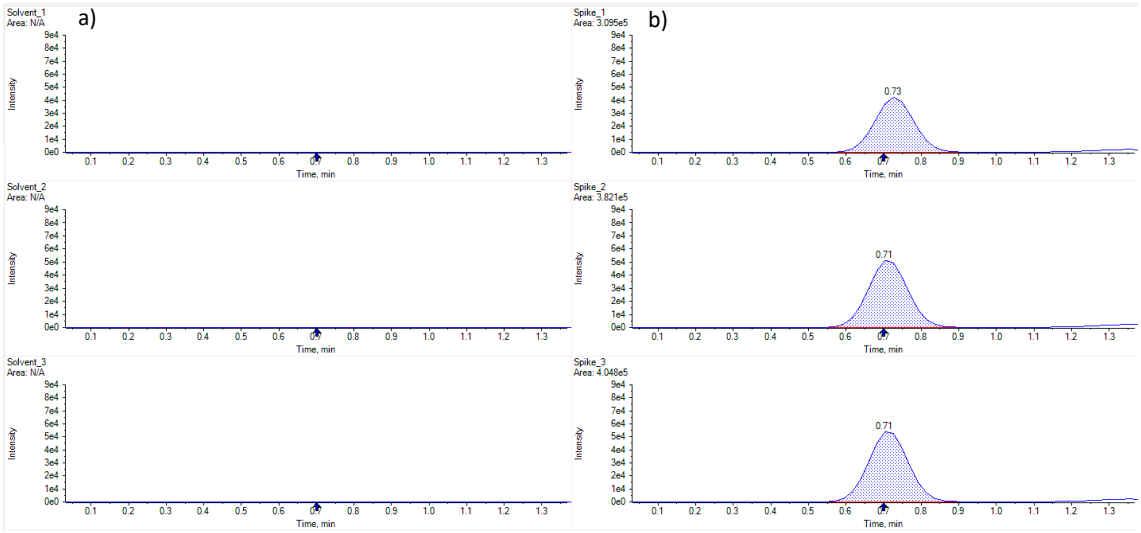

Figure 8.17. Chromatographic spectra of the fragment with m/z 119.1 of 3-methoxytyramine for the selectivity in solvent. a) Three different solutions constituted by methanol that were not spiked with any compound (negative samples). b) Three solvent solutions spiked with a mix containing the analytes and the internal standards (positive samples).

Table 8.5. Application of the acceptance WADA criteria for the identification of 3,4-dihydroxyphenylacetic acid in solvent.

Criteria	Transition	Relative abundance		S/N		ΔRT	
	167.0/122.2	1.635	4.905	>3		3.326	3.462
	167.0/123.2	90.000	110.000			3.322	3.458
	Transition	**Absolute area**	**Relative area**	**S/N**	**RT_A**	**RT_{IS}**	**RT_{ratio}**
Positive #1	167.0/122.2	4457.460	3.270	139.153	3.394	3.373	1.006
	167.0/123.2	136305.025	100.000	3296.957	3.390	3.373	1.005
Negative #1	167.0/122.2	-	-	-	-	-	-
	167.0/123.2	-	-	-	-	-	-
Positive #2	167.0/122.2	5427.623	2.965	109.820	3.375	3.367	1.002
	167.0/123.2	183052.274	100.000	2728.204	3.381	3.367	1.004
Negative #2	167.0/122.2	-	-	-	-	-	-
	167.0/123.2	-	-	-	-	-	-
Positive #3	167.0/122.2	4254.346	3.360	110.317	3.374	3.362	1.004
	167.0/123.2	126632.315	100.000	2318.150	3.377	3.362	1.005
Negative #3	167.0/122.2	-	-	-	-	-	-
	167.0/123.2	-	-	-	-	-	-

Table 8.6. Application of the acceptance WADA criteria for the identification of homovanillic acid in solvent.

	Transition	Relative abundance		S/N		ΔRT	
Criteria	181.0/136.7	59.468	79.468	>3		3.613	3.761
	181.0/137.2	90.000	110.000			3.612	3.760
	Transition	**Absolute area**	**Relative area**	**S/N**	**RT_A**	**RT_{IS}**	**RT_{ratio}**
Positive #1	181.0/136.7	33223.318	69.468	993.050	3.687	3.677	1.003
	181.0/137.2	47825.366	100.000	1909.399	3.686	3.677	1.003
Negative #1	181.0/136.7	-	-	-	-	-	-
	181.0/137.2	-	-	-	-	-	-
Positive #2	181.0/136.7	44187.864	72.806	1243.658	3.669	3.662	1.002
	181.0/137.2	60692.504	100.000	2211.710	3.669	3.662	1.002
Negative #2	181.0/136.7	-	-	-	-	-	-
	181.0/137.2	-	-	-	-	-	-
Positive #3	181.0/136.7	37412.401	78.787	1321.142	3.689	3.679	1.003
	181.0/137.2	47485.470	100.000	1863.659	3.686	3.679	1.002
Negative #3	181.0/136.7	-	-	-	-	-	-
	181.0/137.2	-	-	-	-	-	-

Table 8.7. Application of the acceptance WADA criteria for the identification of 3-methoxytyramine in plasma.

Criteria	Transition	Relative abundance		S/N		ΔRT	
	168.3/91.0	90.000	110.000	>3		0.730	0.760
	168.3/119.1	50.711	70.711			0.728	0.758
	Transition	**Absolute area**	**Relative area**	**S/N**	**RT_A**	**RT_{IS}**	**RT_{ratio}**
Positive #1	168.3/91.0	108406.439	100.000	528.002	0.745	0.737	1.010
	168.3/119.1	65814.452	60.711	482.206	0.743	0.737	1.008
Negative #1	168.3/91.0	-	-	-	-	-	-
	168.3/119.1	-	-	-	-	-	-
Positive #2	168.3/91.0	111419.417	100.000	447.427	0.747	0.744	1.004
	168.3/119.1	68339.332	61.335	575.721	0.745	0.744	1.001
Negative #2	168.3/91.0	-	-	-	-	-	-
	168.3/119.1	-	-	-	-	-	-
Positive #3	168.3/91.0	111707.141	100.000	479.927	0.747	0.742	1.007
	168.3/119.1	61295.568	54.872	459.948	0.747	0.742	1.007
Negative #3	168.3/91.0	-	-	-	-	-	-
	168.3/119.1	-	-	-	-	-	-
Positive #4	168.3/91.0	109024.064	100.000	468.207	0.749	0.745	1.006
	168.3/119.1	64758.359	59.398	529.936	0.748	0.745	1.004
Negative #4	168.3/91.0	-	-	-	-	-	-
	168.3/119.1	-	-	-	-	-	-
Positive #5	168.3/91.0	95682.922	100.000	426.195	0.751	0.749	1.003
	168.3/119.1	61494.858	64.269	569.538	0.752	0.749	1.003
Negative #5	168.3/91.0	-	-	-	-	-	-
	168.3/119.1	-	-	-	-	-	-
Positive #6	168.3/91.0	93428.628	100.000	427.229	0.752	0.748	1.006
	168.3/119.1	59918.761	64.133	557.426	0.750	0.748	1.003
Negative #6	168.3/91.0	-	-	-	-	-	-
	168.3/119.1	-	-	-	-	-	-

Table 8.8. Application of the acceptance WADA criteria for the identification of 3,4-dihydroxyphenylacetic acid in plasma.

Criteria	Transition	Relative abundance		S/N		ΔRT	
	167.0/122.2	1.279	3.837	>3		3.339	3.475
	167.0/123.2	90.000	110.000			3.327	3.463
	Transition	**Absolute area**	**Relative area**	**S/N**	**RT_A**	**RT_{IS}**	**RT_{ratio}**
Positive #1	167.0/122.2	485.695	2.558	17.759	3.407	3.381	1.007
	167.0/123.2	18987.107	100.000	287.473	3.395	3.381	1.004
Negative #1	167.0/122.2	-	-	-	-	-	-
	167.0/123.2	-	-	-	-	-	-
Positive #2	167.0/122.2	1612.658	3.556	59.663	3.399	3.380	1.006
	167.0/123.2	45344.261	100.000	478.454	3.397	3.380	1.005
Negative #2	167.0/122.2	-	-	-	-	-	-
	167.0/123.2	-	-	-	-	-	-
Positive #3	167.0/122.2	1324.726	3.811	51.441	3.406	3.393	1.004
	167.0/123.2	34760.535	100.000	580.615	3.406	3.393	1.004
Negative #3	167.0/122.2	-	-	-	-	-	-
	167.0/123.2	-	-	-	-	-	-
Positive #4	167.0/122.2	354.280	2.834	13.094	3.413	3.399	1.004
	167.0/123.2	12498.910	100.000	271.457	3.416	3.399	1.005
Negative #4	167.0/122.2	-	-	-	-	-	-
	167.0/123.2	-	-	-	-	-	-
Positive #5	167.0/122.2	1287.536	3.822	45.788	3.418	3.399	1.006
	167.0/123.2	33687.626	100.000	600.758	3.412	3.399	1.004
Negative #5	167.0/122.2	-	-	-	-	-	-
	167.0/123.2	-	-	-	-	-	-
Positive #6	167.0/122.2	112.658	3.603	4.011	3.401	3.381	1.006
	167.0/123.2	3126.550	100.000	46.697	3.394	3.381	1.004
Negative #6	167.0/122.2	-	-	-	-	-	-
	167.0/123.2	-	-	-	-	-	-

Table 8.9. Application of the acceptance WADA criteria for the identification of homovanillic acid in plasma.

Criteria	Transition	Relative abundance		S/N		ΔRT	
	181.0/136.7	69.069	89.069	>3		3.624	3.772
	181.0/137.2	90.000	110.000			3.626	3.774
	Transition	**Absolute area**	**Relative area**	**S/N**	**RT_A**	**RT_{IS}**	**RT_{ratio}**
Positive #1	181.0/136.7	25175.054	79.069	239.620	3.698	3.694	1.001
	181.0/137.2	31839.352	100.000	322.446	3.700	3.694	1.002
Negative #1	181.0/136.7	-	-	-	-	-	-
	181.0/137.2	-	-	-	-	-	-
Positive #2	181.0/136.7	24477.573	73.656	155.559	3.702	3.690	1.003
	181.0/137.2	33232.406	100.000	381.884	3.699	3.690	1.002
Negative #2	181.0/136.7	-	-	-	-	-	-
	181.0/137.2	-	-	-	-	-	-
Positive #3	181.0/136.7	38558.447	88.268	386.616	3.704	3.695	1.003
	181.0/137.2	43683.288	100.000	523.353	3.703	3.695	1.002
Negative #3	181.0/136.7	-	-	-	-	-	-
	181.0/137.2	-	-	-	-	-	-
Positive #4	181.0/136.7	37226.460	81.095	349.076	3.701	3.692	1.002
	181.0/137.2	45905.034	100.000	411.120	3.701	3.692	1.003
Negative #4	181.0/136.7	-	-	-	-	-	-
	181.0/137.2	-	-	-	-	-	-
Positive #5	181.0/136.7	24908.520	76.692	204.493	3.706	3.700	1.002
	181.0/137.2	32478.547	100.000	294.437	3.708	3.700	1.002
Negative #5	181.0/136.7	-	-	-	-	-	-
	181.0/137.2	-	-	-	-	-	-
Positive #6	181.0/136.7	29267.725	86.914	160.137	3.695	3.688	1.002
	181.0/137.2	33674.469	100.000	272.986	3.694	3.688	1.002
Negative #6	181.0/136.7	-	-	-	-	-	-
	181.0/137.2	-	-	-	-	-	-

Appendix 8.5. Example of the linearity analysis for the fragment with m/z 91.1 of dopamine in solvent.

Concentration (pmol/µL)	Peak area ratio	Residuals
0.05	0.037	-0.007
0.10	0.063	-0.013
0.15	0.110	-0.004
0.25	0.139	-0.030
0.50	0.370	0.044
1.0	0.790	0.151
2.0	1.175	-0.092
3.0	1.755	-0.143
4.0	2.509	-0.017
5.0	3.258	0.103

Regression statistics	
m	0.63
b	0.01
R	0.997
R^2	0.994
$S_{y/x}$	0.08
$2xS_{y/x}$	0.16
T-student value	2.31
Upper limit 95%	0.092
Lower limit 95%	-0.067

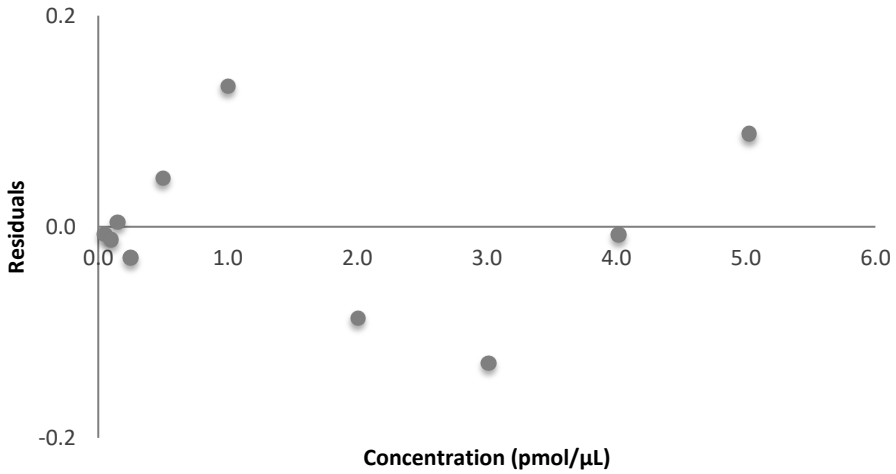

Figure 8.18. Plot of the residuals versus the concentration, used in the linearity study of dopamine in solvent.

Appendix 8.6. Example of the linearity analysis for the fragment with m/z 136.2 of L-tyrosine in solvent.

Concentration (pmol/µL)	Peak area ratio	Residuals
0.05	0.022	-0.007
0.10	0.043	0.001
0.15	0.056	0.001
0.25	0.087	0.006
0.50	0.148	0.003
1.0	0.274	0.000
2.0	0.495	-0.036
3.0	0.806	0.016
4.0	1.105	0.058
5.0	1.263	-0.042

Regression statistics	
m	0.26
b	0.02
R	0.998
R^2	0.997
$S_{y/x}$	0.03
$2xS_{y/x}$	0.06
T-student value	2.30
Upper limit 95%	0.045
Lower limit 95%	-0.012

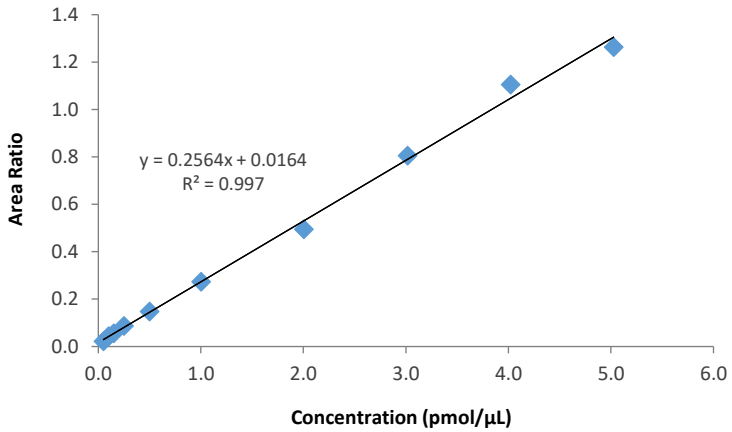

Figure 8.19. Calibration curve for the fragment with m/z 143.2 of L-tyrosine in solvent.

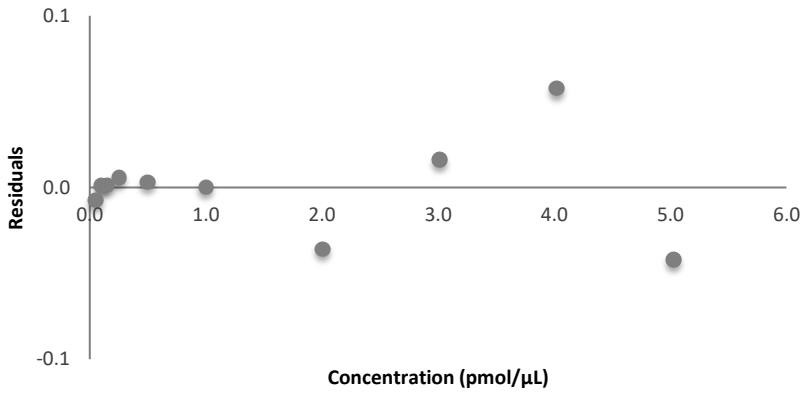

Figure 8.20. Plot of the residuals versus the concentration, used in the linearity study of L-tyrosine in solvent.

Appendix 8.7. Example of the linearity analysis for the fragment with m/z 152.1 of L-DOPA in solvent.

Concentration (pmol/µL)	Peak area ratio	Residuals
0.10	0.038	0.003
0.15	0.052	0.002
0.25	0.074	-0.008
0.50	0.168	0.009
1.0	0.328	0.014
2.0	0.575	-0.048
3.0	0.998	0.063
4.0	1.233	-0.012
5.0	1.483	-0.073
6.0	1.913	0.051

Regression statistics	
m	0.31
b	0.005
R	0.998
R^2	0.996
$S_{y/x}$	0.04
$2xS_{y/x}$	0.09
T-student value	2.31
Upper limit 95%	0.046
Lower limit 95%	-0.038

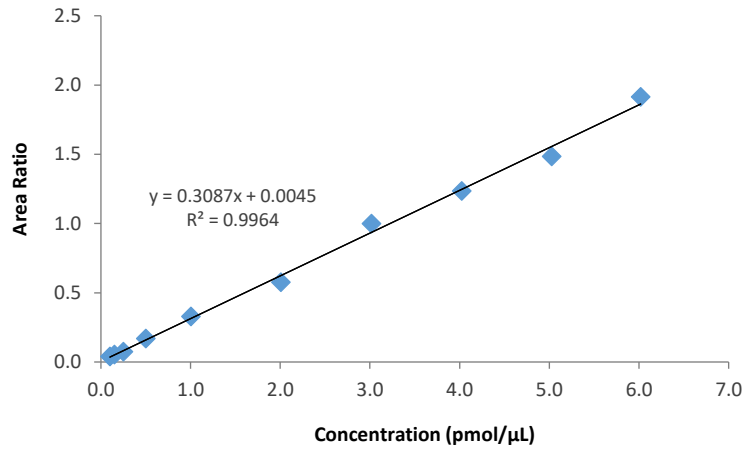

Figure 8.21. Calibration curve for the fragment with m/z 152.1 of L-DOPA in solvent.

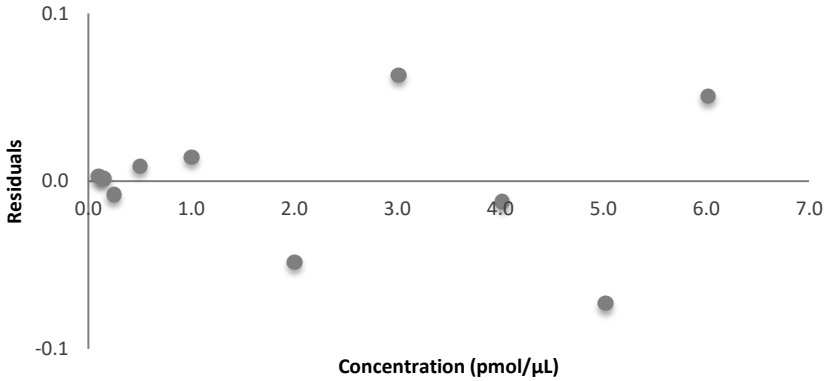

Figure 8.22. Plot of the residuals versus the concentration, used in the linearity study of L-DOPA in solvent.

Appendix 8.8. Example of the linearity analysis for the fragment with m/z 119.1 of 3-methoxytyramine in solvent.

Concentration (pmol/µL)	Peak area ratio	Residuals
0.03	0.022	-0.008
0.05	0.031	-0.008
0.10	0.050	-0.007
0.15	0.065	-0.009
0.25	0.132	0.023
0.50	0.205	0.008
1.0	0.394	0.019
3.0	1.096	0.012
4.0	1.351	-0.087
5.0	1.849	0.057

Regression statistics	
m	0.35
b	0.02
R	0.998
R^2	0.997
$S_{y/x}$	0.04
$2xS_{y/x}$	0.08
T-student value	2.31
Upper limit 95%	0.059
Lower limit 95%	-0.017

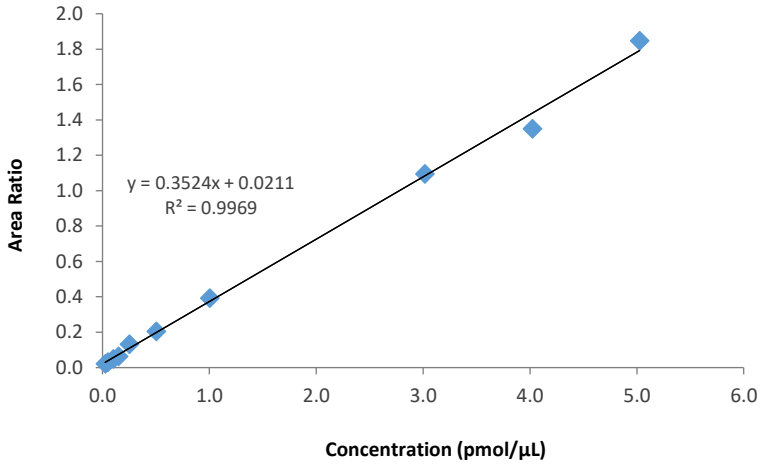

Figure 8.23. Calibration curve for the fragment with m/z 119.1 of 3-methoxytyramine in solvent.

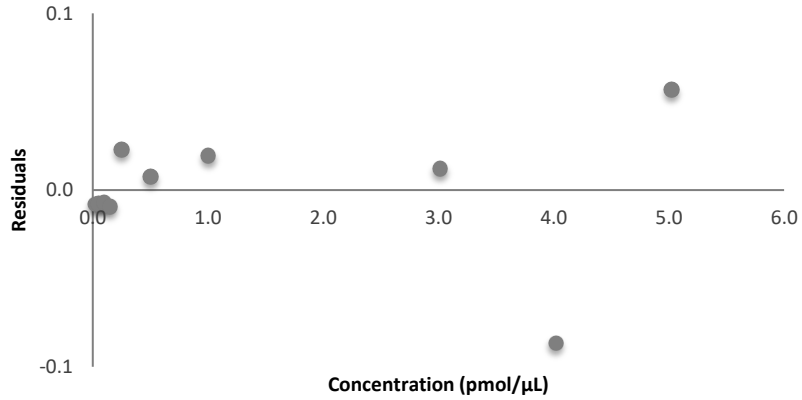

Figure 8.24. Plot of the residuals versus the concentration, used in the linearity study of 3-methoxytyramine in solvent.

Appendix 8.9. Example of the linearity analysis for the fragment with m/z 123.2 of 3,4-dihydroxyphenylacetic acid in solvent.

Concentration (pmol/µL)	Peak area ratio	Residuals
0.10	0.045	0.007
0.15	0.043	-0.008
0.25	0.072	-0.005
0.50	0.139	-0.001
1.0	0.277	0.009
2.0	0.502	-0.020
3.0	0.782	0.003
4.0	1.084	0.050
5.0	1.258	-0.032
6.0	1.540	-0.002

Regression statistics	
m	0.25
b	0.01
R	0.999
R^2	0.999
$S_{y/x}$	0.02
$2xS_{y/x}$	0.05
T-student value	2.31
Upper limit 95%	0.035
Lower limit 95%	-0.009

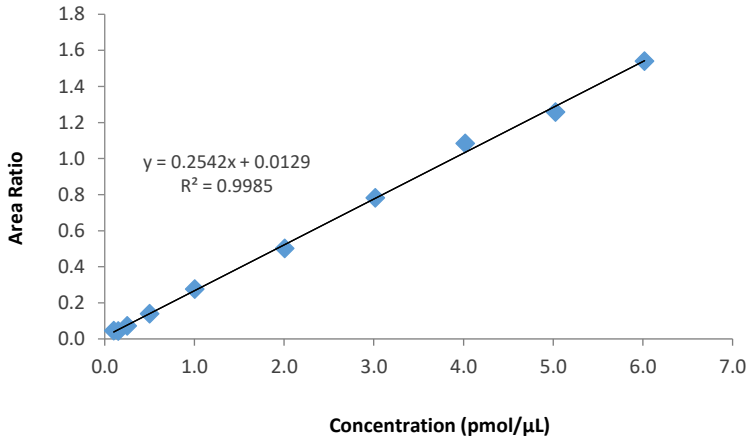

Figure 8.25. Calibration curve for the fragment with m/z 123.2 of 3,4-dihydroxyphenylacetic acid in solvent.

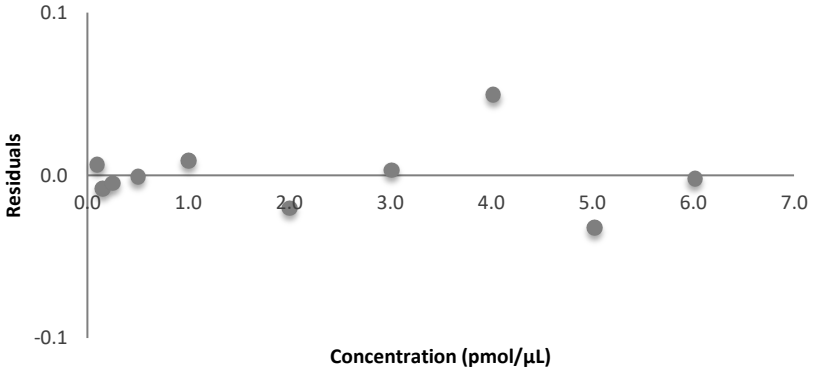

Figure 8.26. Plot of the residuals versus the concentration, used in the linearity study of 3,4-dihydroxyphenylacetic acid in solvent.

Appendix 8.10. Example of the linearity analysis for the fragment with m/z 137.2 of homovanillic acid in solvent.

Concentration (pmol/µL)	Peak area ratio	Residuals
0.03	0.011	0.001
0.05	0.011	-0.002
0.10	0.014	-0.007
0.15	0.021	-0.007
0.25	0.048	0.005
0.50	0.085	0.008
1.0	0.158	0.010
2.0	0.299	0.010
3.0	0.396	-0.036
4.0	0.590	0.017
5.0	0.715	0.001

Regression statistics	
m	0.14
b	0.01
R	0.998
R^2	0.997
$S_{y/x}$	0.01
$2xS_{y/x}$	0.03
T-student value	2.26
Upper limit 95%	0.020
Lower limit 95%	-0.007

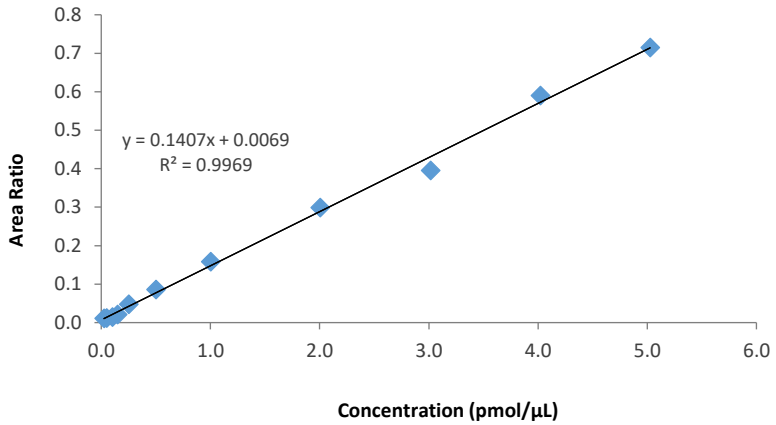

Figure 8.27. Calibration curve for the fragment with m/z 137.2 of homovanillic acid in solvent.

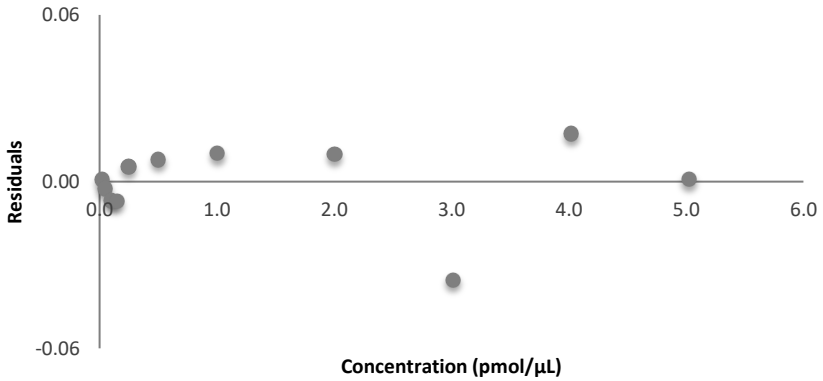

Figure 8.28. Plot of the residuals versus the concentration, used in the linearity study of homovanillic acid in solvent.

Appendix 8.11. Example of the linearity analysis for the fragment with m/z 119.1 of 3-methoxytyramine in plasma.

Concentration (pmol/µL)	Peak area ratio	Residuals
0.05	0.037	-0.033
0.10	0.070	-0.016
0.20	0.131	0.014
0.30	0.151	0.003
0.50	0.185	-0.026
1.0	0.360	-0.006
2.0	0.639	-0.038
4.0	1.469	0.169
6.0	1.850	-0.078
8.0	2.664	0.112
10.0	3.077	-0.100

Regression statistics	
m	0.31
b	0.05
R	0.998
R^2	0.995
$S_{y/x}$	0.08
$2xS_{y/x}$	0.16
T-student value	2.26
Upper limit 95%	0.130
Lower limit 95%	-0.021

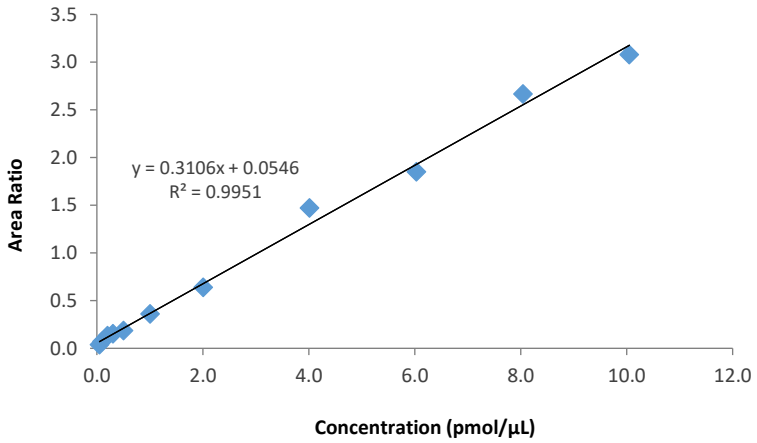

Figure 8.29. Calibration curve for the fragment with m/z 119.1 of 3-methoxytyramine in plasma.

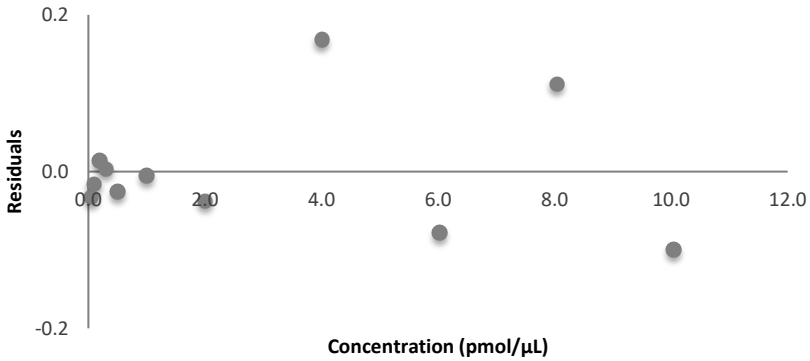

Figure 8.30. Plot of the residuals versus the concentration, used in the linearity study of 3-methoxytyramine in plasma.

Appendix 8.12. Example of the linearity analysis for the fragment with m/z 123.2 of 3,4-dihydroxyphenylacetic acid in plasma.

Concentration (pmol/µL)	Peak area ratio	Residuals
0.05	0.047	0.059
0.10	0.037	0.038
0.20	0.062	0.038
0.30	0.067	0.020
0.50	0.085	-0.010
1.0	0.163	-0.051
2.0	0.421	-0.031
4.0	0.895	-0.032
6.0	1.283	-0.124
8.0	1.867	-0.016
10.0	2.470	0.110

Regression statistics	
m	0.24
b	-0.02
R	0.997
R^2	0.995
$S_{y/x}$	0.07
$2xS_{y/x}$	0.13
T-student value	2.26
Upper limit 95%	0.036
Lower limit 95%	-0.084

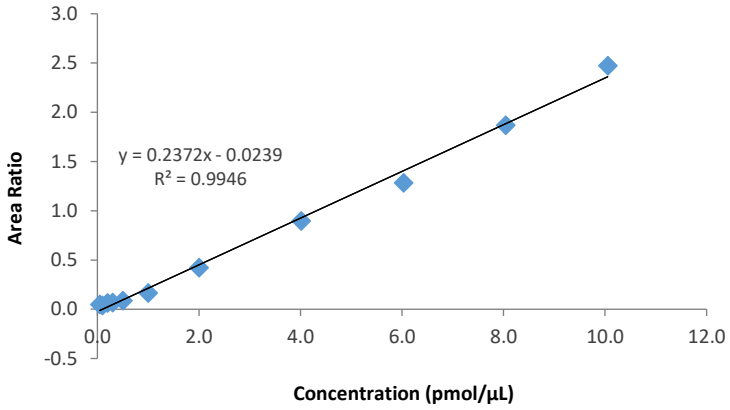

Figure 8.31. Calibration curve for the fragment with m/z 123.2 of 3,4-dihydroxyphenylacetic acid in plasma.

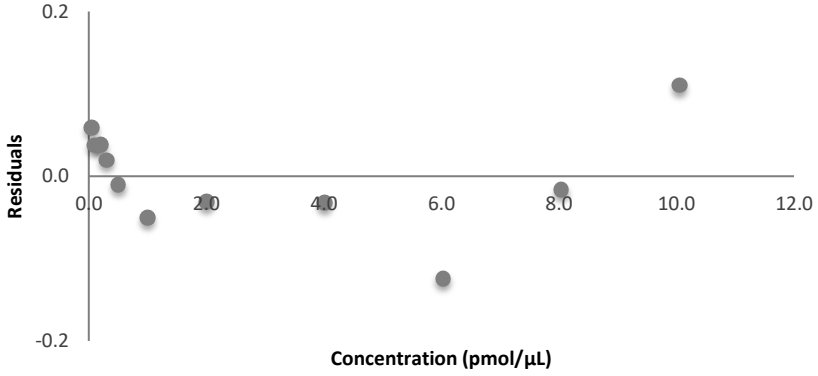

Figure 8.32. Plot of the residuals versus the concentration, used in the linearity study of 3,4-dihydroxyphenylacetic acid in plasma.

Appendix 8.13. Example of the linearity analysis for the fragment with m/z 137.2 of homovanillic acid in plasma.

Concentration (pmol/µL)	Peak area ratio	Residuals
0.05	0.079	0.020
0.10	0.070	0.004
0.20	0.078	-0.001
0.30	0.080	-0.012
0.50	0.119	0.001
1.0	0.189	0.007
2.0	0.307	-0.005
4.0	0.612	0.040
6.0	0.803	-0.031
8.0	1.019	-0.075
12.0	1.663	0.052

Regression statistics	
m	0.13
b	0.05
R	0.998
R^2	0.996
$S_{y/x}$	0.04
$2xS_{y/x}$	0.07
T-student value	2.26
Upper limit 95%	0.086
Lower limit 95%	0.020

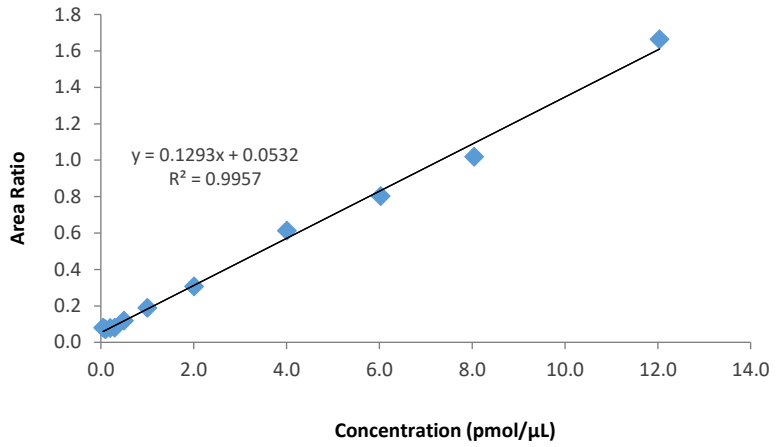

Figure 8.33. Calibration curve for the fragment with m/z 137.2 of homovanillic acid in plasma.

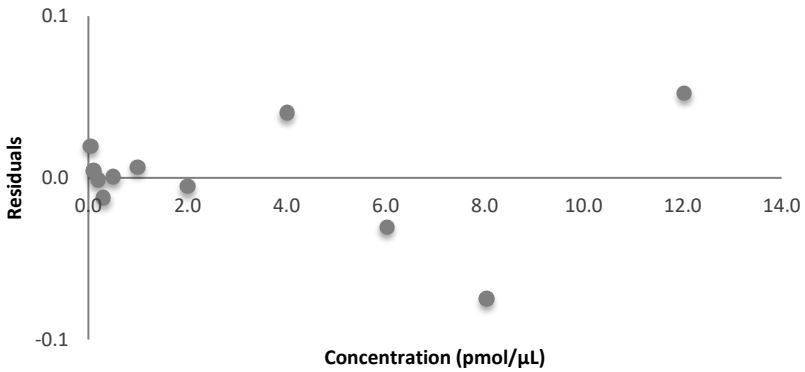

Figure 8.34. Plot of the residuals versus the concentration, used in the linearity study of homovanillic acid in plasma.

Appendix 8.14. Data related to the study of weighted least squares linear regression.

Table 8.10. Relative errors ($\%RE$) and respective sum of the relative errors ($\sum|\%RE|$) calculated by the simplest linear regression and weighted linear regression for each weighting factor (w_i), for the fragment with m/z 136.2 of L-tyrosine in solvent.

Nominal concentration (µM)	Model 1 Unweighted (w_i=1)	Model 2 $\frac{1}{x}$	Model 3 $\frac{1}{x^2}$	Model 4 $\frac{1}{y}$	Model 5 $\frac{1}{y^2}$	Model 6 $\frac{1}{\sqrt{x}}$	Model 7 $\frac{1}{\sqrt{y}}$
0.025	512.24	142.77	70.58	202.521	191.15	199.03	245.67
0.05	236.86	79.17	110.19	102.69	84.68	100.13	115.58
0.1	53.25	61.05	68.83	50.23	59.64	43.72	34.94
0.15	69.10	52.91	56.10	43.79	48.89	43.54	38.53
0.25	46.68	49.89	47.94	44.85	43.36	47.21	44.42
0.5	35.90	30.99	39.87	33.91	37.35	31.54	32.81
1.0	18.16	18.79	21.36	17.90	14.56	18.36	17.74
2.0	18.19	17.98	22.62	17.57	18.13	18.36	18.11
3.0	24.80	22.55	18.02	22.93	18.42	24.03	24.14
4.0	29.36	27.69	41.14	28.22	33.95	28.18	28.60
5.0	19.58	19.90	27.40	20.75	27.42	19.46	19.98
6.0	20.83	22.55	34.22	21.33	24.56	21.92	21.20
$\sum\|\%\boldsymbol{RE}\|$	1084.95	546.22	558.27	606.68	602.10	595.48	641.73
$\boldsymbol{R^2}$	0.99284	0.99470	0.96626	0.99493	0.98386	0.99504	0.99486

Table 8.11. Relative errors ($\%RE$) and respective sum of the relative errors ($\sum|\%RE|$) calculated by the simplest linear regression and weighted linear regression for each weighting factor (w_i), for the fragment with m/z 152.1 of L-DOPA in solvent.

Nominal concentration (µM)	Model 1 Unweighted (w_i=1)	Model 2 $\frac{1}{x}$	Model 3 $\frac{1}{x^2}$	Model 4 $\frac{1}{y}$	Model 5 $\frac{1}{y^2}$	Model 6 $\frac{1}{\sqrt{x}}$	Model 7 $\frac{1}{\sqrt{y}}$
0.025	319.29	68.43	24.50	86.98	43.30	145.37	160.31
0.05	125.23	38.89	47.56	46.22	39.32	45.65	51.57
0.1	66.64	46.41	50.80	40.56	45.67	37.59	36.05
0.15	37.38	28.81	28.80	24.59	24.88	23.15	20.76
0.25	23.39	34.72	32.35	31.22	27.59	32.73	30.46
0.5	51.86	55.27	51.24	56.10	55.09	53.57	53.82
1.0	29.15	27.69	34.37	29.64	38.05	27.61	28.60
2.0	24.19	23.98	21.54	23.72	21.70	24.74	24.58
3.0	27.50	28.01	33.12	27.42	31.35	27.50	27.27
4.0	19.27	19.48	21.11	19.10	19.15	19.39	19.20
5.0	20.70	22.12	31.62	23.13	33.17	21.38	21.81
6.0	4.76	6.02	15.21	6.20	14.70	4.95	4.94
$\sum\|\%\boldsymbol{RE}\|$	749.37	399.83	392.20	414.89	393.97	463.62	479.37
$\boldsymbol{R^2}$	0.99531	0.99577	0.98835	0.99565	0.98946	0.99629	0.99618

Table 8.12. Relative errors ($\%RE$) and respective sum of the relative errors ($\sum|\%RE|$) calculated by the simplest linear regression and weighted linear regression for each weighting factor (w_i), for the fragment with m/z 119.1 of 3-methoxytyramine in solvent.

Nominal concentration (µM)	Model 1 Unweighted (w_i=1)	Model 2 $\frac{1}{x}$	Model 3 $\frac{1}{x^2}$	Model 4 $\frac{1}{y}$	Model 5 $\frac{1}{y^2}$	Model 6 $\frac{1}{\sqrt{x}}$	Model 7 $\frac{1}{\sqrt{y}}$
0.025	1186.69	45.09	19.10	68.56	49.84	129.07	160.22
0.05	603.30	63.49	53.00	69.52	50.98	104.24	119.26
0.1	315.13	36.73	36.97	36.25	36.98	64.275648	67.94
0.15	144.08	40.35	40.37	44.51	48.44	27.36	25.98
0.25	151.31	53.96	50.81	51.78	48.74	57.18	57.59
0.5	46.78	31.13	26.72	31.32	26.93	30.47	30.60
1.0	41.77	30.78	33.66	29.19	34.29	30.81	30.29
2.0	51.32	39.03	40.17	42.88	44.92	41.73	43.55
3.0	27.52	11.60	14.19	14.42	18.14	14.35	15.81
4.0	36.23	28.47	28.25	27.80	29.33	27.81	27.59
5.0	30.70	20.35	16.64	23.49	17.79	22.52	24.17
6.0	47.30	61.67	59.42	59.45	56.64	59.22	58.01
$\sum\|\%\boldsymbol{RE}\|$	2682.12	462.65	419.30	499.18	463.00	609.05	661.03
$\boldsymbol{R^2}$	0.97699	0.99089	0.98212	0.99062	0.98302	0.99013	0.79185

Table 8.13. Relative errors ($\%RE$) and respective sum of the relative errors ($\sum|\%RE|$) calculated by the simplest linear regression and weighted linear regression for each weighting factor (w_i), for the fragment with m/z 123.2 of 3,4-dihydroxyphenylacetic acid in solvent.

Nominal concentration (µM)	**Model 1** **Unweighted (w_i=1)**	**Model 2** $\frac{1}{x}$	**Model 3** $\frac{1}{x^2}$	**Model 4** $\frac{1}{y}$	**Model 5** $\frac{1}{y^2}$	**Model 6** $\frac{1}{\sqrt{x}}$	**Model 7** $\frac{1}{\sqrt{y}}$
0.025	433.80	146.51	70.47	169.42	160.69	245.56	234.35
0.05	293.06	96.65	114.58	70.35	68.95	138.43	115.39
0.1	122.19	95.25	89.22	111.96	117.07	98.57	105.25
0.15	33.61	38.53	36.48	50.23	58.71	29.64	32.64
0.25	36.43	30.85	22.07	30.75	23.48	23.12	24.30
0.5	11.87	15.99	10.60	16.51	15.54	13.24	13.87
1.0	20.71	18.29	15.00	17.64	10.35	17.85	17.52
2.0	28.67	28.01	39.94	28.42	38.58	28.79	29.03
3.0	7.00	5.40	16.79	5.85	14.90	6.75	6.93
4.0	9.95	10.37	21.87	10.02	11.59	10.12	10.02
5.0	15.02	13.57	27.93	13.97	26.11	14.02	14.27
6.0	11.88	14.91	23.28	14.59	16.73	13.30	13.10
$\sum\|\%\boldsymbol{RE}\|$	1024.19	514.33	488.21	539.72	562.70	639.39	616.68
$\boldsymbol{R^2}$	0.99703	0.99669	0.95976	0.99684	0.95954	0.99771	0.99774

Table 8.14. Relative errors ($\%RE$) and respective sum of the relative errors ($\sum|\%RE|$) calculated by the simplest linear regression and weighted linear regression for each weighting factor (w_i), for the fragment with m/z 137.2 of homovanillic acid in solvent.

Nominal concentration (µM)	Model 1 Unweighted (w_i=1)	Model 2 $\frac{1}{x}$	Model 3 $\frac{1}{x^2}$	Model 4 $\frac{1}{y}$	Model 5 $\frac{1}{y^2}$	Model 6 $\frac{1}{\sqrt{x}}$	Model 7 $\frac{1}{\sqrt{y}}$
0.025	274.70	147.32	83.54	144.13	115.14	154.15	143.77
0.05	141.82	131.03	150.04	132.83	141.90	128.56	133.80
0.1	204.92	80.77	68.77	63.38	50.61	109.86	104.17
0.15	112.56	64.80	70.67	59.87	63.01	60.90	58.78
0.25	47.00	73.09	73.62	79.71	85.14	63.78	65.73
0.5	44.95	33.41	43.41	31.88	33.88	36.49	35.65
1.0	29.34	34.87	31.07	37.37	34.49	34.52	35.54
2.0	33.02	32.74	38.46	34.10	38.25	33.59	34.24
3.0	9.42	9.72	12.74	9.73	11.09	9.19	9.80
4.0	14.48	12.89	16.22	13.00	11.28	13.37	14.13
5.0	21.47	18.93	27.48	19.99	22.14	20.15	20.79
6.0	15.47	18.98	25.70	17.64	22.04	17.06	16.37
$\sum\|\%\boldsymbol{RE}\|$	949.16	658.53	641.70	643.62	628.98	681.63	672.75
$\boldsymbol{R^2}$	0.99187	0.99359	0.94770	0.99391	0.97184	0.99434	0.99427

Table 8.15. Relative errors ($\%RE$) and respective sum of the relative errors ($\sum|\%RE|$) calculated by the simplest linear regression and weighted linear regression for each weighting factor (w_i), for the fragment with m/z of 119.1 of 3-methoxytyramine in plasma.

Nominal concentration (µM)	Model 1 Unweighted (w_i=1)	Model 2 $\frac{1}{x}$	Model 3 $\frac{1}{x^2}$	Model 4 $\frac{1}{y}$	Model 5 $\frac{1}{y^2}$	Model 6 $\frac{1}{\sqrt{x}}$	Model 7 $\frac{1}{\sqrt{y}}$
0.05	570.64	255.62	112.99	290.47	197.85	287.58	290.74
0.1	285.03	113.58	157.29	104.86	125.89	123.68	123.39
0.2	184.79	102.35	112.83	95.83	113.22	95.65	95.94
0.3	111.05	110.33	104.91	99.92	101.64	97.12	93.05
0.5	29.24	40.31	35.36	33.03	30.95	31.26	30.18
1.0	34.99	24.90	27.23	23.26	23.60	22.80	21.59
2.0	19.40	21.19	35.71	20.56	19.41	21.40	20.97
4.0	25.16	25.44	28.95	25.51	24.52	25.78	25.79
6.0	23.87	21.54	38.41	19.85	20.37	23.19	22.32
8.0	16.22	15.11	44.50	13.46	20.71	15.35	14.76
10.0	18.32	14.95	33.18	14.76	15.30	16.49	15.87
12.0	25.13	30.77	38.11	32.49	35.48	28.47	29.27
$\sum\|\%\boldsymbol{RE}\|$	1343.83	776.09	769.47	774.01	728.93	788.78	783.86
$\boldsymbol{R^2}$	0.99246	0.99342	0.93927	0.99422	0.97445	0.99452	0.99443

Table 8.16. Relative errors ($\%RE$) and respective sum of the relative errors ($\sum|\%RE|$) calculated by the simplest linear regression and weighted linear regression for each weighting factor (w_i), for the fragment with m/z 123.2 of 3,4-dihydroxyphenylacetic acid in plasma.

Nominal concentration (µM)	Model 1 Unweighted (w_i=1)	Model 2 $\frac{1}{x}$	Model 3 $\frac{1}{x^2}$	Model 4 $\frac{1}{y}$	Model 5 $\frac{1}{y^2}$	Model 6 $\frac{1}{\sqrt{x}}$	Model 7 $\frac{1}{\sqrt{y}}$
0.05	1010.81	316.56	154.27	567.65	551.06	532.88	670.10
0.1	351.34	169.98	291.19	125.24	76.60	141.41	157.05
0.2	191.27	53.62	78.66	58.10	64.31	49.16	76.50
0.3	104.13	105.54	120.30	102.12	120.51	94.13	89.05
0.5	88.50	84.92	77.35	64.93	80.34	68.64	57.86
1.0	83.46	93.24	73.92	84.83	90.26	87.60	82.95
2.0	32.28	43.03	33.77	36.10	30.33	41.66	37.81
4.0	24.85	25.45	65.97	25.74	34.49	27.40	25.41
6.0	19.45	16.36	43.38	14.18	25.03	19.20	17.91
8.0	16.63	13.57	57.22	12.12	33.82	15.04	14.33
10.0	25.63	22.27	51.32	21.84	49.23	23.59	22.89
12.0	29.10	35.07	79.56	36.40	65.19	32.62	33.30
$\sum\|\%\boldsymbol{RE}\|$	1977.46	979.60	1126.91	1149.27	1221.16	1133.35	1285.17
$\boldsymbol{R^2}$	0.98995	0.98759	0.85054	0.98906	0.92358	0.99168	0.99183

Table 8.17. Relative errors ($\%RE$) and respective sum of the relative errors ($\sum|\%RE|$) calculated by the simplest linear regression and weighted linear regression for each weighting factor (w_i), for the fragment with m/z 137.2 of homovanillic acid in plasma.

Nominal concentration (µM)	Model 1 Unweighted (w_i=1)	Model 2 $\frac{1}{x}$	Model 3 $\frac{1}{x^2}$	Model 4 $\frac{1}{y}$	Model 5 $\frac{1}{y^2}$	Model 6 $\frac{1}{\sqrt{x}}$	Model 7 $\frac{1}{\sqrt{y}}$
0.05	857.59	494.30	284.68	770.77	828.94	644.42	771.36
0.1	220.58	265.14	452.32	157.20	115.58	186.94	182.52
0.2	177.96	216.55	265.91	164.37	150.18	192.55	170.57
0.3	89.19	139.47	179.63	112.30	128.44	117.45	102.15
0.5	24.10	53.65	39.59	20.50	21.31	35.18	18.80
1.0	22.48	22.49	53.78	20.10	20.90	19.51	20.11
2.0	25.17	28.00	75.63	28.13	26.54	27.37	26.95
4.0	13.85	14.35	70.27	12.83	16.38	14.03	13.21
6.0	25.66	24.64	70.67	24.80	20.63	25.76	25.49
8.0	30.86	29.19	62.20	29.00	29.71	30.41	29.76
10.0	25.26	28.01	81.52	27.07	31.89	25.99	25.96
12.0	23.79	25.84	86.72	25.52	26.06	24.83	24.92
$\sum\|\%\boldsymbol{RE}\|$	1536.48	1341.63	1722.92	1392.58	1416.55	1344.43	1411.80
$\boldsymbol{R^2}$	0.98998	0.98650	0.72298	0.99193	0.97855	0.99229	0.99206

Appendix 8.15. ANOVA analysis, intermediate precision and repeatability.

Table 8.18. Calculation of a single-factor ANOVA used in the study of intermediate precision and repeatability.

Variation	Sum of squares	Degrees of freedom	Mean squares
Between groups	$SS_{run} = n \sum_{i=1}^{p} (\bar{X}_i - \bar{X})^2$	$p - 1$	$MS_{run} = \frac{n \sum_{i=1}^{p} (\bar{X}_i - \bar{X})^2}{p - 1}$
Within groups (Repeatability)	$SS_r = \sum_{i=1}^{p} \sum_{j=i}^{p} (X_{ij} - \bar{X}_i)^2$	$p.(n - 1)$	$MS_r = \frac{\sum_{i=1}^{p} \sum_{j=i}^{p} (X_{ij} - \bar{X}_i)^2}{p(p - 1)}$
Total	$SS_r = SS_{run} + SS_r$	$p.n - 1$	$MS_T = \frac{SS_T}{n - 1}$

p – number of analytical runs in which the sample is tested;

n – number of replicates performed in every analytical run;

X_{ij} – analytical result of a sample analyzed in the jth replicate and the ith run;

X_i – average of the j replicates obtained in the i run;

$\bar{X}$ – average of the mean results obtained in the p runs.

Table 8.19. Calculation of the variances used in the study of intermediate precision and repeatability.

Variation	Sum of squares
Repeatability variance ($\boldsymbol{S_r^2}$)	$S_r^2 = MS_r$
Between run variance ($\boldsymbol{S_{run}^2}$)	$S_{run}^2 = \frac{MS_{run} - MS_r}{n}$
Intermediate variance ($\boldsymbol{S_I^2}$)	$S_I^2 = S_r^2 + S_{run}^2$
Mean variance ($\boldsymbol{S_x^2}$)	$S_x^2 = \frac{MS_{run}}{n}$

Appendix 8.16. Data related to the study of carry-over effect.

Table 8.20. Area of LOQ of dopamine and dopamine-d4 used to calculate the criteria of carry-over in solvent.

Dopamine			Dopamine-d4		
Transition	**Concentration (µM)**	**Area[1]**	**Transition**	**Concentration (µM)**	**Area[1]**
154.2/91.1	0.050	2560.83	158.3/94.1	0.025	57100.20

[1]The value of the area is the average of the data obtained in the 4 days that the procedure was repeated.

Table 8.21. Results of carry-over effect for dopamine and dopamine-d4 in solvent. Data obtained in the injection of five blanks after the injection of the highest calibrator.

Concentration (µM)	**Injection**	**Dopamine (154.2/91.1)**	**Dopamine-d4 (158.3/94.1)**
		Area[5]	**Area[5]**
6.0	Standard	179168.70	39034.86
	Blank 1	495.80	N/A
	Blank 2	N/A	N/A
	Blank 3	148.00	N/A
	Blank 4	N/A	N/A
	Blank 5	N/A	109.94

[1]The value of the area is the average of the data obtained in the 4 days that the procedure was repeated.

Table 8.22. Area of LOQ of tyrosine and tyrosine-d7 used to calculate the criteria of carry-over in solvent.

Tyrosine			Tyrosine-d7		
Transition	**Concentration (µM)**	**Area[1]**	**Transition**	**Concentration (µM)**	**Area[1]**
182.2/136.2	0.050	7792.20	189.2/143.2	0.025	246027.55

[1]The value of the area is the average of the data obtained in the 4 days that the procedure was repeated.

Table 8.23. Results of carry-over effect for tyrosine and tyrosine-d7 in solvent. Data obtained in the injection of five blanks after the injection of the highest calibrator. The values that did not fulfil these criteria are highlighted.

Concentration (µM)	**Injection**	**Tyrosine (182.2/136.2)**	**Tyrosine-d7 (189.2/143.2)**
		Area[1]	**Area[1]**
6.0	Standard	332303.25	195541.96
	Blank 1	7080.16	1149.04
	Blank 2	4410.40	870.65
	Blank 3	4035.80	634.16
	Blank 4	2476.03	652.90
	Blank 5	2164.47	695.50

[1]The value of the area is the average of the data obtained in the 4 days that the procedure was repeated.

Table 8.24. Area of LOQ of L-DOPA and L-DOPA-d3 used to calculate the criteria of carry-over in solvent.

L-DOPA			L-DOPA-d3		
Transition	**Concentration (µM)**	**Area[1]**	**Transition**	**Concentration (µM)**	**Area[1]**
198.2/152.1	0.050	3587.19	201.2/154.1	0.025	183477.92

[1]The value of the area is the average of the data obtained in the 4 days that the procedure was repeated.

Table 8.25. Results of carry-over effect for L-DOPA and L-DOPA-d3 in solvent. Data obtained in the injection of five blanks after the injection of the highest calibrator.

Concentration (µM)	**Injection**	**L-DOPA (198.2/152.1)**	**L-DOPA-d3 (201.2/154.1)**
		Area[1]	**Area[1]**
6.0	Standard	257956.21	145735.67
	Blank 1	707.10	489.89
	Blank 2	282.98	462.02
	Blank 3	505.76	241.36
	Blank 4	N/A	178.28
	Blank 5	N/A	252.26

[1]The value of the area is the average of the data obtained in the 4 days that the procedure was repeated.

Table 8.26. Area of LOQ of 3-methoxytyramine and 3-methoxytyramine-d4 used to calculate the criteria of carry-over in solvent.

3-methoxytyramine			3-methoxytyramine-d4		
Transition	**Concentration (µM)**	**Area[1]**	**Transition**	**Concentration (µM)**	**Area[1]**
168.3/119.1	0.050	3113.62	172.3/123.1	0.025	124172.53

[1]The value of the area is the average of the data obtained in the 4 days that the procedure was repeated.

Table 8.27. Results of carry-over effect for 3-methoxytyramine and 3-methoxytyramine-d4 in solvent. Data obtained in the injection of five blanks after the injection of the highest calibrator.

Concentration (µM)	**Injection**	**3-methoxytyramine (168.3/119.1)**	**3-methoxytyramine-d4 (172.3/123.1)**
		Area[1]	**Area[1]**
6.0	Standard	199362.27	107505.89
	Blank 1	581.08	N/A
	Blank 2	593.63	N/A
	Blank 3	N/A	N/A
	Blank 4	N/A	N/A
	Blank 5	N/A	N/A

[1]The value of the area is the average of the data obtained in the 4 days that the procedure was repeated.

Table 8.28. Area of LOQ of 3,4-dihydroxyphenylacetic acid and 3,4-dihydroxyphenylacetic acid-d5 used to calculate the criteria of carry-over in solvent.

3,4-dihydroxyphelyacetic acid			3,4-dihydroxyphelyacetic acid-d5		
Transition	**Concentration (µM)**	**Area[1]**	**Transition**	**Concentration (µM)**	**Area[1]**
167.0/123.2	0.100	7728.15	172.2/128.2	0.025	219530,66

[1]The value of the area is the average of the data obtained in the 4 days that the procedure was repeated.

Table 8.29. Results of carry-over effect for 3-methoxytyramine and 3-methoxytyramine-d4 in solvent. Data obtained in the injection of five blanks after the injection of the highest calibrator.

Concentration (µM)	**Injection**	**3,4-dihydroxyphelyacetic acid (167.0/123.2)**	**3,4-dihydroxyphelyacetic acid-d5 (172.2/128.2)**
		Area[1]	**Area[1]**
6.0	Standard	10957.37	223638.87
	Blank 1	N/A	N/A
	Blank 2	N/A	392.02
	Blank 3	N/A	613.16
	Blank 4	N/A	N/A
	Blank 5	N/A	N/A

[1]The value of the area is the average of the data obtained in the 4 days that the procedure was repeated.

Table 8.30. Area of LOQ of homovanillic acid and homovanillic acid-d3 used to calculate the criteria of carry-over in solvent.

Homovanillic acid			Homovanillic acid-d3		
Transition	**Concentration (µM)**	**Area[1]**	**Transition**	**Concentration (µM)**	**Area[1]**
181.0/137.2	0.100	1786.51	184.0/139.8	0.025	114952.20

[1]The value of the area is the average of the data obtained in the 4 days that the procedure was repeated.

Table 8.31. Results of carry-over effect for homovanillic acid and homovanillic acid-d3 in solvent. Data obtained in the injection of five blanks after the injection of the highest calibrator.

Concentration (µM)	**Injection**	**Homovanillic acid (181.0/137.2)**	**Homovanillic acid-d3 (184.0/139.8)**
		Area[1]	**Area[1]**
6.0	Standard	82251.12	102151.43
	Blank 1	N/A	409.16
	Blank 2	N/A	442.89
	Blank 3	N/A	651.91
	Blank 4	N/A	181.01
	Blank 5	N/A	212.37

[1]The value of the area is the average of the data obtained in the 4 days that the procedure was repeated.

Table 8.32. Area of LOQ of 3-methoxytyramine and 3-methoxytyramine-d4 used to calculate the criteria of carry-over in plasma.

3-methoxytyramine			3-methoxytyramine-d4		
Transition	**Concentration (μM)**	**Area[1]**	**Transition**	**Concentration (μM)**	**Area[1]**
168.3/119.1	0.200	1504.32	172.3/123.1	0.050	16498.81

[1]The value of the area is the average of the data obtained in the 4 days that the procedure was repeated.

Table 8.33. Results of carry-over effect for 3-methoxytyramine and 3-methoxytyramine-d4 in plasma. Data obtained in the injection of five blanks after the injection of the highest calibrator.

Concentration (μM)	**Injection**	**3-methoxytyramine (168.3/119.1)**	**3-methoxytyramine-d4 (172.3/123.1)**
		Area[1]	**Area[1]**
6.0	Standard	66658.88	16376.03
	Blank 1	278.90	N/A
	Blank 2	203.42	N/A
	Blank 3	N/A	N/A
	Blank 4	N/A	N/A
	Blank 5	N/A	N/A

[1]The value of the area is the average of the data obtained in the 4 days that the procedure was repeated.

Table 8.34. Area of LOQ of 3,4-dihydroxyphenylacetic acid and 3,4-dihydroxyphenylacetic acid-d5 used to calculate the criteria of carry-over in plasma.

3,4-dihydroxyphelyacetic acid			3,4-dihydroxyphelyacetic acid-d5		
Transition	**Concentration (µM)**	**Area[1]**	**Transition**	**Concentration (µM)**	**Area[1]**
167.0/123.2	0.300	2733.92	172.2/128.2	0.050	42440.06

[1]The value of the area is the average of the data obtained in the 4 days that the procedure was repeated.

Table 8.35. Results of carry-over effect for 3-methoxytyramine and 3-methoxytyramine-d4 in plasma. Data obtained in the injection of five blanks after the injection of the highest calibrator.

Concentration (µM)	**Injection**	**3,4-dihydroxyphelyacetic acid (167.0/123.2)**	**3,4-dihydroxyphelyacetic acid-d5 (172.2/128.2)**
		Area[1]	**Area[1]**
6.0	Standard	139103.60	48430.34
	Blank 1	109.17	N/A
	Blank 2	70.10	N/A
	Blank 3	N/A	N/A
	Blank 4	N/A	N/A
	Blank 5	N/A	N/A

[1]The value of the area is the average of the data obtained in the 4 days that the procedure was repeated.

Table 8.36. Area of LOQ of homovanillic acid and homovanillic acid-d3 used to calculate the criteria of carry-over in plasma.

Homovanillic acid			Homovanillic acid-d3		
Transition	**Concentration (μM)**	**Area[1]**	**Transition**	**Concentration (μM)**	**Area[1]**
181.0/137.2	0.300	5706.80	184.0/139.8	0.050	61526.18

[1]The value of the area is the average of the data obtained in the 4 days that the procedure was repeated.

Table 8.37. Results of carry-over effect for homovanillic acid and homovanillic acid-d3 in plasma. Data obtained in the injection of five blanks after the injection of the highest calibrator.

Concentration (μM)	Injection	Homovanillic acid (181.0/137.2)	Homovanillic acid-d3 (184.0/139.8)
		Area[1]	**Area[1]**
6.0	Standard	110229.56	62772.94
	Blank 1	N/A	264.598
	Blank 2	N/A	251.065
	Blank 3	N/A	229.302
	Blank 4	N/A	82.279
	Blank 5	N/A	494.896

[1]The value of the area is the average of the data obtained in the 4 days that the procedure was repeated.